Fixed and Reconfigurable Multiband Antennas

A thesis submitted for the degree of
Doctor of Philosophy (PhD)

by

Hattan F. Abutarboush

Electronic and Computer Engineering,
School of Engineering and Design,
Brunel University, London, United Kingdom.

July 2011

Abstract

With the current scenario of development of antennas in the wireless communication field, the need of compact multiband, multifunctional and cost effective antenna is on the rise. The objective of this thesis is to present fixed and reconfigurable techniques and methods for small and slim multiband antennas, which are applicable to serve modern small and slime wireless, mobile and cognitive radio applications.

In the fixed designs, independent control of the operating frequencies is investigated to enhance the antennas capabilities and to give the designer an additional level of freedom to design the antenna for other bands easily without altering the shape or the size of the antenna. In addition, for mobile phone antenna, the effect of user's hand and mobile phone housing are studied to be with minimum effect.

Although fixed multiband antennas can widely be used in many different systems or devices, they lack flexibility to accommodate new services compared with reconfigurable antennas. A reconfigurable antenna can be considered as one of the key advances for future wireless communication transceivers. The advantage of using a reconfigurable antenna is to operate in multiband where the total antenna volume can be reused and therefore the overall size can be reduced. Moreover, the future of cell phones and other personal mobile devices require compact multiband antennas and smart antennas with reconfigurable features.

Two different types of frequency reconfigurability are investigated in this thesis: switchable and tunable. In the switchable reconfigurability, PIN diodes have been used so the antenna's operating frequencies can hop between different services whereas varactor diode with variable capacitance allow the antenna's operating frequencies to be fine-tuned over the operating bands. With this in mind, firstly, a switchable compact and slim antenna with two patch elements is presented for cognitive radio applications where the antenna is capable of operating in wideband and narrow bands depending on the states of the switches. In addition to this, a switchable design is proposed to switch between single, dual and tri bands applications (using a single varactor diode to act as a switch at lower capacitance values) with some fine tuning capabilities for the first and third bands when the capacitance of the diode is further increased. Secondly, the earlier designed fixed antennas are modified to be reconfigurable with fine-tuning so that they can be used for more applications in both wireless and mobile applications with the ability to control the bands simultaneously or independently over a wide range.

Both analytical and numerical methods are used to implement a realistic and functional design. Parametric analyses using simulation tools are performed to study critical parameters that may affect the designs.

Finally, the simulated designs are fabricated, and measured results are presented that validate the design approaches.

Acknowledgments

I am grateful to the creator who taught the names to Adam and gave human being authority to pass beyond the zones of heavens and earth, without his blessing and mercy, this thesis would not have been possible.

I owe my deepest gratitude to my parents who gave me love, care, affection and motivation during my whole academic career. Especially, I would like to thank my father and mother for their utmost interest in my education. They are a source of inspiration for me in all my life. Without their help, it would not be possible for me to finish the PhD degree.

I also wish to express my gratitude to my supervisor Dr. R. Nilavalan who supervised my research and guided me all the time. His door was always open. He had been supportive every time I faced a problem; I appreciate all his help and support. In addition, I would like to thank Prof. H. Al-Raweshidy for his useful discussion and support during my PhD degree.

To my wife and son, thanks for patiently listening to all of my complaints during the development of this thesis. You helped me keep my sanity.

I am grateful to a number of colleagues, my friends and family especially my brother Hani Abutarboush, my friend Mr. Thomas Peter, Dave and Lin Shutler who all had been of tremendous help and support.

Thanks go to Prof. S. W. Cheung from Hong Kong University, Dr. K. M. Nasr from National Physical Laboratory in London (NPL) and Dr. D. Budimir from Westminster University for the useful collaboration and discussion during the PhD research.

Table of Contents

List of Figures

List of Tables

List of Abbreviations

IEEE	Institute of Electrical and Electronics Engineering
HF	High Frequency
UHF	Ultra-High Frequency
PIFA	Planar Inverted-F Antenna
WiMAX	Worldwide Interoperability for Microwave Access
WLAN	Wireless Local Area Network
DCS	Digital Communication systems
GSM	Global System for Mobile communications
UMTS	Universal Mobile Telecommunication System
GPS	Global Position System
PCS	Personal Communication System
DVB-H	Digital Video Broadcasting - Handheld
PIN	Positive-Intrinsic-Negative
MEMS	Micro Electro Mechanical Systems
LHCP	Left Hand Circular Polarization
RHCP	Right Hand Circular Polarization
RF	Radio Frequency
RLC	Resistance, Inductance and Capacitance
CR	Cognitive Radio
HFSS	High Frequency Structure Simulator
WMAN	Wireless Metropolitan Area Networks
WiBro	Wireless Broadband
BSs	Base Station Subsystem
VNA	Vector Network Analyzer
dB	Decibel
EM	Electromagnetic
FDTD	Finite Different Time Domain
MOM	Moment of Method
FEM	Finite Element Method
FD	Frequency Domain
TD	Time Domain
LHS	Left Hand Side
RHS	Right Hand Side

Author's Publications

Journals

[R1] Hattan F. AbuTarboush, R. Nilavalan, T. Peter and S. Cheung, "Multiband Inverted-F Antenna with Independent Bands for Small and Slim Cellular Mobile Handsets," IEEE Transaction on Antennas and Propagation, Vol. 59, No. 7, 2011. (**Published in July 2011).**

[R2] H. F. AbuTarboush, R. Nilavalan, K. Nasr, , S. W. Cheung, H. Al-Raweshidy, and D. Budimir " Reconfigurable Tri-Band H-Shaped Antenna with Frequency Selectivity Feature for Compact Wireless Communication Systems," IET Microwave Antennas and Propagation, 2011. **(Accepted July 2011**).

[R3] H. F. AbuTarboush, R. Nilavalan, S. W. Cheung, K. Nasr, T. Peter, and D. Budimir "A Reconfigurable Wideband and Multiband Antenna Using Dual-Patch Elements for Compact Wireless Devices," IEEE Transaction on Antennas and Propagation, 2011. **(Accepted July 2011).**

[R4] H. F. AbuTarboush, R. Nilavalan, K. Nasr, S. W. Cheung and D. Budimir "Multiband Patch Antennas suitable for Fixed and Reconfigurable Wireless Communication Systems," IEEE Transaction on Antennas and Propagation 2010. (**Major Revision**).

[R5] H. F. AbuTarboush, R. Nilavalan, S. W. Cheung, T. Peter and D. Budimir "Reconfigurable Penta-Band PIFA for Small and Slim Mobile Handsets," ", John and Wiley Microwave and Optical Technology Letters. May 2011. (**Accepted 2011**)

[R6] Hattan F. AbuTarboush, R. Nilavalan, D. Budimir and H. Al-Raweshidy, "Double U-Slots Patch Antenna for Tri-Band Wireless Systems International Journal of RF and Microwave Computer-Aided Engineering, Vol.20,no.3,p279-285, May2010.

[R7] T. Peter, R. Nilavalan, H. F. AbuTarboush, and S. W. Cheung, "A Novel Technique and Soldering Method to Improve Performance of Transparent Polymer Antennas," IEEE Antennas and Wireless Propagation Letters, vol.9, pp.918-921, 2010.

Conferences

[R8] H. F. AbuTarboush, R. Nilavalan, T. Peter and S. C. Cheung, "The Effect of the Mutual Coupling on Small Reconfigurable Antenna," international symposium on antennas and propagation. China. ISAP 2010.

[R9] T. Peter, Y. Sun, T. Yuk, H. F. AbuTarboush, R. Nilavalan, S. W. Cheung, "Miniature transparent UWB antenna with tunable notch for green wireless applications," International Workshop on Antenna Technology (iWAT), pp.259-262, March 2011.

[R10] H. F. AbuTarboush, R.Nilavalan, T.Peter and S.Cheung, "Small and Thin Inverted-F antenna with insensitive Ground Plane for Mobile Handsets,"Loughborough Antenna and Propagation Conference. LAPC 2010.

[R11] Hattan F. AbuTarboush, R. Nilavalan, T. Peter and S. C. Cheung, "The Effect of The Ground Plane Size and the Height on Small PIFA," international symposium on antennas and propagation. China. ISAP 2010.

[R12] R. Nilavalan, H. F. AbuTarboush and T. Peter, "PIFA based Reconfigurable Multiband Antenna for Wireless Applications," (**Invited paper for special session on multi-band antennas**), In proceedings of the International Conference in Electromagnetic in Advanced Application, ICEAA 2010, Australia, Sept. 2010.

[R13] H. F AbuTarboush, R. Nilavalan, K. Nasr, H. Al-Raweshidy, D.Budimir, "Widely tunable multiband reconfigurable patch antenna for wireless applications," Antennas and Propagation (EuCAP), 2010 Proceedings of the Fourth European Conference on , vol., no., pp.1-3, 12-16 April 2010

[R14] H. F AbuTarboush, R. Nilavalan, K. Nasr, H. Al-Raweshidy, D. Budimir, "A reconfigurable H-shape antenna for wireless applications," Proceedings of the Fourth European Conference on Antennas and Propagation (EuCAP), 2010, vol., no., pp.1-4, 12-16 April 2010

[R15] H. F AbuTarboush, R. Nilavalan, K. Nasr, H. Al-Raweshidy, D.Budimir, and M. Alexander, "A compact printed antenna for multiband wireless applications," International Workshop on Antenna Technology (iWAT), 2010, vol., no., pp.1-4, 1-3 March 2010

[R16] T. Peter, R. Nilavalan, H. F. AbuTarboush, S. W. Cheung, "A non-thermal soldering technique to improve polymer based antenna performance," European Microwave Conference (EuMC), pp.1476-1479, 28-30 Sept. 2010.

[R17] U. Chandra, H. F. AbuTarboush, H. S. Al-Raweshidy, R. Nilavalan, "Wideband slotted patch antennas using EBG structures," International Workshop on Antenna Technology (iWAT), pp.1-4, 1-3 March 2010.

[R18] A. Rathore, R. Nilavalan, H. F. AbuTarboush, T. Peter, "Compact dual-band (2.4/5.2GHz) monopole antenna for WLAN applications," International Workshop on Antenna Technology (iWAT), pp.1-4, 1-3 March 2010

[R19] H. F. AbuTarboush, R. Nilavalan, H. S. Al-Raweshidy and D. Budimir, "Design of planar inverted-F antennas (PIFA) for multiband wireless applications," (**Invited paper for special session on modern antennas**), International Conference on Electromagnetics in Advanced Applications, 2009. ICEAA '09, pp. 78-81, 2009.

[R20] H. F. A. Tarboush, S. Khan, R. Nilavalan, H. S. Al-Raweshidy and D. Budimir, "Reconfigurable wideband patch antenna for cognitive radio," Antennas & Propagation Conference, 2009. LAPC 2009. Loughborough, pp. 141-144, 2009.

[R21] H. F. AbuTarboush, R. Nilavalan, D. Budimir and H. S. Al-Raweshidy, "Compact planar inverted-F antenna (PIFA) for WiMAX application," IEEEAntennas and Propagation Society International Symposium, 2009. APSURSI 09 pp. 1-4, 2009.

[R22] H. F. AbuTarboush, D. Budimir, R. Nilavalan and H. S. Al-Raweshidy, "Wide-band planar inverted-F antenna for cognitive radio," European Microwave Conference, pp. 1504-1507, 2009.

[R23] Hattan F. AbuTarboush, Karim M. Nasr, R. Nilavalan, H. S. Al-Raweshidy and Martin J. Alexander, " Design and Measurements of a Five Independent Band Patch Antenna for Different Wireless Applications", COST 2100 TD(09) 913, Vienna, Austria Sept. 2009.

[R24] H. F. AbuTarboush, H. S. Al-Raweshidy and R. Nilavalan, "Multi-band antenna for different wireless applications," IEEE International Workshop on Antenna Technology, iWAT 2009, California, USA. pp. 1-4, March 2009.

[R25] H. F. AbuTarboush, H. S. Al-Raweshidy and R. Nilavalan, "Bandwidth enhancement for small patch antenna using PBG structure for different wireless applications," IEEE International Workshop on Antenna Technology, iWAT 2009, California, USA. pp. 1-4, March 2009.

[R26] H. F. AbuTarboush, H. S. Al-Raweshidy and R. Nilavalan, "Bandwidth enhancement for microstrip patch antenna using stacked patch and slot," IEEE International Workshop on Antenna Technology, iWAT 2009, California, USA. pp. 1-4, March 2009.

[R27] D. Zayniyev, H. F. AbuTarboush and D. Budimir, "Microstrip Antenna Diplexer for Wireless Communications," European Microwave Week" (EUM), Roma. September 2009.

[R28] Hattan F. AbuTarboush, R. Nilavalan and H. S. Al-Raweshidy, Antennas for 4G mobile phone and future wireless applications, The 3rd Saudi Innovative Conference (SIC09), UK, June, 2009.

[R29] H. F. AbuTarboush, H. Al-Raweshidy, R. Nilavalan, "Compact Wideband Patch Antenna for 5 and 6GHz WLAN Applications", international symposium on Antenna and Propagation, Taiwan, Oct. 2008.

[R30] H. F. AbuTarboush, H. S. Al-Raweshidy, R. Nilavalan, "Triple Band Double U-Slots Patch Antenna for WiMAX Mobile Applications", The 14th Asia-Pacific Conference on Communications (APCC'08), Japan, 2008.

[R31] H. F. AbuTarboush, H. S. Al-Raweshidy, "A Connected E-Shape and U-Shape Dual-Band Patch Antenna for Different Wireless Applications", The Second International EURASIP Workshop on RFID Technology (EURASIP'08), Budapest, Hungary, July, 2008.

[R32] H. F. AbuTarboush, H. S. Al-Raweshidy, R. Nilavalan, "Compact double U-Slots Patch Antenna for Mobile WiMAX Applications", international symposium on Antenna and Propagation, Taiwan, October 2008.

Chapter 1

Introduction

1.1 Antennas

Antennas are key components of any wireless communication system and it is a device that provides a way for radiation or receiving electromagnetic waves. IEEE standard definition of terms for antenna (IEEE Std 145-1983) defines antenna as a means for radiating or receiving radio wave [1]. Figure 1.1 shows an antenna as a conversion device [1]. The arrows displayed in Figure 1.1 correspond to the electric field lines as the wave is transitioned into free space.

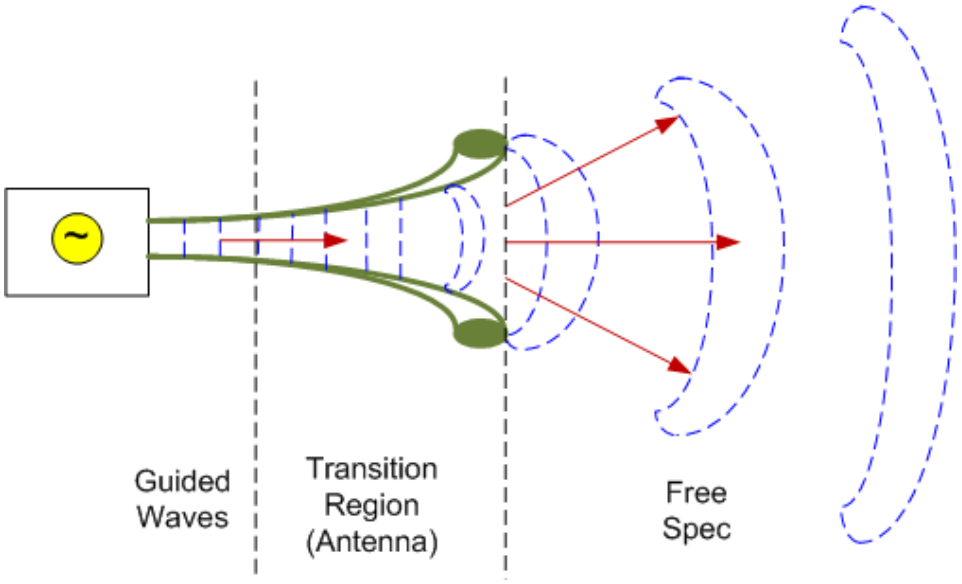

Figure 1-1: Antenna as a transition device

Antennas are usually made of metals but also other materials are possible. Patch antennas have been used in commercial and military application. In military applications, patch antennas are used for radar systems and peer-to-peer communications.

1.2 General Background

1.2.1 Types of Antenna

There are different types of antenna for different applications. Some of the common antennas are discussed in this section.

1.2.1.1 Wire Antenna

Wire Antennas are mainly used in cars and T.V where they are made of conducting wires. Therefore, the cost is usually low and fabrication is inexpensive. Wire antennas can include dipole, helical and Yagi-Uda. It usually operates at low frequencies (HF-UHF) and they have low gain [2].

Dipole: Developed by Heinrich Rudolph Hertz [3] in the late 19th century. Dipole antennas are the most popular type of antenna. Dipole antennas consist of two metals wires with equal length. It can operate in the low frequencies. The evolution of a dipole is shown in Figure 1-2 and an example of a prototype of dipole antenna is shown in Figure 1-3 [2].

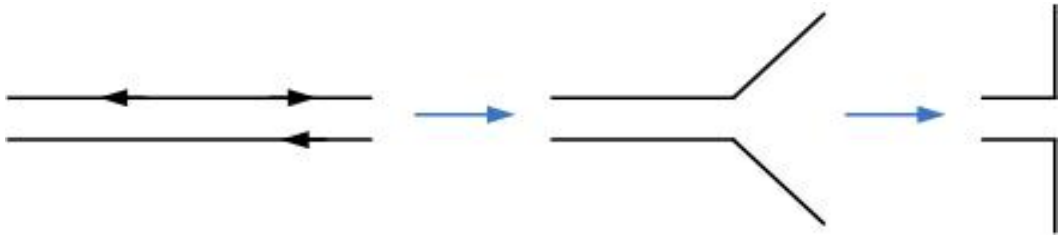

Figure 1-2: Evolution of dipole antenna

Figure 1-3: Prototype of dipole antenna

Monopole: In the early days, monopole antennas (Figure 1-4) were the choice for mobile phone and they are still being used in countries that have limited coverage [2]. The advantages of monopole antennas when they are used in mobile phone are:

- Low SAR
- High efficiency

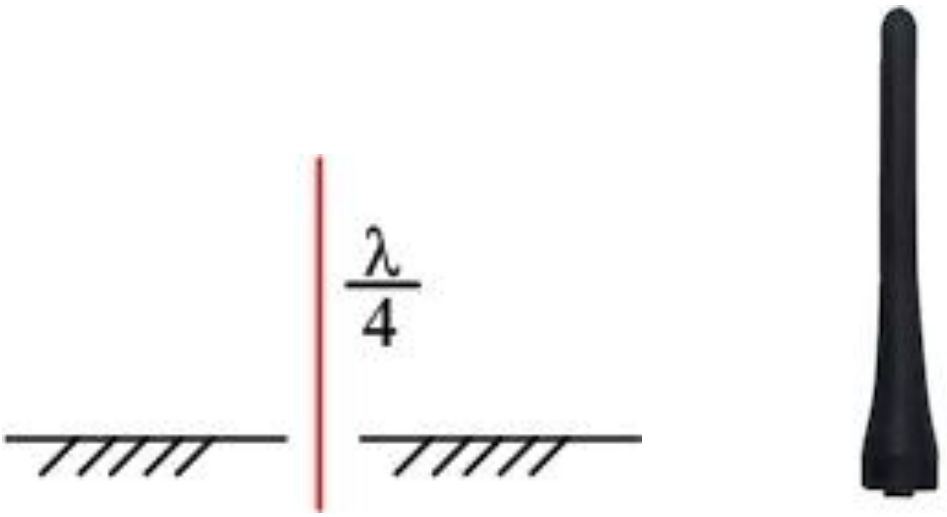

(a) **(b)**

Figure 1-4: (a) Model of monopole antenna and (b) Prototype of monopole antenna

Helical: The helical antenna, which is simply called helix. It is first introduced and investigated in 1950 [4]. In the 1990s, helical antennas were widely used in mobile handsets [2]. They have the advantages of wideband impedance characteristic, circularly polarized radiation and using less space inside mobile phones where the biggest part placed outside the mobile phone [5] case as shown in Figure 1-5. Some mobile phone companies have stopped using this type of antenna in mobile phone because helical antenna is placed outside the handset, which can get broken easily by users.

(a) (b)

Figure 1-5: (a) Model of Helix antenna (b) Helix antenna in Ericson mobile phone

1.2.1.2 Microstrip Antenna

Since 1970s microstrip antennas have become very popular mainly for space borne applications [6] However, now they are being used for commercial applications as well. Microstrip patch antenna consists of a metal patch on a substrate and a ground plane as shown in Figure 1-6.

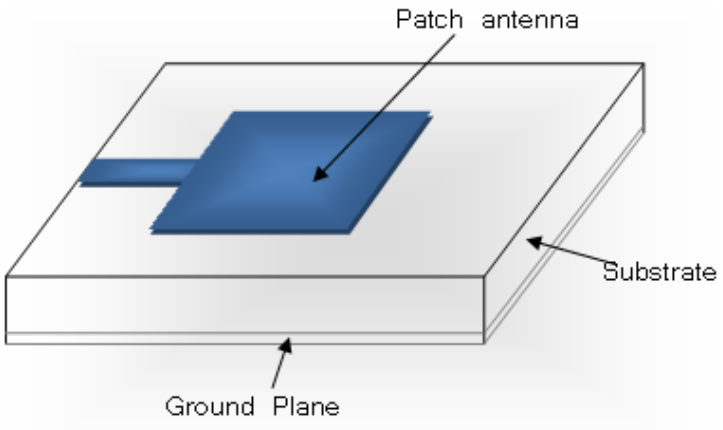

Figure 1-6: Patch Antenna

To meet different design requirements, the patch can take different forms of shapes [1] such as rectangular, circular, triangle and elliptical as shown in Figure 1-7.

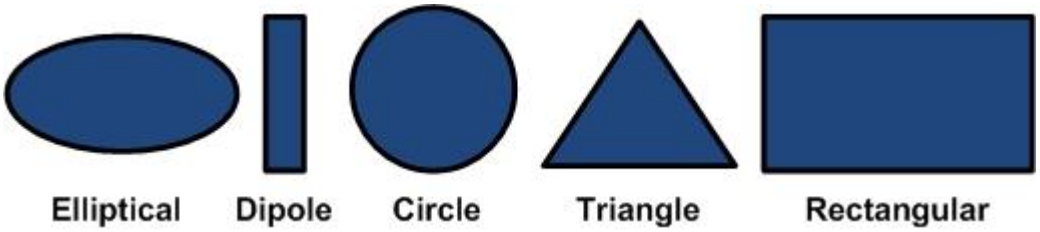

Figure 1-7: Different Configuration of Microstip antennas

The advantages of patch antennas are [1]:

- Low cost.
- Easy and simple to manufacture.
- Low profile.
- Can be confirmable if thin substrate is used.

The disadvantages of patch antennas are:

- Low efficiency.
- Narrow bandwidth.

Patch antenna can be fed using different feed configuration such as coaxial feed and microstrip line as shown in Figure 1-8 [5].

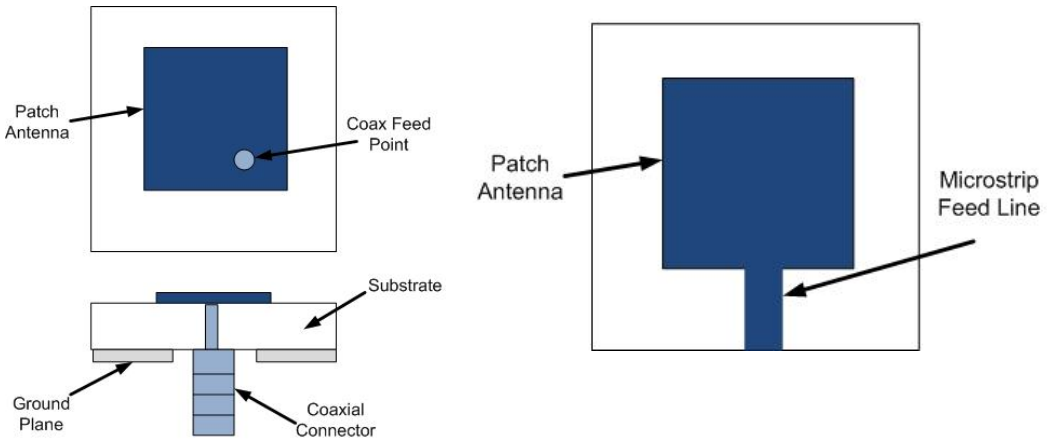

(a) (b)

Figure 1-8 Different feed the can be used in patch antennas

1.2.1.3 Planar Inverted-F Antenna (PIFA)

Planar Inverted-F Antenna (PIFA) is popular antenna for mobile phones since 1990s [7] due to low profile, light weight, easy integration and manufacturability. The PIFA typically consists of a rectangular planar element located above a ground plane, a short circuiting plate or pin, and a feeding mechanism for the planar element as shown in Figure 1-9.

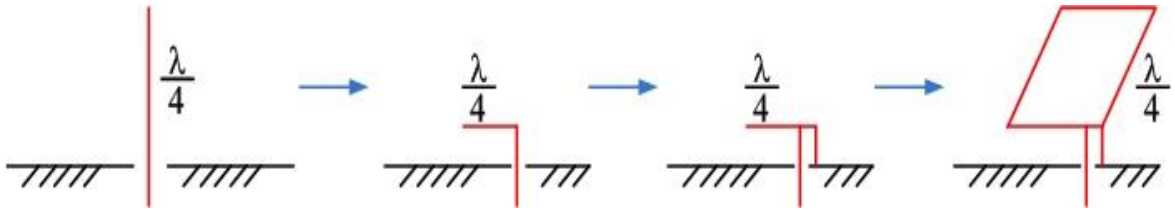

Figure: 1-9 Evolution of a PIFA from a monopole antenna

1.2.2 Main Parameters of an Antenna

There are several fundamental parameters that have major impact on the performance of an antenna such as [1]:

- S-parameters
- Impedance Bandwidth (B.W)
- Radiation pattern
- Directivity
- Efficiency
- Gain
- Polarisation

These parameters must be considered while designing any antenna. Some of these parameters are discussed in this section.

1.2.2.1 S-Parameters

In the Vector Network Analyzer (VNA), the data is normally presented in the form of S-parameters and they are defined by measuring the voltage travelling waves between the N-

ports shown in Figure 1-10. S-parameters describe the response of an N-port network to voltage signals at each port [8, 9].

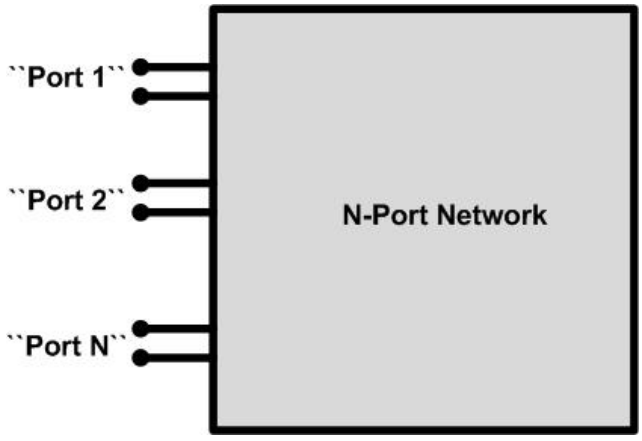

Figure 1-10 An N-Port Network

The responding port is the first number in the subscript and the incident port is the second number. Thus S_{12} means the response at port 1 due to a signal at port 2 and S_{21} means the response at port 2 due to a signal at port 1. In microwave engineering, the most common "N-port" are single ports and dual ports or three ports network [10].

To discuss this in more detail, dual ports are used as an example as shown in Figure 1-11.

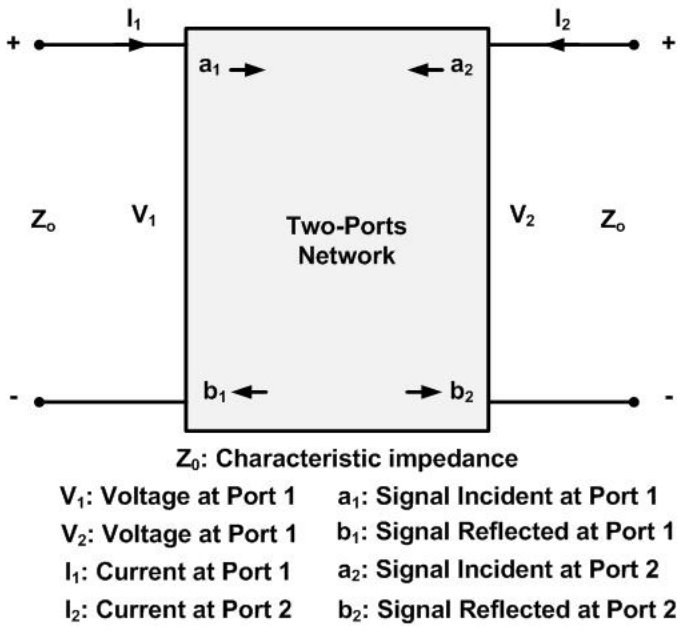

Figure 1-11 Two-Ports Network

S-Parameters for such a network are defined as:

$$\begin{pmatrix} b_1 \\ b_2 \end{pmatrix} = \begin{pmatrix} S_{11} & S_{12} \\ S_{21} & S_{22} \end{pmatrix} \times \begin{pmatrix} a_1 \\ a_2 \end{pmatrix} \quad (1\text{-}1)$$

If we assume that each port is terminated in impedance Z_0, we can define the four S-parameters of the 2-port as:

$$S_{11} = \frac{b_1}{a_1} \Big| a_2 = 0 \quad (1\text{-}2)$$

$$S_{21} = \frac{b_2}{a_1} \Big| a_2 = 0 \quad (1\text{-}3)$$

$$S_{12} = \frac{b_1}{a_2} \Big| a_1 = 0 \quad (1\text{-}4)$$

$$S_{22} = \frac{b_2}{a_2} \Big| a_1 = 0 \quad (1\text{-}5)$$

In this case, if S_{11} is to be measured the port one would be used to inject the signal so the reflected signal will measured. a_2 will be equal to 0 as there is no signal injected in port 2.

1.2.2.2 Impedance Bandwidth (BW)

Impedance bandwidth is used to describe the bandwidth over which the antenna has acceptable losses due to mismatch. From Figure 1-12, the bandwidth of broadband antenna can be calculated using the equation (1-6).

$$B.W = \frac{f_2 - f_1}{f_0} \times 100\% \quad (1\text{-}6)$$

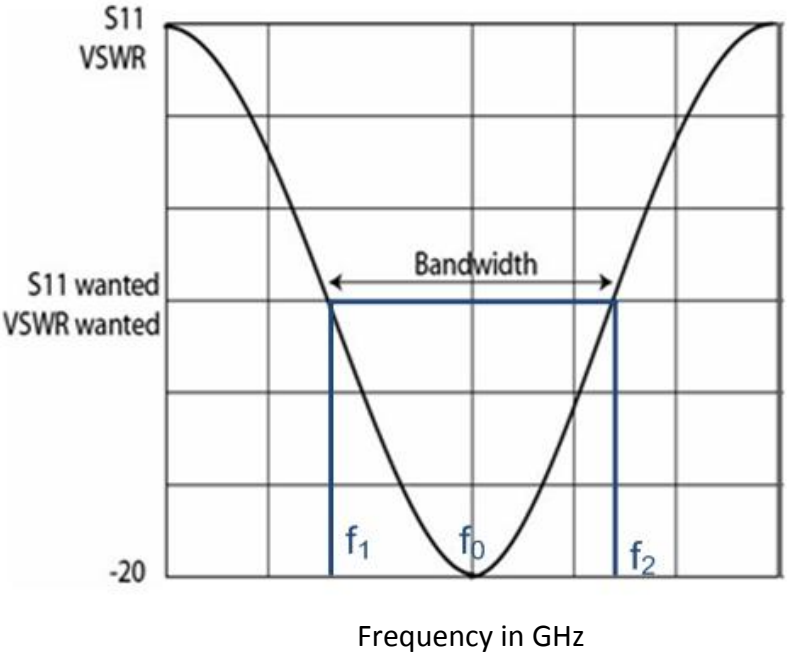

Figure 1-12: Bandwidth measuring

Where f_0 is the centre frequency,

f_1 is the lower frequency

f_2 is the Higher frequency

1.2.2.3 Radiation Patterns

Antenna's radiation pattern is defined in the IEEE Standard Definitions of Terms for Antennas [1] as:

"*A mathematical function or a graphical representation of the radiation properties of the antenna as a function of space coordinates. In most cases, the radiation pattern is determined in the far-field region and is represented as a function of the directional coordinates. Radiation properties include power flux density, radiation intensity, field strength, directivity, phase or polarisation.*"

Radiation patterns have main lobe, side lobes and back lobe as shown in Figure 1-13.

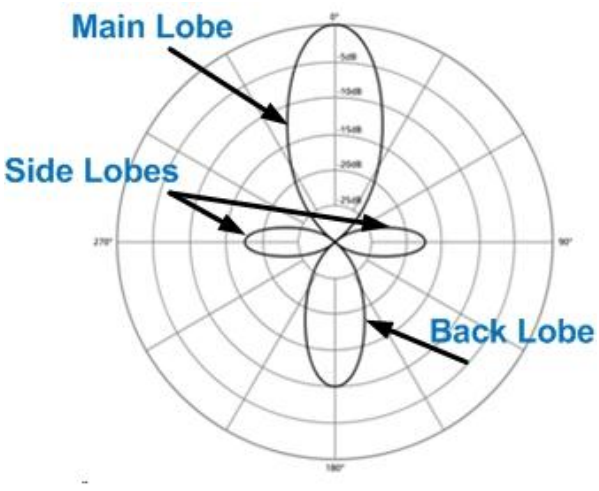

Figure 1-13: Radiation Lobes and beam width of an antenna Pattern

Radiation patterns can be omnidirectional as shown in Figure 1-14(a) or directional as shown in Figure 1-14(b). Omnidirectional antennas tend to have low gain because the power radiates in all directions [11] where directional antennas have high gain as the power is directed toward one direction [12]. Omnidirectional radiation patterns are suitable for many applications including mobile phone applications whereas directional antennas are suitable for wireless applications such as point to point applications.

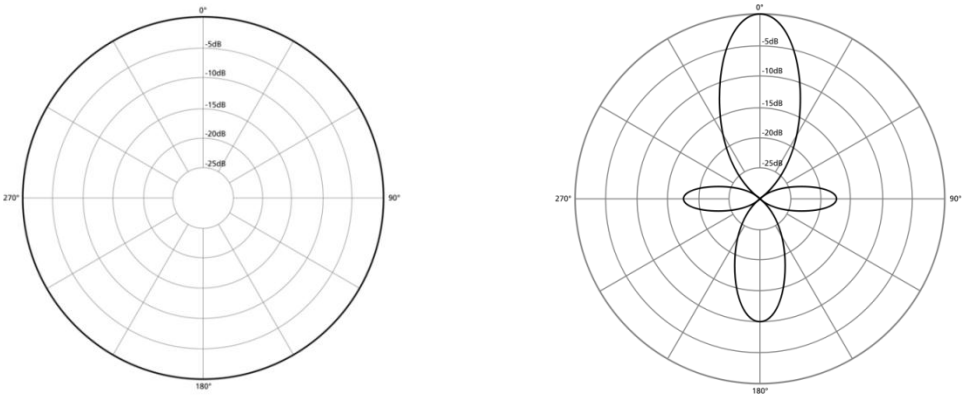

(a) (b)

Figure 1-14 (a) Omnidirectional radiation pattern and (d) Directional radiation pattern

1.2.2.4 Directivity

Directivity of an antenna is “the ratio of the radiation intensity in a given direction from the antenna to the radiation intensity averaged over all directions” [1]. It is a measure of how

'directional' an antenna's radiation pattern can be. If an antenna radiates in all directions i.e. oimnidirectional patterns, the directivity of this type of antenna would be 1 or 0 dB whereas directional antenna would have a high directivity as shown in Figure 1-15 [13].

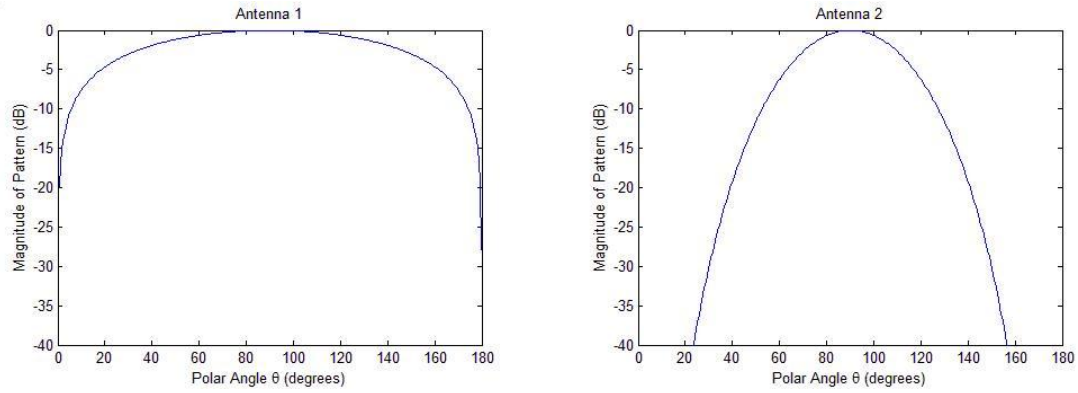

(a) **(b)**

Figure 1-15 Radiation Patterns for Antennas that have (a) low directivity and (b) high directivity

1.2.2.5 Gain

For a given antenna, it is defined as the ratio of power radiated or received by particular antenna in a given direction, to the power radiated or received by an isotropic antenna both fed by the same power and it is measured in dBi.

Gain of any antenna is closely related to the directivity of the antenna. Therefore, in order to find the gain of any antenna, the directivity should be found. Equation (1-7) can be used to determine gain.

$$Gain = \eta \, . \, D \tag{1-7}$$

Where η is the efficiency

D: is the directivity

1.2.2.6 Radiation Efficiency

The efficiency of an antenna relates the power delivered to the antenna and the power radiated or dissipated within the antenna. A high efficiency antenna has most of the power

present at the antenna's input radiated away. A low efficiency antenna has most of the power absorbed as losses within the antenna, or reflected away due to impedance mismatch.

1.2.3 Antenna Field Region

The electromagnetic field distribution of a radiated antenna changes as the radiation moves away from the antenna. These changes are classified into three different groups as shown in Figure 1-16 [1, 14].

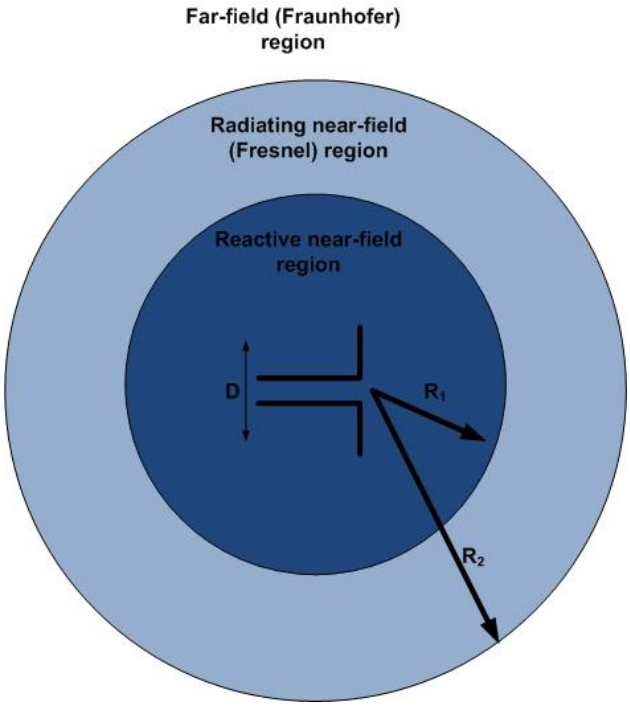

Figure 1-16 Field regions of an antenna

1.2.3.1 Reactive Near-Field Region

From Figure 1-16, the immediate field is considered to be the reactive near field region of the antenna. For the majority of antennas this region exists at $R_1 < 0.62\sqrt{D^3/\lambda}$ from the antenna.

R: Radius

D: Maximum antenna dimension.

1.2.3.2 Radiating Near-Field or Fresnel Region

The radiating near field or Fresnel region is the region between the near and far fields. The boundaries for this region are between $0.62\sqrt{D^3/\lambda} \le R_2 \le 2D^2/\lambda$. If the antenna is very small compared to wavelength this region may not exist.

1.2.3.3 Radiating Far-Field or Fraunhofer Region

In the radiating far-field or Fraunhofer region the field components are transverse to the radial direction from the antenna and all the power flow is directed outwards in a radial fashion. In this region the shape of the field pattern is independent of the distance, R, from the antenna. The inner boundary is taken to be the distance $R_1 > 2D^2/\lambda$, where D is the largest dimension of the antenna.

1.3 Motivation

The advent of wireless communication and mobile phone devices has revolutionized our life styles. Through the evolutionary process of development, a numerous of antennas have been developed for these applications. The requirements of new small and multiband antennas are becoming even more challenging with time. To cope up with such challenging demands, a constant and even thorough research is required for developing new antennas capable of operating in multiple bands with small size.

In this thesis, novel antennas are designed and developed to be used in fixed and reconfigurable terminals for wireless, mobile phone and cognitive radio applications to enhance the system capability. These novel antennas offer smaller size, slim and independently controlled bands, in addition to the added functionality in the performance of wireless systems.

Throughout the discussion, the designs are verified with experimental implementation.

1.4 Scope of the Thesis

The aims of the research presented in this thesis are mainly two folds: i) Design small and slim fixed multiple bands antennas for mobile and wireless applications. The aim here is to make mobile phone smaller and slimmer with reduce user's hand effect on the antenna's performances and to generate multiple bands from a single band antenna to reduce the size of wireless devices. Moreover, adding the independent control feature to allow the

antenna to be designed to other applications easily. ii) Design of compact and slim reconfigurable multifunctional antennas for mobile, wireless and cognitive radio applications. The aim here is to propose a switchable method to switch between wideband and multi-narrow bands to be used for cognitive radio applications. Moreover, proposed a new method through a switchable antenna that introduces multiple bands without the need to incorporate any additional parts and by only using a single varactor diode. Finally, introduce a tunable reconfigurable antennas with independently and simultaneously controlled multiple bands over a wide range to enhance the antenna capability in serving other standard.

The research primarily focuses on achieving the following objectives:

1. In the fixed designs, using slots technique with different shape which can reduce the size of the antennas as well as allowing the antenna to generate multiple bands. The shape of the radiators or the slots must be simple and easy to optimise. To achieve independent control, the current distribution is an essential way to identify the key parameter for each band. To achieve insensitive antenna to user's hand and to the housing of mobile phones, the ground plane should not radiate and it should be less sensitive. Therefore, the bands should be obtained mainly from the main radiator not from the ground plane. Again, the current distribution on the structure must be mentor while designing and optimising the antenna.

2. In the reconfigurable designs, studying the best location to place the switches in order to achieve a wide tuning range and independent bands over wide range. Slot must be used in order to disturb the current path on the antenna and to allow the antenna to generate multiple band operations. Varactor diodes should be used to achieve fine tuning or PIN diode should be used to switch between the operating frequencies.

1.5 Contribution to Knowledge*

The key contributions of this thesis are summarized as follows:

1- Employment of U-slots technique to generate multiband operations and to minimise the size of the antenna [R6, R29, and R31]

2- Proposed novel compact multiband antennas with the capability to operate over five-band for fixed and reconfigurable systems. The designs were specifically constructed to allow the operating frequencies to be controlled independently over a wide range. In the fixed design, the five-band can be optimised independently [R4, R14 and R2]. In the reconfigurable design, the independent control is performed electrically using varactor diodes [R4, R12].

3- Extended the capabilities of Planar Inverted-F Antenna (PIFA) to operate as ultra-slim tri-band handsets antenna [R1, R9 and R10] with switching and tuning functions [R5 and R10].

4- Introduced a technique to switch between wideband and multi-narrow band operations for cognitive radio applications [R3, R19 and R8].

5- Introduced a multiband selection method with a single varactor diode to select and operate as a single, dual and three bands [R2 and R13]. Moreover, the antenna has some fine tuning capabilities toward the lower frequencies [R2].

1.6 Organisation of the Thesis

This thesis consists of six chapters. The chapters are inter-dependent and the reader should follow the right order to better understand the contributions presented in the thesis.

After the introductory and the basic theory of antennas and the fundamental parameters in chapter-1, chapter-2 gives a brief overview and some previous work in the area of fixed and reconfigurable multiband antennas. General information about PIN and varactor diodes is provided. This is followed by an introduction to modelling techniques used in different simulations software and then giving a brief introduction to the chosen simulation software that was used to design and predict the performance of the antennas.

Chapter-3 presents three different techniques to design fixed multiple-band antennas for wireless and mobile applications. The effect of user's hand, mobile phone housing and the size of the ground plane are discussed in this chapter. Finally, the independent control concept on fixed antennas is presented in this chapter.

Chapter-4 presents two antennas using switchable techniques. The first antenna is to be

---

* References are relative to the numbered list in page XV (Author's Publications)

used in cognitive radio applications where the antenna can be switchable between wideband and multiband operations. The second antenna introduces a new technique to select the number of bands (single, dual or tri bands) with some fine tuning capabilities.

Chapter-5, wide tunable antennas using varactor diodes are introduced to cover the major wireless and mobile services and standards. Then, the concept of independent tuning on reconfigurable antenna is introduced in this chapter.

Finally, Chapter-6 concludes the research findings of the thesis and presents the future work to be carried out in connection with the research presented in this thesis.

1.7 References

[1] Constantine A. Balanis: “Antenna theory, analysis and design” Third edition, John Wiley & Sons, Inc. ISBN 0-471-60639-1.

[2] Yi Huang, and Kevin Boyle, "Antennas: From Theory to Practice", John Wiley & Sons, ISBN: 978-0-470-510'''t28-5, 2008.

[3] F.R. Terman,” Electronic Radio and Engineering”. MacGraw-Hill.

[4] J. D. Kraus, ”The Helical *Antennas*”, Antennas, Chapter 7. McGraw-Hill: New York, 1950.

[5] J. Volakis, "Antenna Engineering Handbook," McGraw Hill, 2007. Ch. 13.

[6] J. R. James, P. S. Hall, and C. Wood, Microstrip Antenna Theory and Design, INSPEC/IEE (London and New York : Peter Peregrinus on behalf of the IEE, 1980.

[7] J. Volakis, "Antenna Engineering Handbook," McGraw Hill, 2007. Ch. 36.

[8] D. Budmir, "Advanced CAD of RF, Microwave and Millimetre-wave Circuits for Modern Digital Communication Systems", Master degree course, Westminster University, 2007.

[9] David M. Pozar, “Microwave Engineering”, Third Edition (Intl. Ed.); John Wiley & Sons, 2005, pp 170-174. ISBN 0-471-44878-8.

[10] J Choma & WK Chen. “Feedback networks: theory and circuit applications”. Singapore: World Scientific. Chapter 3, p. 225 ff, 2007. ISBN 981-02-2770-1.

[11] G. Augustin, P.Bybi, V.Sarin, P. Mohanan, C. Aanandan and K. Vasudevan, "A Compact Dual-Band Planar Antenna for DCS-1900/PCS/PHS,WCDMA/IMT-2000, and WLAN Applications", IEEE Antennas and Wireless Propagation Letters, vol.7, pp.108-111, 2008.

[12] H. Wang, X. B. Huang and D. G. Fang, "A Single Layer Wideband U-Slot Microstrip Patch Antenna Array", IEEE Antennas and Wireless Propagation Letters, vol.7, pp. 9-12, 2008.

[13] http://www.antenna-theory.com/

[14] J. S. Seybold, Introduction to RF Propagation: John Wiley & Sons, Inc., 2005.

Chapter 2

Fixed and Reconfigurable Antenna

2.1 Introduction

The research presented in this thesis deals with different types of antenna for different wireless communications bands such as the Global System for Mobile Communications (GSM900 and 800), Personal Communication System (PCS 1800 and 1900), Digital Communication Systems (DCS), Global Positioning System (GPS), Universal Mobile Telecommunications System (UMTS), Wireless Local Area Networks (WLAN) and Worldwide Interoperability for Microwave Access (WiMAX) etc...

Some of these applications requires fixed antenna where the antenna is designed and optimized to operate at particular frequencies and some requires adaptive antenna (reconfigurable) where the antenna's operating frequencies can change to other bands by using reconfigurable elements (multifunctional antenna). Different techniques have been used in the past to reduce the size of the antenna or to allow the antenna to operate in multiple band operations or to generate a wide bandwidth. Slots are usually employed in antenna's structure and it has been widely used to achieve these techniques.

This chapter gives a brief overview of the latest techniques used to achieve multiple bands on fixed antennas and to achieve a wide tunability range in reconfigurable antennas. Then the types of reconfigurability are discussed. To change the performances of the antenna electrically, switches such as varactor and PIN have been used in order to tune/switch the operating frequencies or control the position of the radiation patterns or change the polarization of the antenna. This is introduced in brief in this chapter. Finally, modelling techniques and High Frequency simulation software (HFSS) software are discussed.

2.2 Fixed multiband antennas

Antennas for mobile and wireless terminals supporting several standards simultaneously are currently receiving a lot of interest. Therefore, there is an increasing demand for multiband antennas which can be easily integrated in a wireless device supporting multiple standards.

The term fixed means that the operating frequencies, radiation patterns and polarization are fixed upon the designer goal and once the antenna is fabricated and placed in the system, the performances of the antenna cannot be changed.

Printed antennas, monopole antennas and Planar Inverted-F Antennas (PIFA) are the most suitable antennas to be used in wireless systems thanks to their low profile, low fabrication cost, and simple feeding structures.

Printed antenna is characterized by the length and width of the radiator shape, the height of the substrate above the ground plane and the dielectric constant of the substrate material.

Printed antennas usually consist of radiated elements and a dielectric substrate material, such as FR-4 and Duriod, on one side and a ground plane on the other.

Different techniques have been used in printed antennas to achieve wideband or multiband operation. Some of these techniques are pointed here.

- Modifying the radiators shape: the radiators can take different shapes, as shown in Figure 1-7, and hence multiple-band can be obtained.
- Slotted radiators: the slot can disturb the current path on the radiators and hence change the performance of the antenna. Slots technique is employed in the design of many antennas and it became the most commonly used technique when multiple band operation is the aim [1] – [5].
- Using foam layer between the radiator and the substrate can generate multiband and wideband performance [6]
- Shorting wall: the shorting wall allow the current to travel longer distance where the bandwidth can be increased and the antenna size can be minimised. [7] - [8].
- Shorting pins: shorting pins can improve the bandwidth of the antenna by few more percentages [9].

- Stack multi-layers and fractal shape [10]. The fractal shape also can be used in the ground plane to generate multiple band operations [11] as shown in Figure 2-1 (a)-(c)

The above techniques may result in larger dimensions and thickness of the physical antenna, which sometimes make it difficult to fit into small and slim devices.

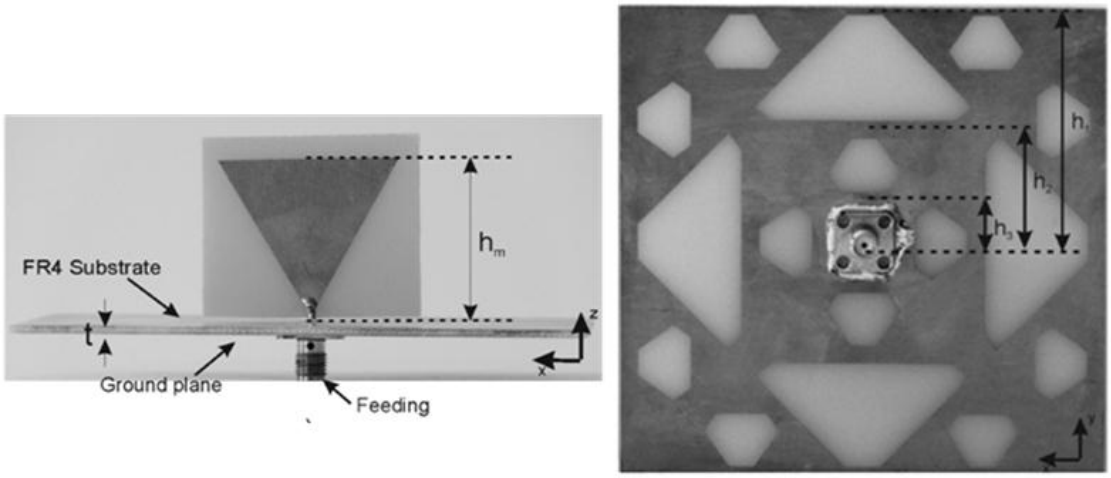

(a) **(b)**

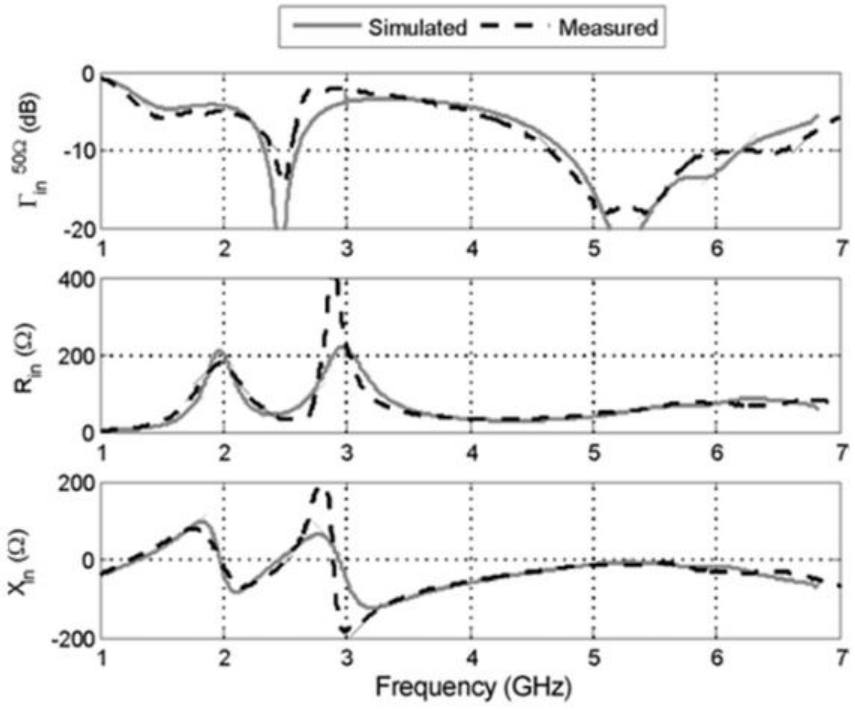

(c)

Figure 2-1 (a) Multiband Antenna and (b) Fractal-based ground plane (c) S_{11} [11]

Planar Inverted-F Antennas are widely used in a variety of communication systems especially in mobile phone handsets due to low profile, light weight, easy integration and

manufacturability [12-14]. The first portable mobile terminal shown in Figure 2-2 (a) was produced by Motorola in 1983 [15]. It is clear that this antenna is bulky and heavy compared to the recent mobile phone shown in Figure 2-2 (b) produced by Nokia [16].

(a) **(b)**

Figure 2-2: (a) Early single band mobile phone 1980 (b) Latest multiband mobile phone from Nokia in 2009

In PIFA, different techniques have been used to generate wideband or multiple band operations. Some of these techniques are:

- Truncated corner technique [17]
- Meandered strips [18]
- Meandered shapes [19-20]
- Branch line slit [21]
- Slot in the ground [22]
- Optimising the height of radiators[23]

The PIFA offers high radiation efficiency and wide bandwidth, 10%, for mobile applications in a compact structure.

The size and the shape of the radiators, the height of the plate above the ground plane, the size, shape and position of the shorting plate or shorting pin, and the feed point location along the substrate all have considerable impact on the impedance matching, bandwidth, frequency bands, efficiency and gain of the antenna. Normally the size of the radiator can be calculated by using equation 2-1.

$$\lambda = 4 (L + W) \tag{2-1}$$

Where L and W are the length and width of the radiator respectively.

2.2.1 Independent Control on Fixed Terminals

To design an antenna with multiple bands operation, it is desirable to have an independent frequency control on two or more separate frequencies. Achieving this option is very challenging. Very often, when one parameter is changed, all the other frequencies are affected [24]-[25] as shown in Figure 2-3 and Figure 2-4. Therefore, independent control can be a difficult task and sometimes the whole structure has to be altered when other bands are required.

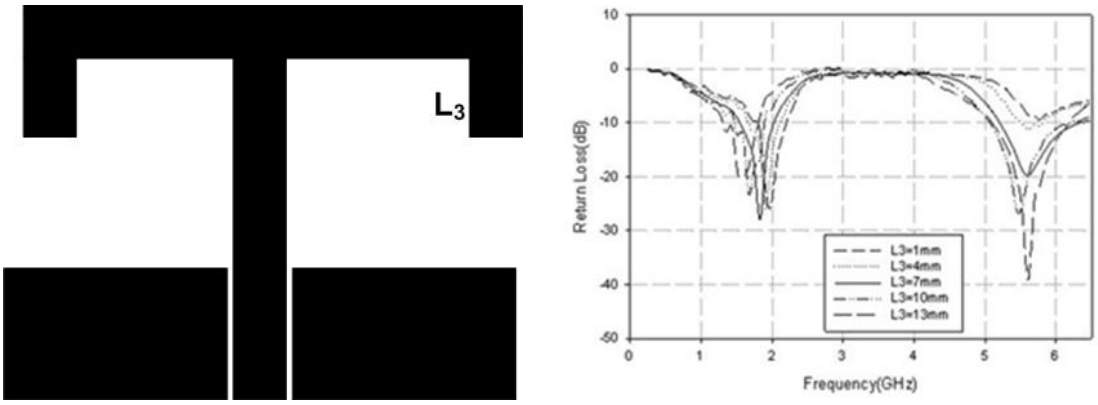

(a) (b)

Figure 2-3: Changing one parameter (L_3) of the T-Shaped Antenna [24]

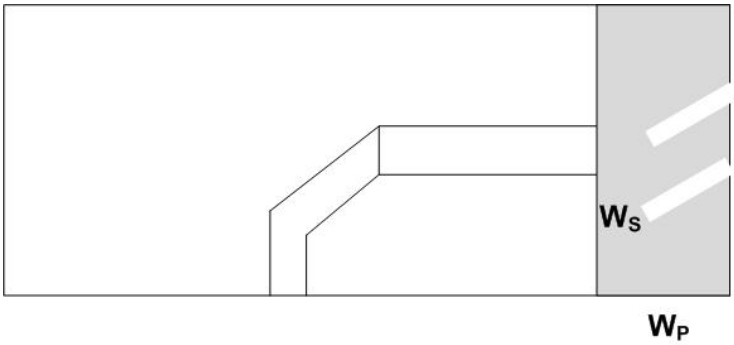

(a)

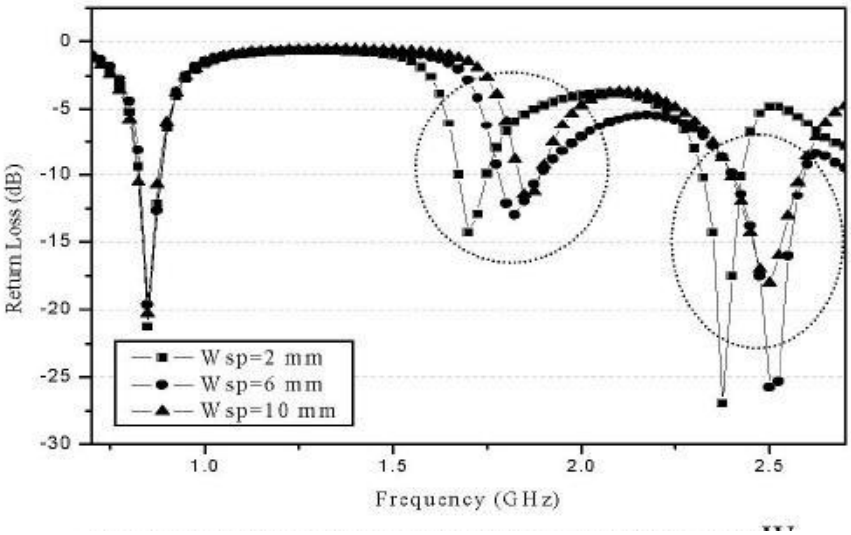

(b)

Figure 2-4: Effect of changing some parameters (Ws&p) of the PIFA [25]

Some work has been done to achieve frequency independent control for a small-size and thin antenna. For example in [26], a Planer Inverted-F Antenna (PIFA) was thoroughly studied to control three resonant frequencies for GSM/DCS/DMB with an overall size of 105 x 30 x 9 mm^3. In [27], a switchable design for dual bands at (1.9 GHz, 5.2 GHz) and (1.9 GHz, 3.5 GHz) was presented with some tuning capability for a reconfigurable system. In [27], the dual-band can be controlled independently. Moreover, in the patent reported in [28], a multi-frequency band antenna, capable of tuning the low-band portion to a low frequency band and the first high-band portion to a first high frequency band, was introduced for use in mobile handsets applications which of a larger size.

Most of the reported antennas offering this feature either has large ground plane, high profile or the control range is not wide enough to cover the major services and standard.

2.2.2 Effect of Mobile Phone Housing and User's Hand on Antenna's Performances

An antenna is designed in the real operating environment with the handset. Handsets must have a housing, which is made usually of plastic as shown in Figure 2-6 [29]. This plastic, or any other type of material, might sometimes affect the impedance matching, gain and efficiency of the antenna [30]. Therefore, the effect of the mobile phone housing should be considered before placing the antenna in mobile phones [31].

Many designed PIFA for mobile phone handsets have not taken into account the effect of user's hand and the housing of mobile phone [33] – [35].

Figure 2-6: Housing of a mobile phone [29]

Not only the plastic but also user's hands or user's interactions which can have a huge impact on the impedance matching, gain and efficiency of the antenna [36] as shown in Figure 2-7(a)-(c). Therefore, antennas should be designed to have minimum effect when user's hold the phone in different positions as discussed in [37].

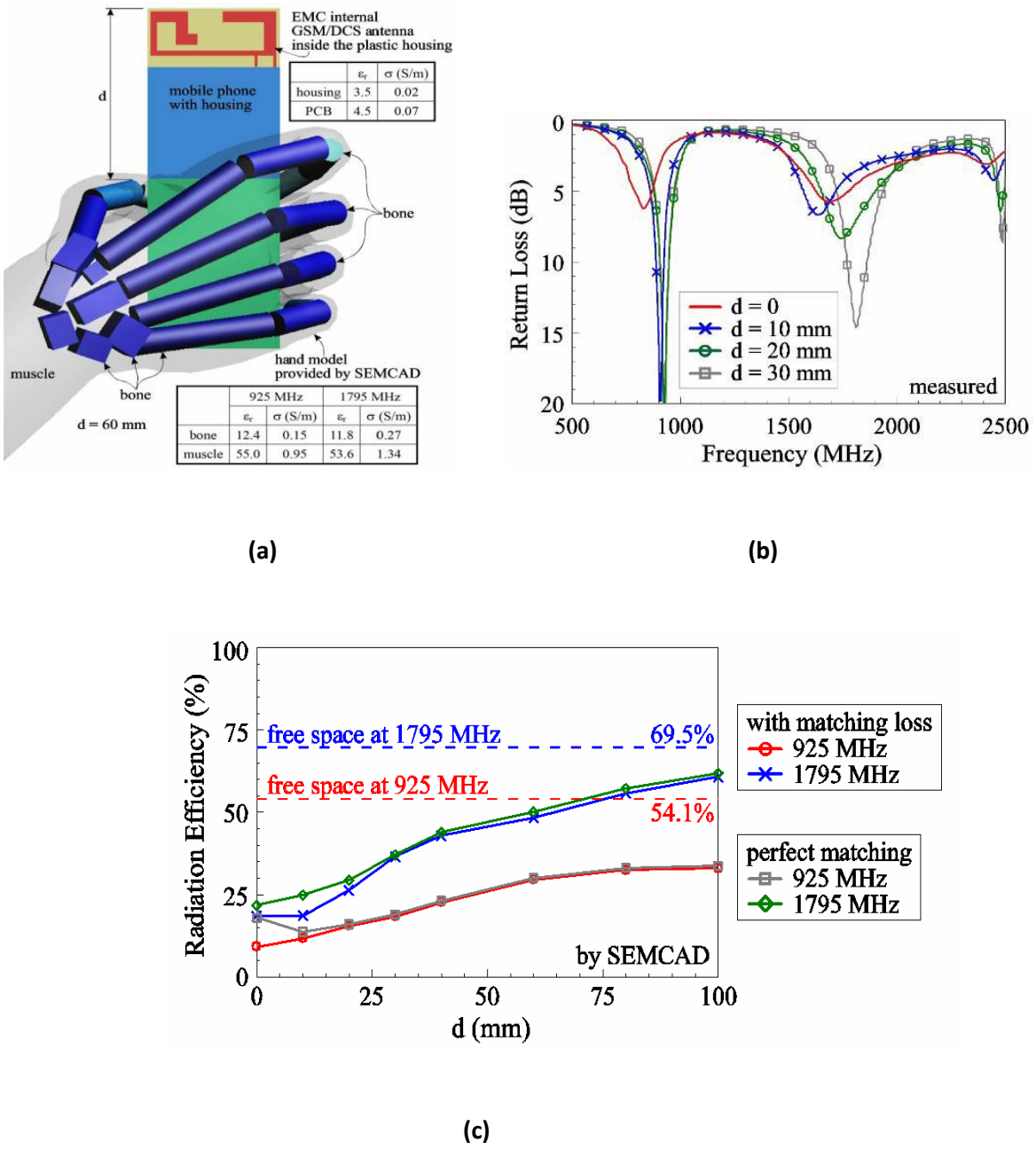

	ε_r	σ (S/m)
housing	3.5	0.02
PCB	4.5	0.07

	925 MHz		1795 MHz	
	ε_r	σ (S/m)	ε_r	σ (S/m)
bone	12.4	0.15	11.8	0.27
muscle	55.0	0.95	53.6	1.34

(a) **(b)**

(c)

Figure 2-7: Effect of user's hand on mobile phone antenna [36]

2.3 Reconfigurable Antennas

Although fixed multiband antennas can widely be used in many different systems or devices, they lack the flexibility to accommodate new services compared with reconfigurable antennas [38]. A reconfigurable antenna can be considered as one of the key elements in future wireless communication transceivers. The advantage of using a reconfigurable antenna is the ability to operate in multiple bands where the total antenna

volume can be reused thus enabling the overall size to be reduced. Modern wireless communication systems relying on multiband reconfigurable antennas are becoming more popular for their ability to serve multiple standards. Devices using a single compact antenna allow reduction in the dimensions of the device and more space to integrate other electronic components. Different reconfigurable antenna techniques have been proposed in [38].

2.3.1 Types of Reconfigurable Antennas

Reconfigurable antennas can be classified into three different categories, namely,

- Frequency reconfigurable
    - Continuous (Tunable Antenna)
    - Coarse (Switchable Antenna)
- Radiation pattern reconfigurable
- Polarization reconfigurable

2.3.1.1 Frequency Reconfigurable:

The first category is based on frequency reconfigurability. The aim is to tune/switch the operating frequency of the antenna and to have a single multifunctional antenna in a small terminal for many applications [38]-[39]. The shape of the radiation patterns of these reported antennas remain unchanged when the frequencies are tuned/switched from one band to the other.

Frequency reconfigurable antennas are classified into two categories:

Continuous tuning: This can be achieved by using varactor diodes where the antenna allows for smooth transitions within or between operating bands without hops as in [40]

Coarse tuning: This can be achieved by using PIN diode switches. Coarse tuning employs different switching mechanisms to operate at multiple bands. Examples include a widely tunable antenna using PIN switches [39], switching different feeding location to reconfigure the operating frequencies [41] and reconfigurable patch antenna [42] for satellite and terrestrial applications.

2.3.1.2 Radiation Pattern Reconfigurability

The second category is based on pattern reconfigurability, where the frequency band remains unchanged while the radiation pattern changes based on system requirements. The antenna can steer its radiation pattern main beam in different directions. This type of pattern reconfigurability has been reported recently in [43] by using a CPW fed antenna. In [44], a reconfigurable antenna combining both frequency and radiation pattern reconfigurability was introduced.

2.3.1.3 Polarization Reconfigurability

The third category is based on polarization reconfigurability, where the polarization is switched from linear to circular [45] and from left hand (LHCP) to right hand (RHCP) circular as reported in [46]. A novel reconfigurable patch antenna with both frequency and polarization diversity was also reported in [47].

2.3.2 Independent Control on Reconfigurable Terminals

Independent tuning in reconfigurable antennas has received much attention recently. The technique is to fix one band at a particular frequency and tunes the other band to other frequencies. This can be done by fixing the voltage at the first varactor diode and vary the voltage on the other varactor diode. This is not an easy task as the radiators have to be designed carefully in order to allow the one band to be controlled without affecting the other. The location of the switch has to be optimised and placed in the highest current density location. A number of techniques have been proposed to achieve independent control (electrically) for one or more bands over a wide range. For example in [48], a reconfigurable slot antenna with dual-band operations has been proposed with a wide tuning range (2020 MHz) as shown in Figure 2-8 and Figure 2-9(a)-(b). The total size of this antenna is 150 x 110 mm^2.

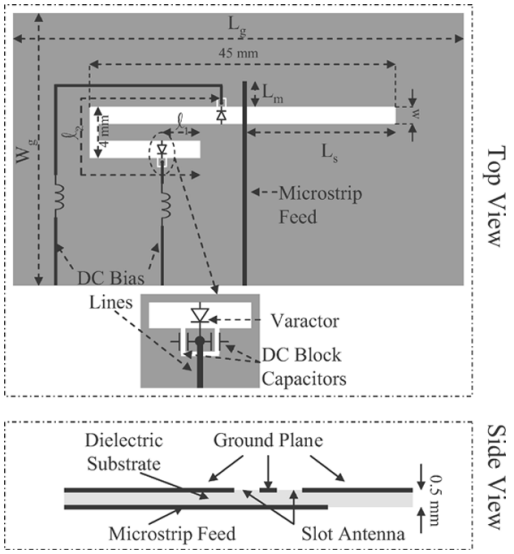

Figure 2-8: Multiband Slot Antenna [48]

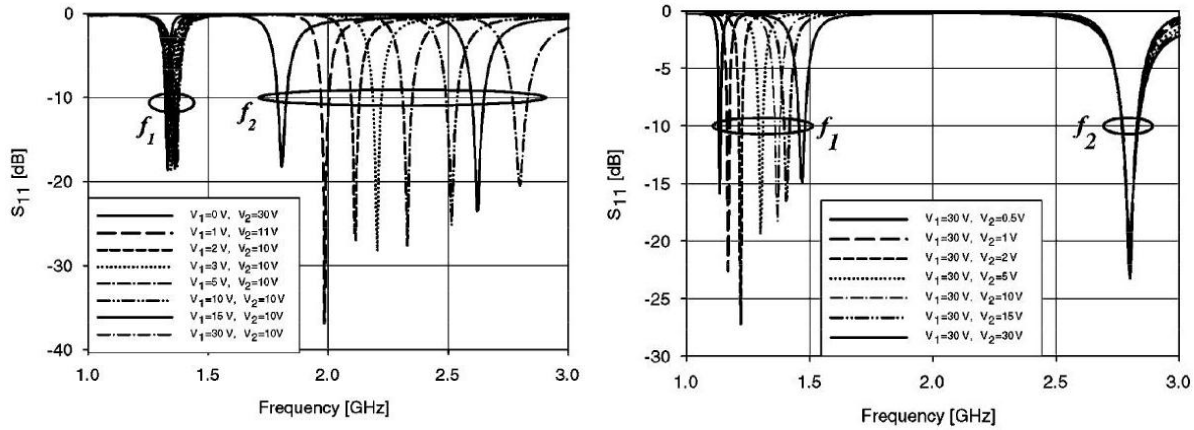

(a) **(b)**

Figure 2-9: input reflection coefficients of the dual-band tunable antenna [48].

2.4 Switching Technology

2.4.1 PIN Diode Switches

PIN diode is a semiconductor device that operates as a variable resistor at RF and Microwave frequencies. It can also be used as a switch and Limiter. PIN diodes are popular in microwave circuit applications due to its fast switching times and relatively high current handling capabilities [49]. The construction of a PIN diode is showing in Figure 2-10.

Figure 2-5: PIN diode

The P and N types are separated by an intrinsic region, the P contact is the anode, and the N contact is the cathode as shown in Figure 2-11 where the anode is the side with the arrow, the cathode is the side with the plate. Between the P and N region is the intrinsic where the width of this region has an important role on the performance of the PIN diode [49].

Figure 2-6: Circuit symbol for PIN diode

Figure 2-12 shows a simple equivalent circuit of a switch that can be ON or OFF. In the ON state, the switch can be represented as a resistor and a series capacitor in the OFF state.

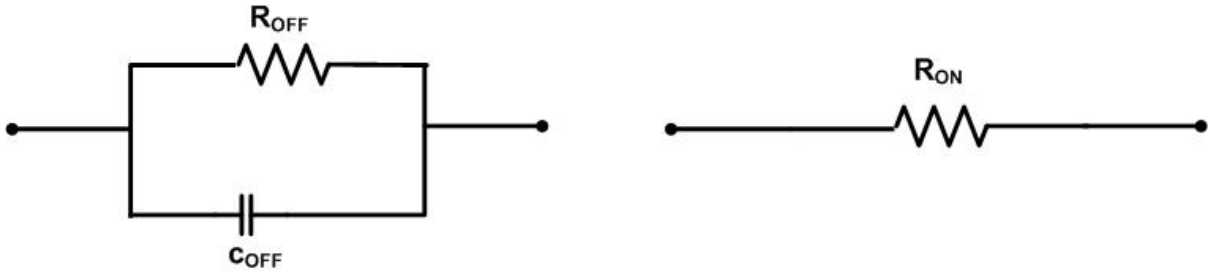

Figure 2-7: Simple switch equivalent circuit (a) ON state (b) OFF state

PIN diode has been widely used to prove the concept of many switchable antennas as shown in Figure 2-13 (a)-(c) as an example.

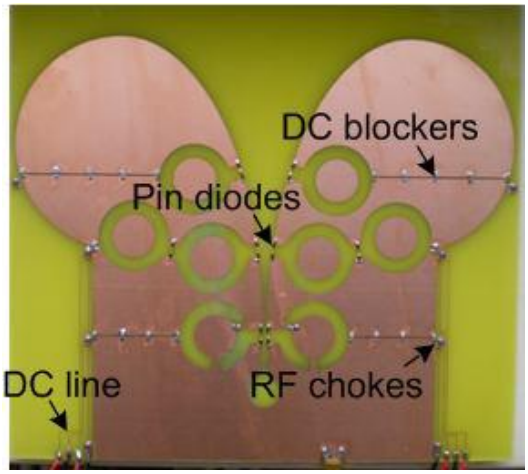

Figure 2-8: Prototype of switchable Vivaldi antenna using PIN diodes [50]

2.4.2 Varactor Diode Switches

Varactor diode also called varicaps is a semiconductor diode with a small junction capacitance that varies it values depending on the bias voltage applied to the diode. They are an important component of radio frequency or RF applications. Varactor diodes are widely used in communication applications when tuning is needed. The circuit symbol for a varactor diode is shown in Figure 2-14.

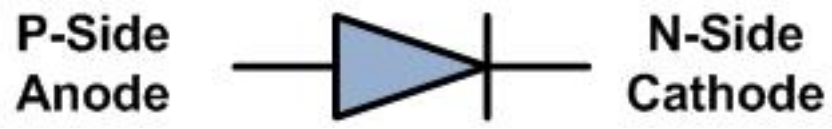

Figure 2-9 Circuit symbol for a varactor diode / varicap diode

The capacitance of a varactor decreases when the voltage gets larger. A tuning varactor can be represented by the following electrical equivalent circuit (Figure 2-15) [30].

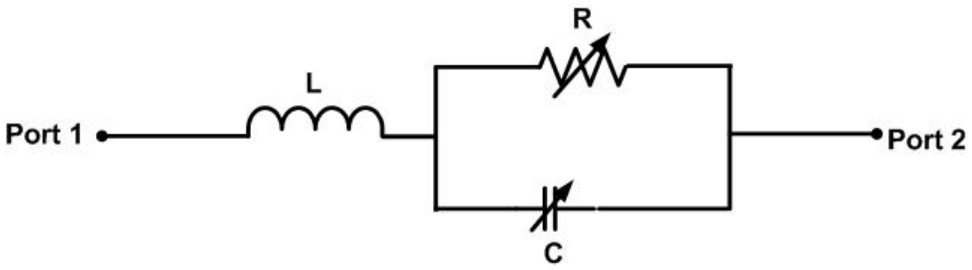

Figure 2-10: Equivalent circuit for a varactor

PIN diode has been also been widely used to achieve fine tuning and to prove the concept of many reconfigurable antennas as shown in Figure 2-16 (a)-(c) [51].

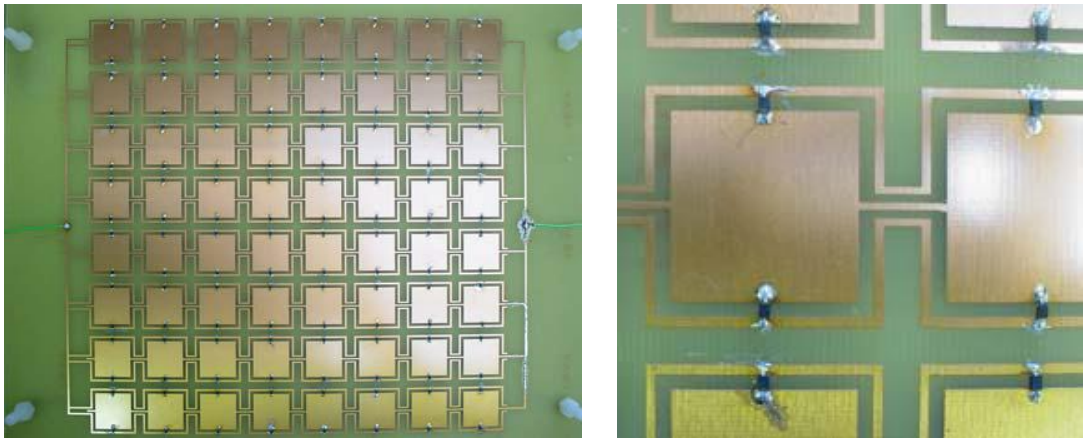

Figure 2-11: Illustration of Manufactured Multilayered EBG with varactor diodes [51].

2.4.3 MEMS

MEMS switches are devices that use mechanical movement to achieve a short circuit or an open circuit in the RF transmission line. RF MEMS switches are the specific micromechanical switches that are designed to operate at RF-to-millimetre-wave frequencies.

In the last ten years, RF MEMS switches have been used for telecommunication applications due to many advantages compared to other switches such as small in size, good linearity and good isolation. However, they require high DC actuation voltages [30].

MEMS switch are used in different applications such as phase array phase shifter, switching, reconfigurable networks and low power oscillator [52]-[53]. Cross-section view

of a MEMS switch is shown in Figure 2-17 [54] and an example of practical MEMS on an antenna is shown in Figure 2-18 [54].

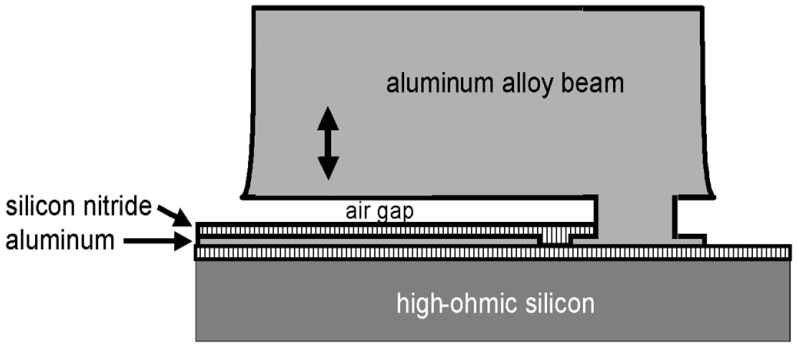

Figure 2-12: Cross-sectional view of a capacitive MEMS switch realized in the NXP [54]

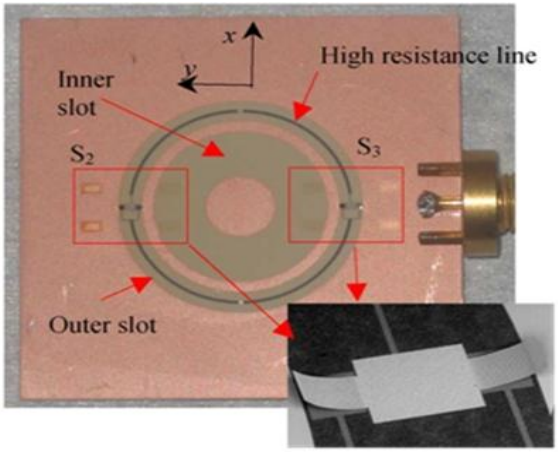

Figure 2-18 Photograph of the annular slot integrated with two double-arm MEMS actuators [55].

2.5 Modelling Techniques

Many methods have been developed over the past years for a wide range of applications in RF engineering. These methods or techniques can be divided into: i) Time Domain (TD) such as Finite Different Time Domain (FDTD) and ii) Frequency Domain (FD) such as Moment Of Methods (MOM) and Finite Element Method (FEM).

Many different commercial software have been developed using one of these methods, and it is therefore not necessary any longer to write a new code but just utilize any of them

to aid the modelling of the RF design. In this section, the foundation principles on which these methods are based are briefly introduced.

2.5.1 Moment of Method (MOM)

The Method of Moment (MoM) is a numerical method of solving electromagnetic problems or volume integral equation in the frequency domain. MoM can be used to solve problems in several areas of engineering and sciences including electromagnetic. In the 1960's Roger F. Harrington was the first to use MoM to solve electromagnetic problem. Numerical Electromagnetic Code (NEC) is the most well known of the codes using MoM to solve problems that can be defined as sets of one or more wires. Although, it is an adaptable and thoroughly simple method, it requires large amounts of computation. The Method of Moments is broadly used to solve electromagnetic scattering and radiation problems. This technique is based on reducing the operator equations to a system of linear equations that is written in matrix form. The MoM applied to wire antennas for instance, is used by the commercial software IE3D. Results accuracy is considered an advantage using this method as it uses essentially exact equations and provides a direct numerical solution of these equations. Another advantage is that, in practice, it is applicable to geometrically complex scatters [56]-[57].

2.5.2 Finite-Difference Time-Domain (FDTD)

The Finite Difference Time Domain is a method that is broadly used to stimulate several electromagnetic problems. The literature on (FDTD) is extensive and has been used for various microwave analysis such as, antenna designs, propagation, filter design, and many other microwave analysis. However, FDTD is not suitable for electrically huge system but is good for system involving pulses. This method did not gain considerable attention despite its usefulness to handle electromagnetic problems until the computing costs became low. FDTD method was first proposed by Yee in 1966 for a simple Cartesian co-ordinate system [58]. The FDTD algorithm iteratively calculates the field values in the problem space that is discretised into unit cells. Each unit cell is assigned with three orthogonal electric and three orthogonal magnetic fields as shown in Figure 2-19 [59].

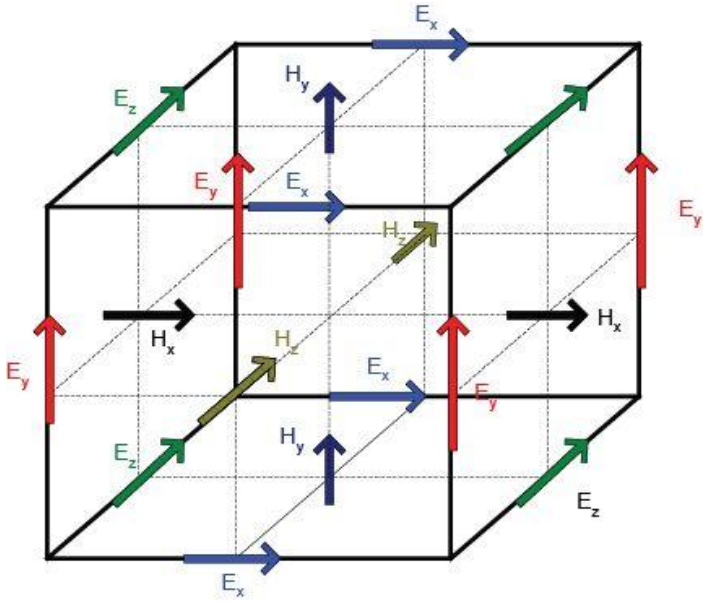

Figure 2-19: Yee cell [59]

2.5.3 Finite Element Method (FEM)

The finite element method (FEM) is a mathematical technique used for finding approximate solutions of partial differential equations (PDE) as well as of integral equations. The solution is based on reducing the differential equation completely, or rendering the PDE into an approximating system of common differential equations, which are then numerically integrated using Euler's method which is a standard technique such as the Runge-Kutta. FEM is a method used to solve frequency domain boundary valued electromagnetic problems using a variational form. There are generally two types of analysis that are used in FEM 2-D and 3-D canonical elements of differing shape. While 2-D conserves simplicity and allows itself to be run from a normal computer, it however, tends to give less accurate results. Three-dimensional canonical element, however, gives more accurate results by working effectively on faster computers. The FEM is often used in the frequency domain for computing the frequency field distribution in complex, closed regions such as cavities and waveguides [30, 56].

2.6 High Frequency Simulation Software (HFSS)

2.6.1 Introduction to HFSS

There are many different commercial software available to design antennas such as Zeland, CST, HFSS, M-Sonnet and Feko... etc. HFSS is an interactive simulation system whose basic mesh element is tetrahedron. The reason for choosing HFSS is that it uses FEM methods, which deals with very complex structures and it predicts accurate results. The HFSS software is used in the design of all the antennas in this thesis, partly due to the hands on experience gained using it for the RF designs.

The name HFSS stands for High Frequency Structure Simulator, which employs the Finite Element Method (FEM). It is a high-performance full-wave electromagnetic field simulator for 3D volumetric passive device modelling. It integrates simulation, visualization, solid modelling, and automation in an environment that facilitates learning and where solutions to 3D electromagnetic (EM) problems are quickly and precisely attained [60].

2.6.2 Modelling Diodes in HFSS

Since it is difficult to model diodes, surface mount ceramic chip capacitors, inductors and resistors in a full-wave solver, the diode was modelled with a RLC boundary sheet.

PIN diode: The PIN diode can be modelled using RLC sheet. When the PIN diode is in the ON state, it act as a resistance and if the PIN diode is in the OFF state, it act as a capacitance. In the simulation, different module can be created to check the results when switching the diode ON and OFF.

Varactor diode: Vatractor diode is a variable capacitance. Depending on the capacitance range of the practical diode, the diode can be simulated with these values.

2.7 Summary

In this chapter, literature review on fixed and reconfigurable antennas has been introduced. It has been noticed from the reported researches in the literature review that, the size of antennas are still needed to be slimmer as well as small to meet the demand for slim devices like the Ipad and Ipod devices. It has also been noticed that when designing an antenna for mobile phone, the effect of user's hand and mobile phone housing are usually neglected which is not the case in real world. Therefore, research is needed to design

antennas for handsets which can be less sensitive when user's hold the phone in different direction.

Types of reconfigurable antennas have also been discussed. Reconfigurable antennas are become very popular and many projects are aiming to achieve multifunctional antennas. Researches in this area are still needed to design and develop antennas capable of operating in all the major wireless services and standard. The number of switches and the size of the antenna are still the case in achieving good designs.

The concept of independent control in fixed and reconfigurable antennas was discussed. The wide control to cover as many bands as possible has not been achieved yet.

Switches component such as PIN, varactor and MEMS have been briefly introduced. Finally, modelling technique and HFSS software are introduced in brief.

2.8 References

[1] M Sanad, "Double C-Patch Antennas Having Different Aperture Shapes", IEEE Proceedings on Antennas and Propagation, pp.2116-2119, June 1995.

[2] H. F. AbuTarboush, R. Nilavalan, D. Budimir and H. S. Al-Raweshidy, "Double U-Slots Patch Antenna for Tri-Band Wireless Systems", John and Wiley International Journal of RF and Microwave Computer-Aided Engineering, Vol. 20, no. 3, pp. 279-285, May 2010.

[3] M. Ali, G. Hayes, H. Hwang and R. Sadler, "Design of a multiband internal antenna for third generation mobile phone handsets," IEEE Transactions on Antennas and Propagation, vol. 51, pp. 1452-1461, 2003.

[4] S. Chen, Y. Jiao, W. Wang and F. Zhang, "Modified T-shaped planar monopole antennas for multiband operation," IEEE Transactions on Microwave Theory and Techniques, vol. 54, pp. 3267-3270, 2006

[5] Sheta, "A novel H-shaped patch antenna," Microwave Optical Technology Letter P.62–65, 2001.

[6] H. Elsadek and D. Nashaat, "Multiband and UWB V-Shaped Antenna Configuration for Wireless Communications Applications," IEEE Antennas and Wireless Propagation Letters, vol. 7, pp. 89-91, 2008.

[7] C. L. Mak, R. Chair, K. F. Lee, K. M. Luk and A. A. Kishk, "Half U-slot patch antenna with shorting wall", Electronics Letters, vol. 39, pp. 1779-1780, 2003.

[8] X. Liu, "Bandwidth-expanded U-slot patch antenna with shorting wall," International Symposium on Signals Systems and Electronics (ISSSE), vol.1, pp.1-3, 17-20 Sept. 2010

[9] Y. Junho, R. Mittra, L. Yoonjae, S. Ganguly, "A novel modified Sierpinski patch antenna using shorting pins and switches for multiband applications," IEEE Antennas and Propagation Society International Symposium, vol.4, pp. 90- 93 vol.4, 2002.

[10] J. Anguera, C. Puente, C. Borja and J. Soler, "Dual-Frequency Broadband-Stacked Microstrip Antenna Using a Reactive Loading and a Fractal-Shaped Radiating Edge", IEEE Antennas and Wireless Propagation Letters, vol. 6, pp. 309-312, 2007.

[11] J. Gemio, J. Granados and J. Castany, "Dual-Band Antenna with Fractal-Based Ground Plane for WLAN Applications," IEEE Antennas and Wireless Propagation Letters, vol. 8, pp.748-751, 2009.

[12] Z. Ying, "Some important antenna innovations in the mobile terminal industry in the last decade, “First European Conference on Antennas and Propagation, pp.1-5, Nov. 2006.

[13] P. S. Hall, E.Lee, C. T. P. Song, "Planar Inverted-F Antennas", Chapter7, Printed Antennas for wireless Communications Edited by R. Waterhouse, John Wiley & Sons, Ltd, 2007.

[14] Thomas G. Moore, "multiband PIFA antenna for portable devices", Application number: 9/814,171 Publication number: US 2002/0135521 A1 Filing date: 21 Mar 2001.

[15] www.en.wikipedia.org/wiki/Motorola

[16] www.Nokia.co.uk

[17] C.-Y.-D Sim, "Dual and triple-band PIFA design for WLAN applications", Microwave and Optical Technology Letters, Volume 49, Issue 9, pages 2159–2162. 2007.

[18] P.W Chan, H. Wong, E. Yung, "Wideband planar inverted-F antenna with meandering shorting strip," Electronics Letters , vol.44, no.6, pp.395-396, March 13 2008.

[19] P.Chan, H.Wong, E.Yung, "Dual-band printed inverted-F antenna for DCS, 2.4GHz WLAN applications," Loughborough Antennas and Propagation Conference, pp.185-188, 2008

[20] W.P. Dou and Y.W.M.Chia, “Novel meandered planar inverted- F antenna for triple frequency operation”, Microwave Optical Technology Letter Vol.27, pp.58-60, 2000.

[21] Fu-Ren Hsiao, Hong-Twu Chen, Tzung-Wern Chio1, Gwo-Yun Lee, Kin-Lu Wong, "A dual-band planar inverted-F patch antenna with a branch-line slit", Microwave and Optical Technology Letters, vol. 32, no. 4, pp. 310–312, Feb. 2002.

[22] A. Cabedo, J. Anguera, C. Picher, M. Ribo, C. Puente, "Multiband Handset Antenna Combining a PIFA, Slots, and Ground Plane Modes," IEEE Transactions on Antennas and Propagation, vol.57, no.9, pp.2526-2533, Sept. 2009.

[23] H. Chen, Y. Lin, P. Cheng, H. Lin, C. Song, P. Hall, "Parametric study on the characteristics of planar inverted-F antenna," IEE Proceedings Microwaves, Antennas and Propagation, pp. 534- 538, Dec. 2005.

[24] R. Sujith, V. Deepu, D. Laila, C. Aanandan, K. Vasudevan, P. Mohanan, "A compact dual-band modified T-shaped CPW-fed monopole antenna", Microwave and Optical Technology Letters, vol. 51, no. 4, pp. 937-939, 2009.

[25] S. Lee, H. Park, S. Hong, and J. Choi, "Design of a Multiband Antenna using a Planner Inverted-F Structure," The 9th International Conference on Advanced Communication Technology, vol. 3, pp.1665-1668, Feb. 2007.

[26] D. Kim, J. Lee, C. Cho, and T. Lee, "Design of a Compact Tri-Band PIFA Based on Independent Control of the Resonant Frequencies", IEEE Transactions on Antennas and Propagation, vol. 56, pp. 1428-1436, 2008.

[27] J.H.Lim, G.T.Back, Y.I.Ko, C.W.Song, T.Y.Yun, "A Reconfigurable PIFA Using a Switchable PIN-Diode and a Fine-Tuning Varactor for USPCS/WCDMA/m-WiMAX/WLAN", IEEE Transactions on Antennas and Propagation, vol.58, no.7, pp.2404-2411, July 2010.

[28] Z. Ying, “Multi frequency-band antenna,” Patent No WO01/91 233, May 2001. Z. Ying and A. Dahlstroem, "Multi frequency band antenna for mobile telephone", patent No WO200191233-A; EP1168491-A; WO200191233-A1.

[29] http://www.telcomponents.com/Generic_Housing_Nokia_6230_-_Black.html

[30] Yi Huang, and Kevin Boyle, "Antennas: From Theory to Practice", John Wiley & Sons, ISBN: 978-0-470-510'''t28-5, 2008.

[31] S. Yong-Sun, P. Seong-Ook, L. Manjai, "A broadband interior antenna of planar monopole type in handsets," IEEE Antennas and Wireless Propagation Letters, vol.4, pp.9-12, 2005

[32] H. Min-Seok, K. Hong-Teuk, "Compact Five Band Internal Antenna for Mobile Phone," IEEE Antennas and Propagation Society International Symposium, pp.4381-4384, 2006.

[33] Chia-Ling Liu; Yi-Fang Lin; Chia-Ming Liang; Shan-Cheng Pan; Hua-Ming Chen; , "Miniature Internal Penta-Band Monopole Antenna for Mobile Phones," Antennas and Propagation, IEEE Transactions on , vol.58, no.3, pp.1008-1011, March 2010

[34] C. Fang-Hsien, W. Kin-Lu, "Simple Folded Monopole Slot Antenna for Penta-Band Clamshell Mobile Phone Application," IEEE Transactions on Antennas and Propagation, vol.57, no.11, pp.3680-3684, Nov. 2009.

[35] Kin-Lu Wong; Saou-Wen Su; Chia-Lun Tang; Shih-Huang Yeh; , "Internal shorted patch antenna for a UMTS folder-type mobile phone," Antennas and Propagation, IEEE Transactions on , vol.53, no.10, pp. 3391- 3394, Oct. 2005

[36] Chih-Ming Su; Chih-Hsien Wu; Kin-Lu Wong; Shih-Huang Yeh; Chia-Lun Tang; , "User's hand effects on EMC internal GSM/DCS mobile phone antenna," IEEE Antennas and Propagation Society International Symposium, pp.2097-2100, 9-14 July 2006.

[37] Hattan F. AbuTarboush, R. Nilavalan, T. Peter and S. Cheung, "Multiband Inverted-F Antenna with Independent Bands for Small and Slim Cellular Mobile Handsets," IEEE Transaction on Antennas and Propagation, Vol. 59, No. 7, 2011.

[38] S. Yang, C. Zhang, H. Pan, A. Fathy and V. Nair, "Frequency-reconfigurable antennas for multiradio wireless platforms," IEEE Microwave Magazine, vol. 10, pp. 66-83, 2009.

[39] Sheta and S. F. Mahmoud, "A Widely Tunable Compact Patch Antenna," IEEE Antennas and Wireless Propagation Letters, vol. 7, pp.40-42 2008

[40] Viet-Anh Nguyen; Manh-Tuan Dao; Yun Tack Lim; Seong-Ook Park; , "A Compact Tunable Internal Antenna for Personal Communication Handsets," IEEE Antennas and Wireless Propagation Letters, vol.7, pp.569-572, 2008.

[41] Mak, C. Rowell, R. D. Murch and C. Mak, "Reconfigurable Multiband Antenna Designs for Wireless Communication Devices," IEEE Transactions on Antennas and Propagation, vol. 55, pp. 1919-1928, 2007.

[42] M. Ali, A. Sayem and V. Kunda, "A Reconfigurable Stacked Microstrip Patch Antenna for Satellite and Terrestrial Links," IEEE Transactions on Vehicular Technology, vol. 56, pp. 426-435, 2007.

[43] W. S. Kang, J. A. Park and Y. J. Yoon, "Simple reconfigurable antenna with radiation pattern," Electronics Letters, vol. 44; 44, pp. 182-183, 2008.

[44] M. Lai, T. Wu, J. Hsieh, C. Wang and S. Jeng, "Design of reconfigurable antennas based on an L-shaped slot and PIN diodes for compact wireless devices," IET Microwaves, Antennas & Propagation, vol. 3, pp. 47-54, 2009.

[45] R. Chen and J. Row, "Single-Fed Microstrip Patch Antenna with Switchable Polarization," IEEE Transactions on Antennas and Propagation, vol. 56, pp. 922-926, 2008.

[46] Kim, B. Pan, S. Nikolaou, Y. Kim, J. Papapolymerou and M. Tentzeris, "A Novel Single-Feed Circular Microstrip Antenna With Reconfigurable Polarization Capability," IEEE Transactions on Antennas and Propagation, vol. 56, pp. 630-638, 2008.

[47] N. Jin, F. Yang and Rahmat-Samii, "A novel patch antenna with switchable slot (PASS): dual-frequency operation with reversed circular polarizations," IEEE Transactions on Antennas and Propagation, vol. 54, pp. 1031-1034, 2006.

[48] N.Behdad, K.Sarabandi, "Dual-band reconfigurable antenna with a very wide tunability range," IEEE Transactions on Antennas and Propagation, vol.54, no.2, pp.409-416, 2006.

[49] K. Chang, Microwave Solid-State Circuits and Applications, John Wiley& ons, USA, 1994.

[50] M. Hamid, P. Gardner, P. S. Hall, F. Ghanem, "Switched Band Vivaldi Antenna," IEEE Transactions on Antennas and Propagation, no.99, pp.1, 2011 (Early Access)

[51] L. Hyung-Joo, L. Ford, R. Langley, "Independent multiband antenna tuning using an active EBG," Loughborough Antennas and Propagation Conference, pp.141-144, 2008.

[52] K.J. Vinoy, Hargsoon Yoon, Taeksoo Ji and Vijay K. Varadan, RF MEMS and Reconfigurable Antennas for Communication Systems, MEMS Components and Applications for Industry, Automobiles, Aerospace, and Communication II, Proceedings of SPIE Vol.4981, pp.164-175, 2003.

[53] Vijay K. Varadan, K.J. Vinoy and K.A. Jose, RF MEMS and their applications, John Wiley and sons, Chichester, UK, 2003.

[54] K. R. Boyle, P. G. Steeneken, "A Five-Band Reconfigurable PIFA for Mobile Phones," IEEE Transactions on Antennas and Propagation, vol.55, no.11, pp.3300-3309, Nov. 2007.

[55] B. Cetiner, G. Crusats, L. Jofre, N. Biyikli, "RF MEMS Integrated Frequency Reconfigurable Annular Slot Antenna," IEEE Transactions on Antennas and Propagation, vol.58, no.3, pp.626-632, March 2010

[56] W. C. Gibson, The Method of Moments in Electromagnetics, Chapman & Hall/CRC, 2008

[57] Edward, H. Newman, Ronald J, “Overview of MoM and UTD Methods at the Ohio State University”, IEEE, pp.700-708, 1989.

[58] K. S. Yee, "Numerical Solution of Initial Boundary Value Problems Involving Maxwell’s Equations in Isotropic Media", IEEE transaction on Antenna and Propagation, vol. AP-14, pp. 302-307, 1966.

[59] R. Nilavalan, “FDTD Manual” Brunel University, West London, 2009.

[60] www.ansoft.co.uk

Chapter 3

Fixed Multiband Antennas

3.1 Introduction

Modern wireless devices or systems are getting smaller and thinner in addition to the increase in the number of services required to be integrated in one device. Therefore, antennas are required to fulfil these needs with multiple bands capabilities and with small and slim overall size. Different techniques have been investigated to achieve multiband operation for printed antennas and for PIFA as discussed earlier in section 2.2.

In PIFA, the ground plane can play an important role to enhance the performance of the antenna [1]. For example, for low frequency operation such as for the GSM 900/800 bands, the ground plane has to be used as a radiating part. However, if the ground plane also acts as a radiating part, the effect of the user's hand is likely to degrade the antenna performance when the antenna is fitted inside the mobile phone. This causes several practical engineering problems [2] - [5]. In some designs, the location of the antenna on the substrate is also an important factor to be considered as it can enhance the bandwidth of the antenna by few more percentages [6].

Although there is extensive literature on multiband antenna for wireless and mobile applications, the following important issues need to be addressed:

- The independent control of the operating bands with a wide controlled range.
- Small and low profile structures to suite modern slim designs.
- Antennas performance in its operating environment specially the effect of the:
  (a) Antenna housing

(b) User's hand

- Many designs have not studied the sensitivity of the antenna when user's hold the mobile phone and when the antenna is cover with a plastic (housing of mobile phone). In Iphone 4, from apple, the antenna was designed perfectly but when it was fitted inside the handsets, user's found that, the matching of the antenna is affected when they hold the phone in different positions. Therefore, this should be taken into account when designing an antenna for handsets. These issues may results in a significant changes in the performance.

This chapter addresses the above issues with some novel designs.

In section 3.2, U-slots have been used to show how possible this technique can be used to minimise the size of the antenna and to create multiple bands from a single band antenna. The design is optimised to operate in the WiMAX bands with enough bandwidth to cater this application.

Then, in section 3.3, a PIFA is proposed for small and ultra-slim mobile phone handsets. Slots are also used in this design to create multiple bands. The effect of the ground plane size is studies comprehensively. In addition, user's hand and mobile phone housing effect have been studies with the design to have less effect on the performance of the antenna.

Finally, in section 3.4, a sub-patches technique has been used to generate multiple band operations. In this case, size reduction and multiple bands operations have been achieved with small and thin structure.

The independent control concept that was discussed in section 2.2 is achieved in all the antennas presented in this chapter and hence the antennas can be controlled independently over a wide range. This feature gives an additional level of freedom for the antenna designer to design the antenna to any other band of interest.

All the antennas presented in this chapter have simple structures to manufacture. Moreover, they are designed for fixed terminals i.e. once they are placed in the system, their operating bands are fixed.

3.2 Compact U-Slot antenna for Tri-band WiMAX applications

3.2.1 Introduction

This section discusses the following points:

- Reduce the size of the antenna.
- The possibility of obtaining multiple bands for WiMAX applications.
- Independent control of the WiMAX bands.
- Studying the effect of the coaxial cable in the radiation pattern measurements.

Therefore, the antenna proposed in this section is focused on using U-Slot shape to introduce multiple bands and to minimize the size of the antenna. The proposed design was optimised to operate at three bands for use in WiMAX applications. Other frequencies can be obtained by changing key dimensions of the antenna.

3.2.2 WiMAX Applications

The IEEE 802.16 working group has established a new standard known as WiMAX (Worldwide Interoperability for Microwave Access) which can reach theoretically up to 30-mile radius coverage. Moreover, in the case of WiMAX, the highest theoretically achievable transmission rates are possible at 70 Mbps. As currently defined through IEEE Standard 802.16, a wireless MAN provides network access to buildings through exterior antennas communicating with central radio base stations (BSs). One of the potential applications of WiMAX is to provide backhaul support for mobile WiFi hotspots. In order to satisfy the integration of WiFi, WiBro and WiMAX for WMAN applications, multiband compact antennas are the preferred front-end for mobile terminals [7].

3.2.3 Antenna Structure and Design Procedure

The design specifications for the proposed antenna are:

- The dielectric material selected for the design is FR-4.
- Dielectric constant 4.4
- Height of substrate (h) = 1.57 mm.

The antenna is fed by 50 Ω microstrip line. It has two U-slot shaped and two bridges to connect both shapes together as shown in Figure 3-1.

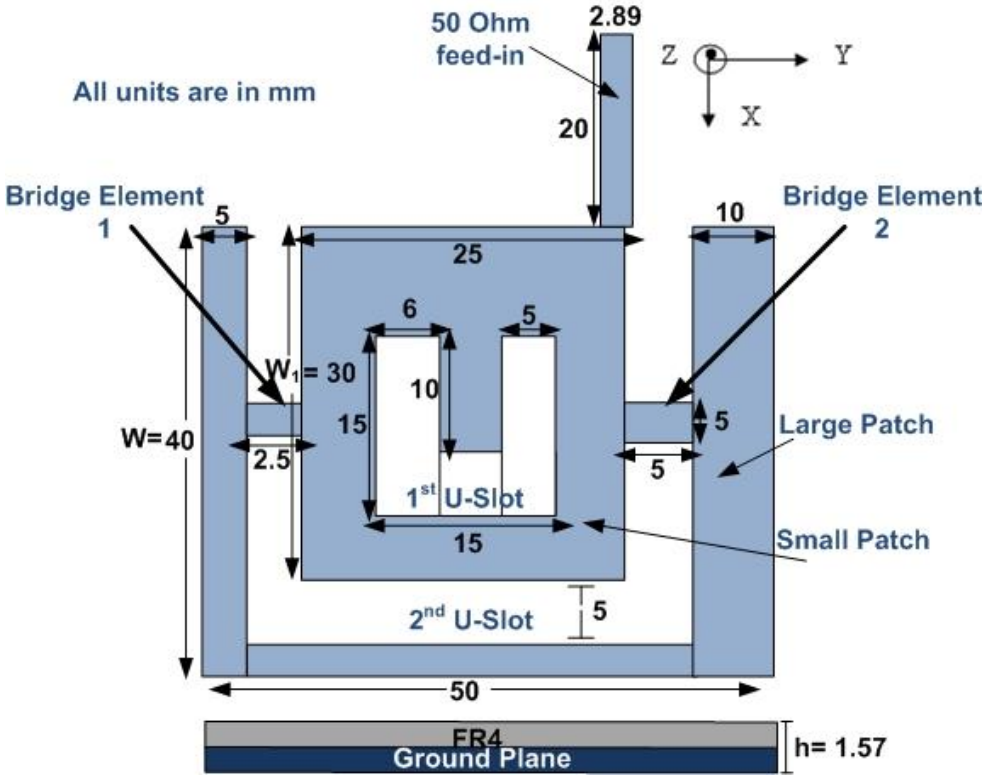

Figure 3-1: Structure and detailed dimensions of proposed patch antenna

The proposed antenna is optimised to operate at the three WiMAX frequency bands 2.7, 3.3 and 5.3 GHz with simulated impedance bandwidth of 4.8 %, 3 % and 2.5 % respectively. Thus the three bands satisfied the required bandwidth for the WiMAX compliant transmitters. The proposed antenna consists of a ground plane, a printed patch with large and small U-slots and a microstrip feed line. In step one; basic formulas have been used to design the total size of the patch [8]. The total size of the small patch is 25 x 30 mm^2 this can generate a single band at 4.68 GHz which is about half wavelength. When cutting a U-Slot shape on the small patch the currents travel over a longer path which results in shifting the band to lower frequency at 4.26 GHz. Two other bands have been generated when cutting a U-Slot shape on the small patch at 3.26 GHz and 5.4 GHz. However, WiMAX has allocated three frequency bands, the low band (2.5 to 2.8 GHz), the middle band (3.2 to 3.8 GHz) and the high band (5.2 to 5.8 GHz). Therefore, by increasing the size of the small patch, cutting a larger U-slot and then adding two bridge elements in appropriate place to connect both shapes together, the currents can travel longer distance which results in shifting the bands to lower frequencies and also the fine tuning of the length, width and the location of the bridges and

the feed line results in the final targeted frequencies at 2.7 GHz, 3.3 GHz and 5.3 GHz as shown in Figure 3-2 and table 3-1. The mobile WiMAX requires an operating bandwidth of 1.25 MHz [9]. The proposed antenna operates with adequate bandwidths at the specified operating frequencies within these WiMAX bands.

An edge feed approach was employed in the design as it will be convenient to integrate the antenna with other microstrip circuits printed on the same board and also to reduce space requirements. The offset feeding arrangement was found to give a better input match at these operating frequencies and hence it was adopted.

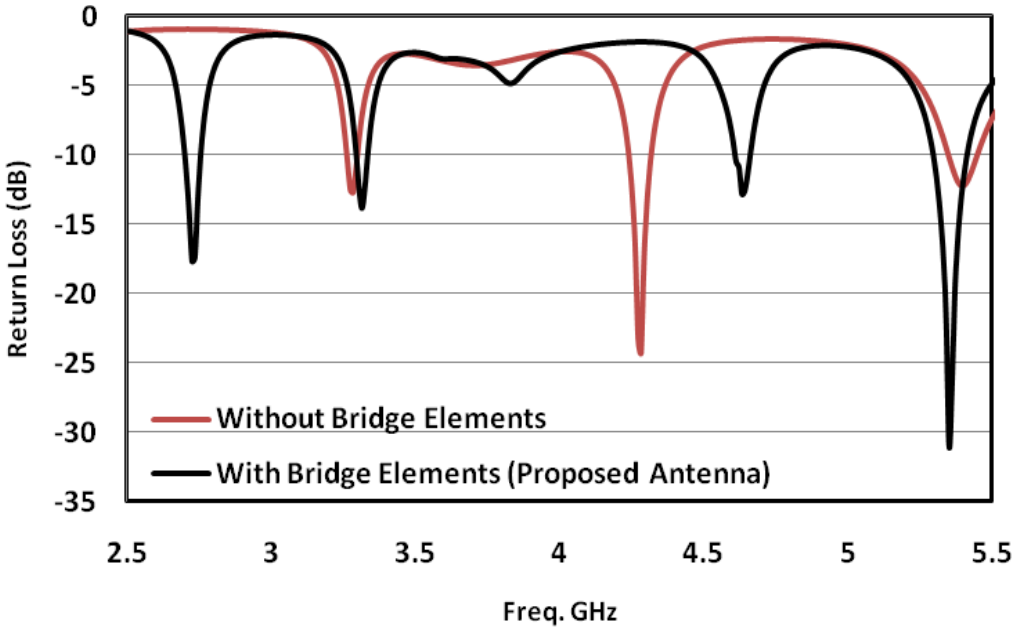

Figure 3-2: S_{11} with and without bridge elements.

Table 3-1: The effect of the bridges on the proposed U-Slot antenna

	Band I	Band II	Band III
Without Bridges	3.2 GHz	4.3 GHz	5.4 GHz
With Bridges	2.7 GHz	3.3 GHz	5.3 GHz

3.2.4 Parametric Analysis

Of all the investigated design parameters, two of them have a very noticeable effect in determining the performance of the antenna. The parameters that show the most effect are W and W_2. In order to check the changes of the frequencies shift or bandwidth changes, parametric studies for each parameter have been carried out and obtained from iterative simulation with initial data.

3.2.4.1 Effect of Changing (W)

In Figure 3-3, it shows the S_{11} based on variation in the parameter (W). The first and second bands are not affected, however, there is a noticeable change on the impedance matching of the third band when decreasing the size of (W) from 45 mm to 35 mm. A better characteristic for S_{11} and the bandwidth is obtained when (W) is 40 mm.

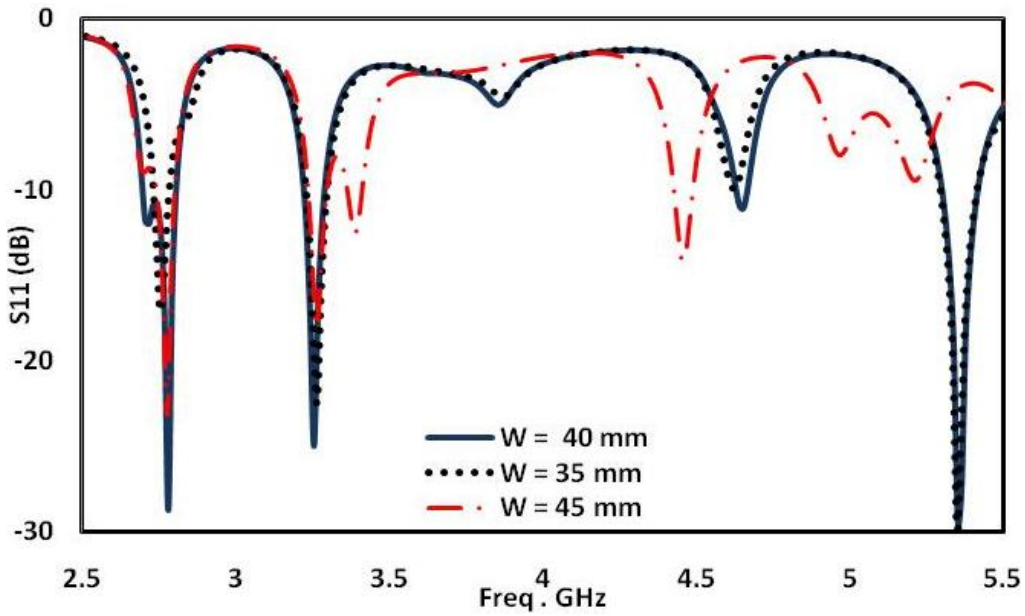

Figure 3-3: Variation of the (W) parameter on the S_{11} response

3.2.4.2 Effect of Changing (W_2)

Figure 3-4 describes the S_{11} based on increasing and decreasing the width (W_2) of the first U-slot. (W_2) affects the resonance frequency of the first band (2.7 GHz) only. Therefore, when (W_2) is 15 mm the first band is at 2.7 GHz. By increasing the value to 17 mm the resonance is shifted to a lower band whereas by decreasing the value to 13 mm, the resonant is shifted to a higher frequency. A better characteristic for S_{11} and the bandwidth is obtained when (W_2) is 40 mm. As a result, the antenna can be easily constructed on any other band by choosing the appropriate width for both U-slots.

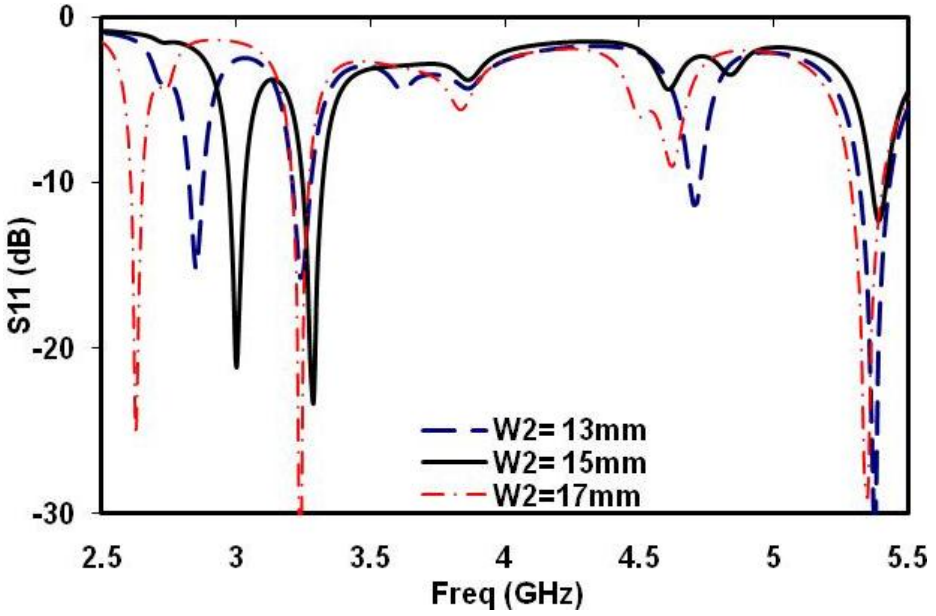

Figure 3-4: Variation of (W_2) parameter on the S_{11} response

3.2.5 Simulation and Measurements

3.2.5.1 S_{11} and Current Distributions

In order to validate the simulation results from HFSS software, the proposed antenna has been fabricated according to the specifications given in section 3.2.3. Figure 3-5 (a) shows the prototype of the antenna. The measured data for the proposed antenna showing that the antenna operates at 2.7 GHz, 3.3 GHz and 5.3 GHz, and measured using Agilent N5230A vector network analyser. In Figure 3-5 (b), the simulated values of the S_{11} in the final design

are compared with the measured data and it was found that the simulated and measured results are in good agreement, confirming that the simulated results were obtained with reasonable accuracy. The discrepancy between the simulated and measured results might be attributed to the fabrication process.

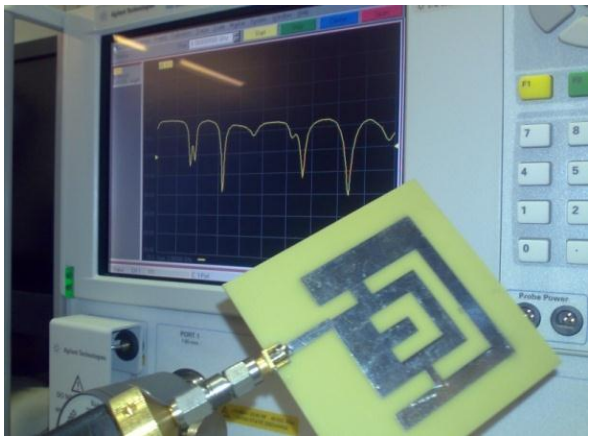

(a)

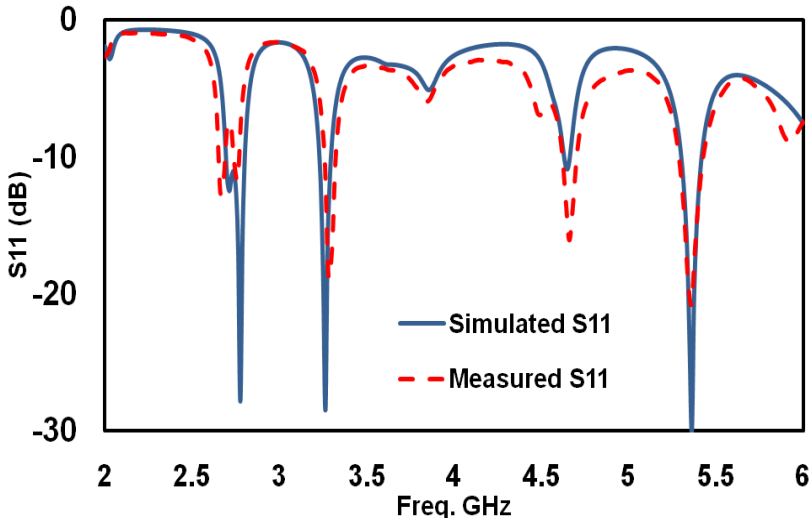

(b)

Figure 3-5: (a) Fabricated prototype and (b) measured and simulated results for the proposed antenna

The current distributions on the proposed antenna at 2.7 GHz, 3.3 GHz and 5.3 GHz are shown in Figure 3-6 (a)-(c) respectively. Figure 3-6 (a) shows that the current distribution at 2.7 GHz band is concentrated mainly in the X direction and results in H-plane in Y-Z plane and it can also be observed that high cross-polar components due to high current densities

in the Y direction. Similarly Figure 3-6 (b) and (c) show current concentration in Y direction at 3.3GHz and X direction at 5.3GHz resulting in H-planes in X-Z and Y-Z planes respectively. The current path lengths correspond to respective resonance frequencies.

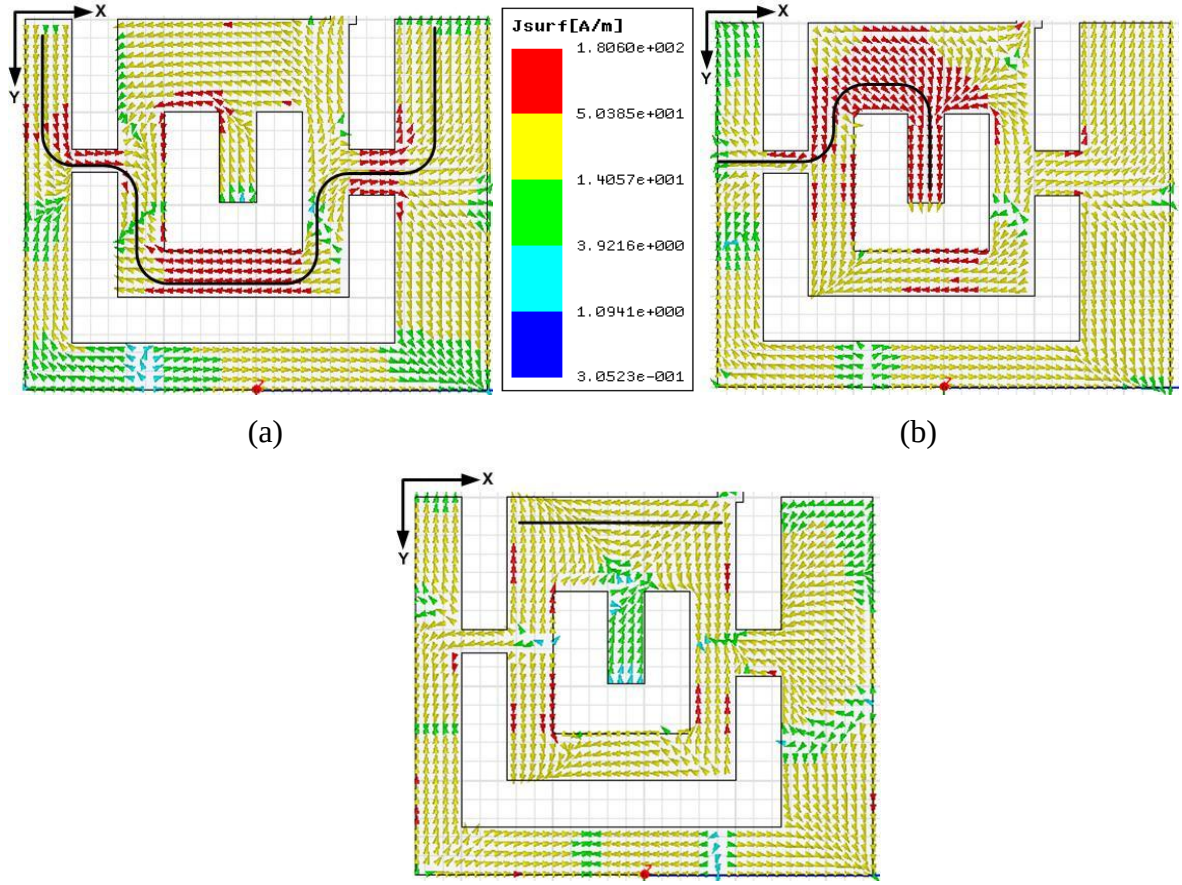

(a) (b)

(c)

Figure 3-6: Current distribution for U-Slot antenna at (a) 2.7 GHz, (b) 3.3 GHz and (c) 5.3 GHz

3.2.6 Radiation Patterns and Gain

The Co and X polarization for E-Plane and H-Plane radiation patterns at the centre frequencies 2.7, 3.3 and 5.3 GHz are plotted as shown in Figure 3-7 (a)-(c). From the radiation patterns it can be observed that there is a stable response throughout the three bands with -8 dB low cross polarization for the first band and below -10 dB for the second and third bands. The antenna gain is 1.7 dBi at 2.7 GHz, 2.3 dBi at 3.3 GHz and 4.1 dBi at 5.2 GHz.

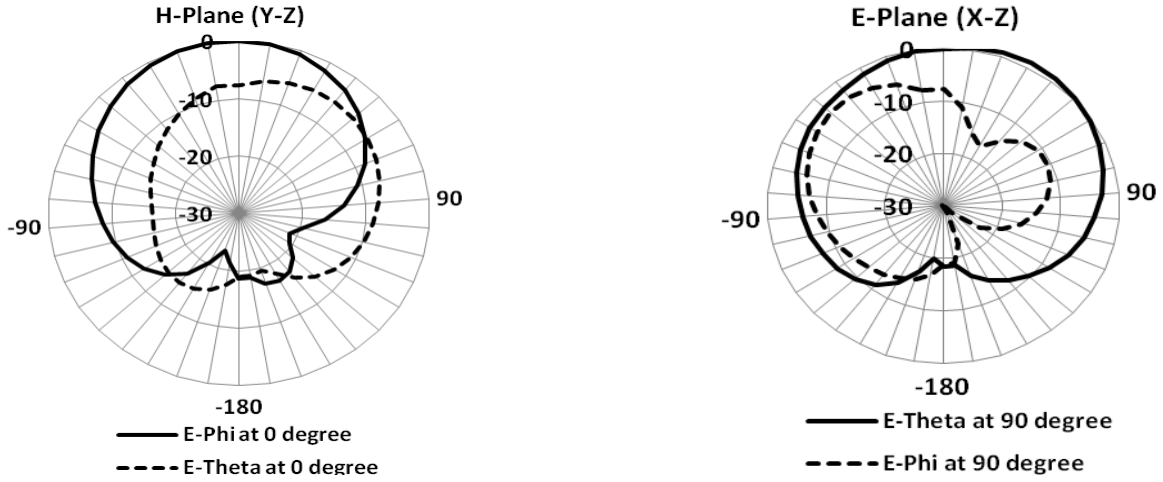

(a)

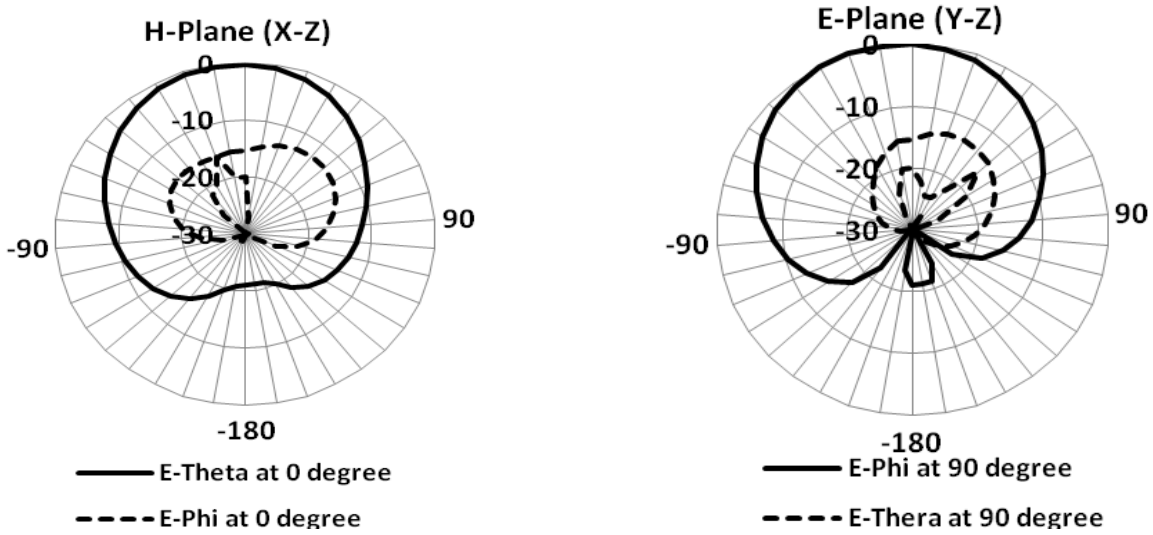

(b)

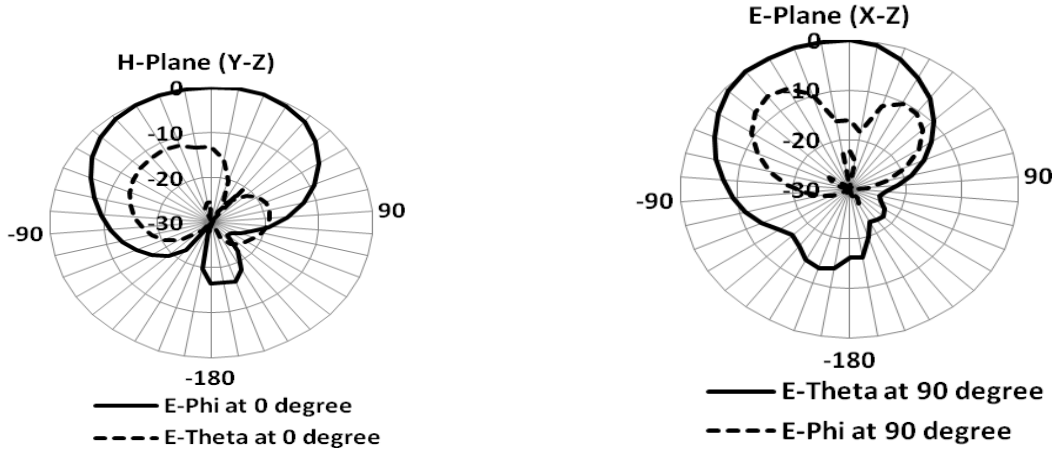

(c)

Figure 3-7: Co and Cross polarization for E-plane and H-plane at (a) 2.7 GHz. (b) 3.3 GHz. (c) 5.3 GHz

During the radiation pattern measurements, an RF-optical cable was used to connect the antenna instead of traditional coaxial cable to eliminating the large distortion associated with the unwanted radiation from a coaxial cable as shown in Figure 3-8 (a)-(b).

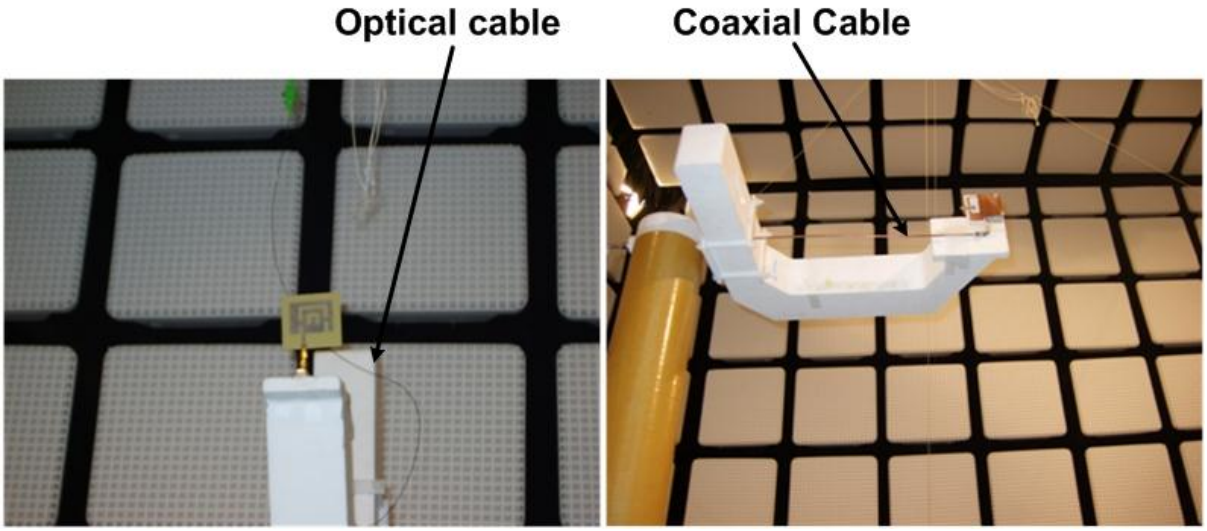

(a) (b)

Figure 3-8: Experimental setup for radiation pattern measurement of the U-Slot antenna using: (a) coaxial cable; (b) optical fibre

The measurements were made in the NPL SMART chamber. The use of optical fibre on the receiving antenna eliminates cable reflections [10-11]. Results of the radiation patterns of the proposed antenna with coaxial cable and with optical fibre are compared as shown in Figure 3-9 (a)-(c). The results in Figure 3-9 show that the optical cable has slightly improved the shape of the radiation patterns and some nulls have been cleared which reflect that the coaxial cable has some effects on the radiation patterns.

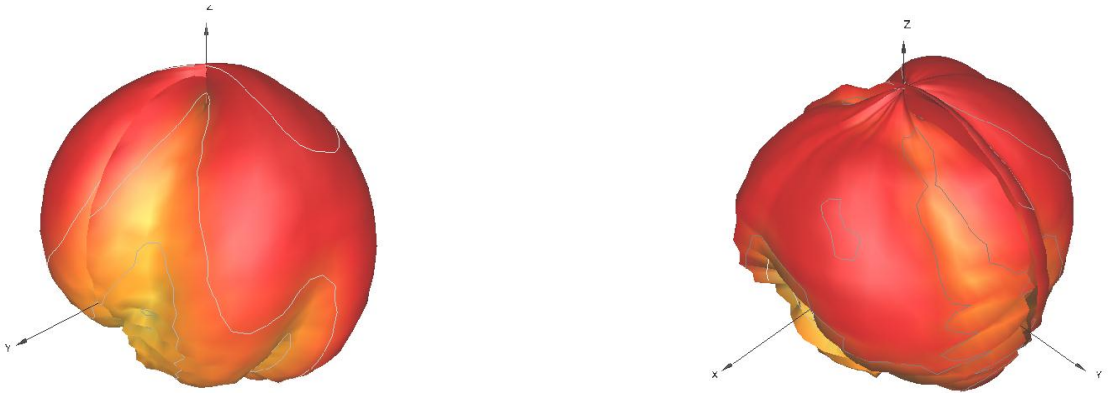

2.7 GHz with optical **2.7 GHz with coaxial**

(a)

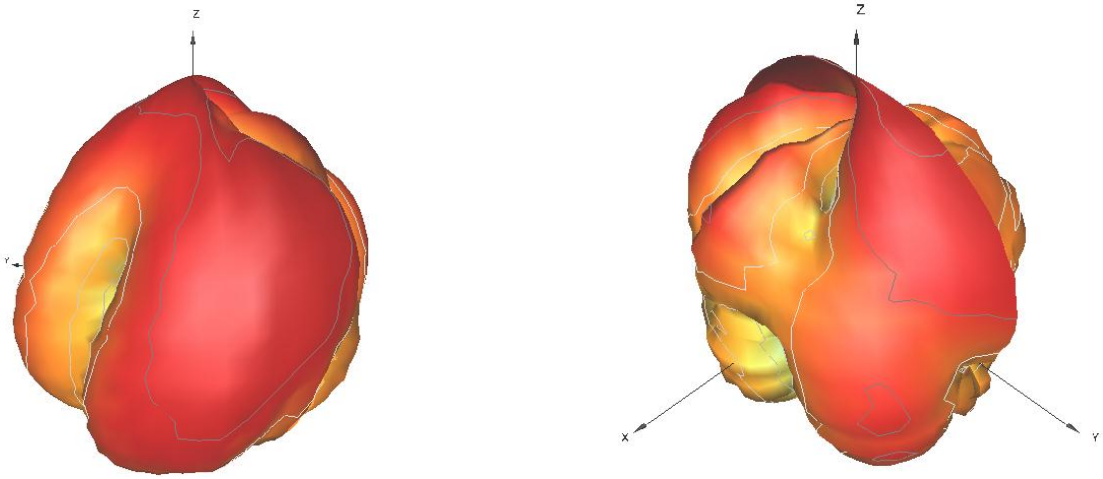

3.3 GHz with optical **3.3 GHz with Coaxial**

(b)

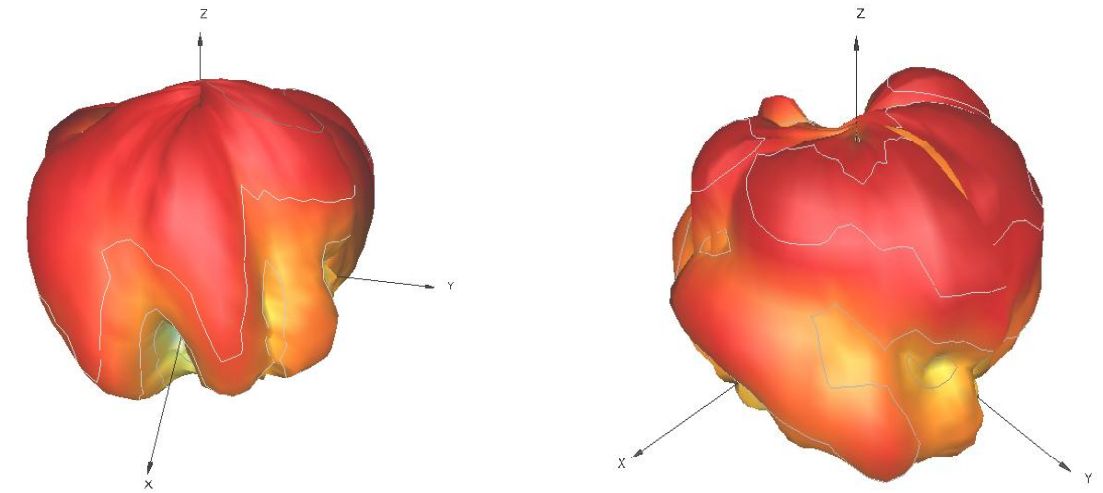

5.3 GHz with optical **5.3 GHz with coaxial**

(c)

Figure 3-9: 3D measured radiation patterns with optical cable and with coaxial cable

3.3 Multiband Inverted-F Antenna for Small and Slim Mobile Handsets

3.3.1 Introduction

Based on the discussion in section 3.1, this section tackles the following points:

- The effect of the ground plane size, the height of PIFA and the location of the feeding point.
- The independent control over a wide range.
- The effect of the housing and user's hand on the antenna's performance.
- The overall size of the antenna.

Therefore, the design of a small ultra-thin Printed Inverted-F Antenna (PIFA) with independent frequency control is proposed. The antenna consists of a slotted radiator supported by shorting walls and a small ground plane. The structure is designed and optimized to operate at 2.09, 3.74 and 5 GHz with achievable bandwidths of 11%, 8.84% and 10%, respectively. These three bands cover the existing wireless communication frequency bands from 1.5 - 6.8 GHz. Each of the three bands can be controlled independently without affecting the other two bands. The 2.09 GHz band can be controlled to operate between 1.5 – 2.09 GHz (33.33%), the 3.74 GHz band can be controlled over the range of 3.57 – 4.18GHz (15.76%) and the 5 GHz band can be controlled to cover the band from 5.00 – 6.80 GHz (30.50%). Results of intensive investigations using computer simulations and measurements show that the ground plane and the feed locations of the antenna have marginal effects on the performance of the antenna. The effects of the user's hand and mobile phone housing on the return loss, radiation patterns, gains and efficiency are characterized. The measured peak gains of the prototype antenna at 2.09, 3.74 and 5GHz are 2.05, 2.32 and 3.47 dBi, respectively. The measured radiation efficiencies for the corresponding three bands are 70.12, 60.29 and 66.24 % respectively.

3.3.2 Antenna Configuration and S_{11} Measurements

Figure 3-10 (a) shows the structure of the proposed antenna with detailed dimensions given in Figure 3-10 (b) and Table 3-2. The proposed antenna consists of a main radiator with an irregular shape, a rectangular slot, shorting walls, and a ground plane. The material

used is FR-4 substrate with a dielectric constant of 4.4, a loss tangent of 0.02 and a substrate height of 1.57mm. The proposed antenna has a very small size and is physically thin. The total volume of the radiator with feed point is 25.6 x 26 x 3.57 mm^3, while the overall volume of the antenna including the ground plan is 40 x 40 x 3.57 mm^3. The EM software, High Frequency Structure Simulator (HFSS) V.11.4 package, is used for full wave analysis of the antenna and material losses is taken into account in the simulation studies.

To validate the simulated results, the proposed antenna is also fabricated on a FR-4 substrate with the same characteristics used in simulation. The thickness of the copper used in the prototype is 0.15 mm. The simulated and measured reflection coefficient (S_{11}) of the proposed antenna is presented in Fig 3-11 (a) and the prototype is shown in Fig. 3-10 (b). It can be seen that the simulated and measured results are in good agreements. The little discrepancies might be due to many factors such as the soldering proficiency and accuracy of cutting the edges of the copper. The results in Fig. 3-11 (a) show three distinct bands are generated at 2.09 GHz, 3.74 GHz and 5 GHz. The corresponding bandwidths defined by -6 dB for the three bands are 11 % (1.978–2.2 GHz) for the 2.09 GHz band, 8.84 % (3.571 –3.9 GHz) for the 3.74 GHz band and 10 % (4.887–5.391 GHz) for the 5 GHz band. These bandwidths satisfy the requirements for most of the wireless applications. The antenna achieves a wider bandwidth, smaller ground plane size and thinner structure than the designs reported in [12] and [13].

Table 3-2: Detailed dimensions of proposed antenna (in millimeter)

Parameter	**W**	**W_1**	**W_2**	**W_3**	**W_4**	**W_5**
Dimension	40	6	2	2	11.6	4
Parameter	**L**	**L_1**	**L_2**	**L_3**	**L_4**	**L_5**
Dimension	40	25.6	25.6	20	20	12
Parameter	**S_1**	**S_2**	**S_3**	**S_4**	**Ground Plane**	
Dimension	2	3.57	4	3	40 x 40	

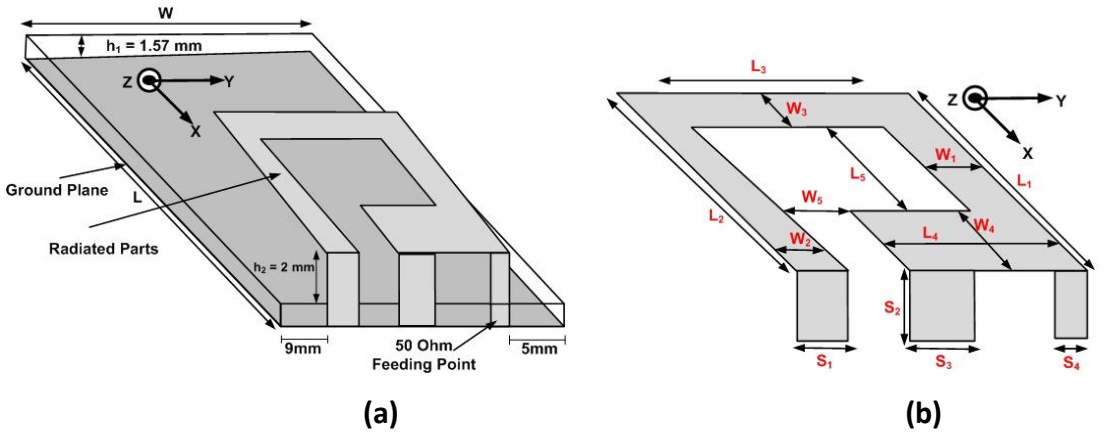

Figure 3-10: Layout of proposed antenna (a) 3D View and (b) detailed dimensions

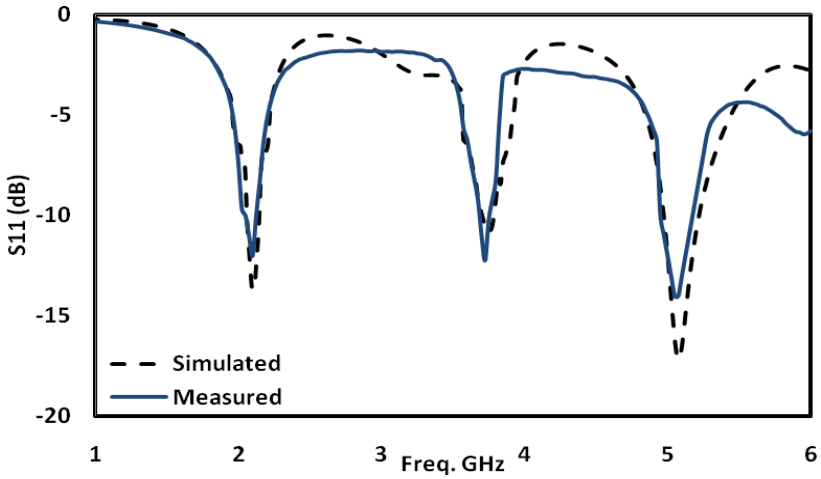

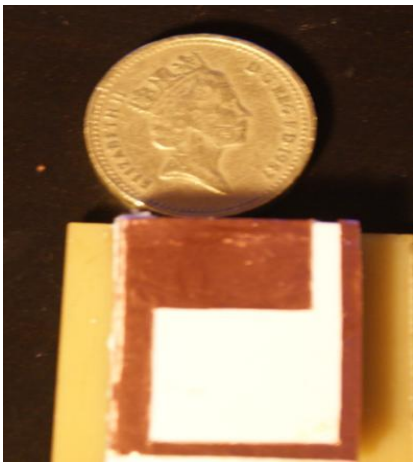

(b)

Figure 3-11: (a) Simulated and measured S_{11} for the proposed antenna (b) prototype antenna

3.3.3 Radiation Mechanism and Current Distributions

Further understanding of the antenna behaviour can be observed from the current distribution plots shown in Figure 3-12 (a) - (c). These current distribution plots can be used to identify the electrical lengths for the first, second and third resonant frequencies, f_1, f_2 and f_3, at 2.09 GHz, 3.74 GHz and 5 GHz, respectively. It can be seen in Figure 3-12 (a) that there are two major current paths on the radiator generating the 2.09 GHz band. The first current path is along L_1 and W_1 whereas the second current path is along L_2 and W_2 of Figure 3-10 (b). Both paths have an electrical length of about a quarter wavelength at 2.09 GHz. At 3.74 GHz, Figure 3-12 (b) shows that there is only one major current path concentrated along L_3 and W_3 on the radiator. This path has an electrical length of about a quarter wavelength at 3.74 GHz. In Figure 3-12 (c), there are two major current paths on the radiator. The first path is formed around W_1 and (L_1 - W_4) whereas the second path is formed around L_4 and W_4. The electrical lengths for both paths are about a quarter wavelength at 5 GHz. Thus by varying these parameters, the current paths for the first, second and third resonances can be independently controlled over a wide range, which is further elaborated in the next section.

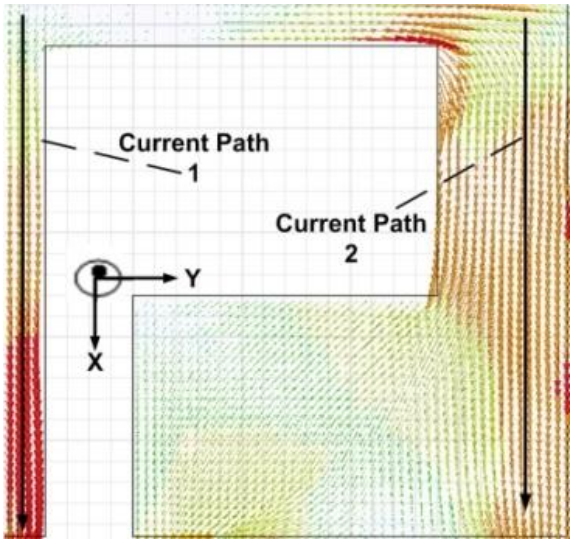

(a)

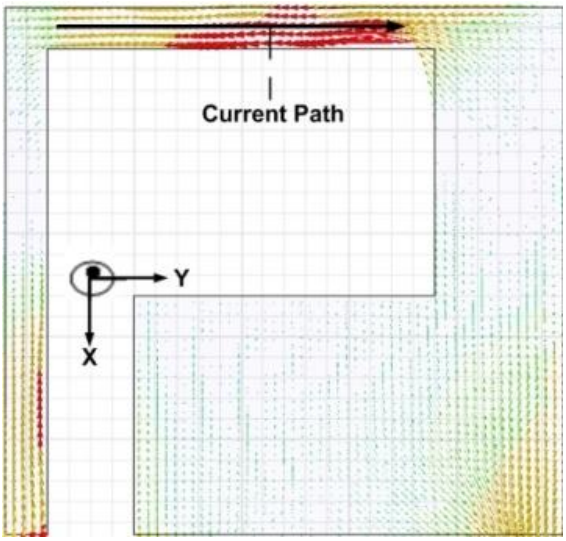

(b)

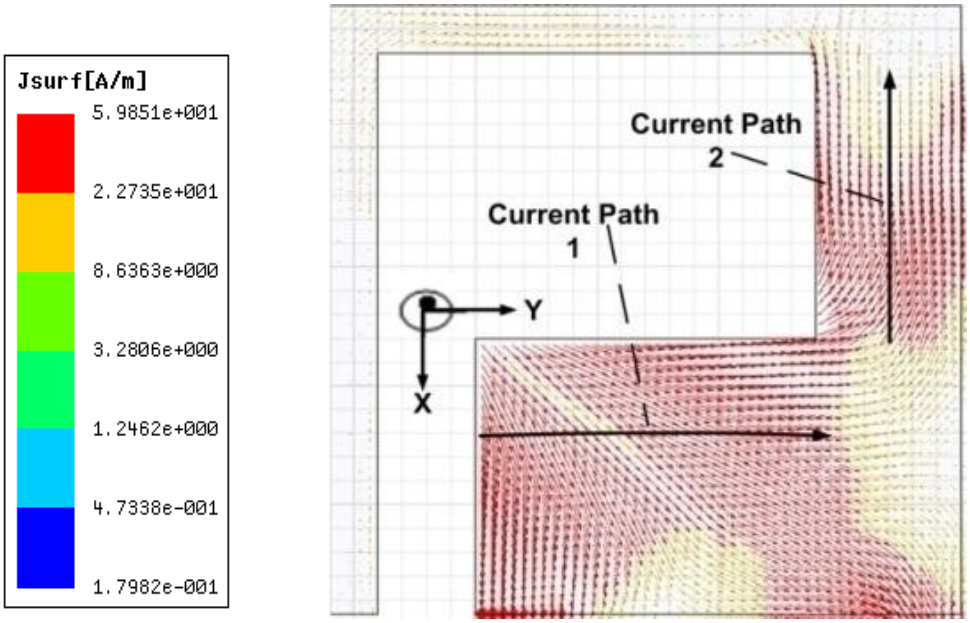

(c)

Figure 3-12: Currents distribution for proposed antenna at (a) 2.09 GHz, (b) 3.74 GHz and (c) 5 GHz

3.3.4 Parametric Analysis and Independent Control over a Wide Range

To design an antenna with multiple band operation, it is desirable to have an independent frequency control on two or more separate frequencies. Achieving this option is very challenging as discussed in section 2.2.

The idea proposed in this work to achieve an independent frequency control on different frequencies of a single antenna is to find out the radiation elements of the antenna responsible for individual bands. From the current distribution discussions in section 3.3.3, we can identify the key radiation elements by observing the current paths for each resonance frequency, so we can control each band independently. For example, the current path along L_2 and W_2 is for the 2.09 GHz band. Increasing the length of L_2 in the X-direction moves the lower order mode resonance (at 2.09 GHz) toward the lower frequencies as shown in Figure 3-13 (a) and Table 3-4. The 2.09 GHz band can be controlled over 33.33% between 1.5 – 2.09 GHz. Similarly, the current path for 3.74 GHz is along L_3 and W_3 , so by changing the size of the width of W_3 in the X-direction (without changing the parameters (L_1 and W_1)), the 3.74 GHz band can be tuned to a lower or higher frequency, as shown in

Figure 3-13 (b) and Table 3-4. Here, we can tune the 3.74 GHz band over 15.75% between 3.57 – 4.188 GHz. For the 5 GHz band, the current path is formed along L_4 and W_4. By varying the length and the width simultaneously, we can tune the 5 GHz band over 30.50% between 5 – 6.8 GHz without affecting the 2.09 GHz band and the 3.74 GHz bands, as shown in Figure 3-13 (c) and Table 3-3.

It should be noted that the 2.09 GHz and 5 GHz bands have one common current path around L_1 and W_1, so by changing the length or the width of L_1, these two bands can be controlled without affecting the 3.74 GHz band. Since these three bands can be controlled independently over wide frequency ranges (compared with the design reported in [12] and [14]), the antenna can be designed easily for other applications.

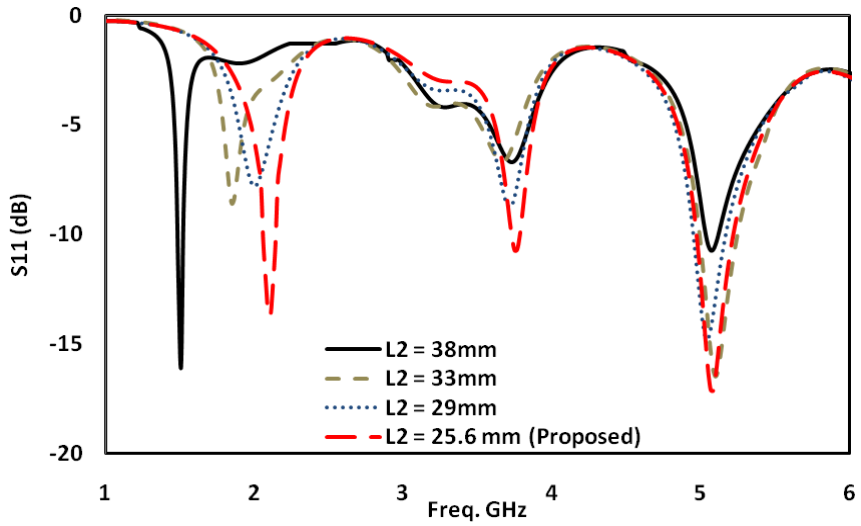

(a)

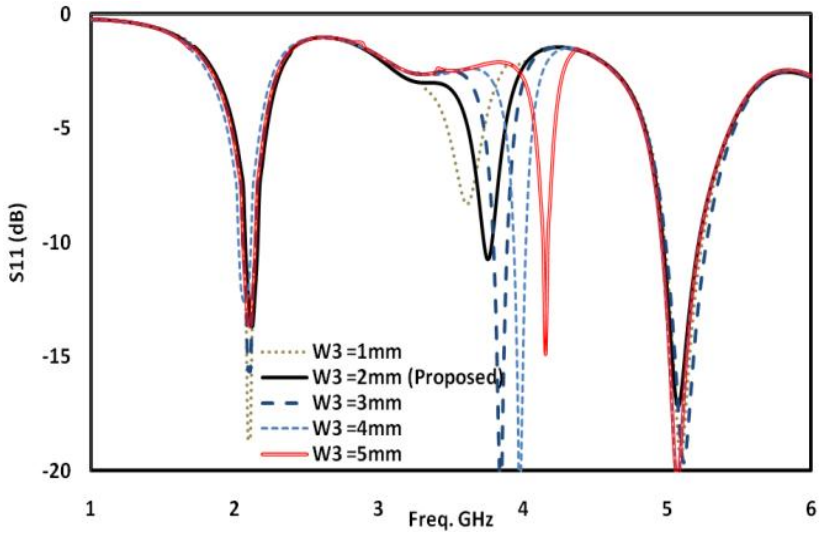

(b)

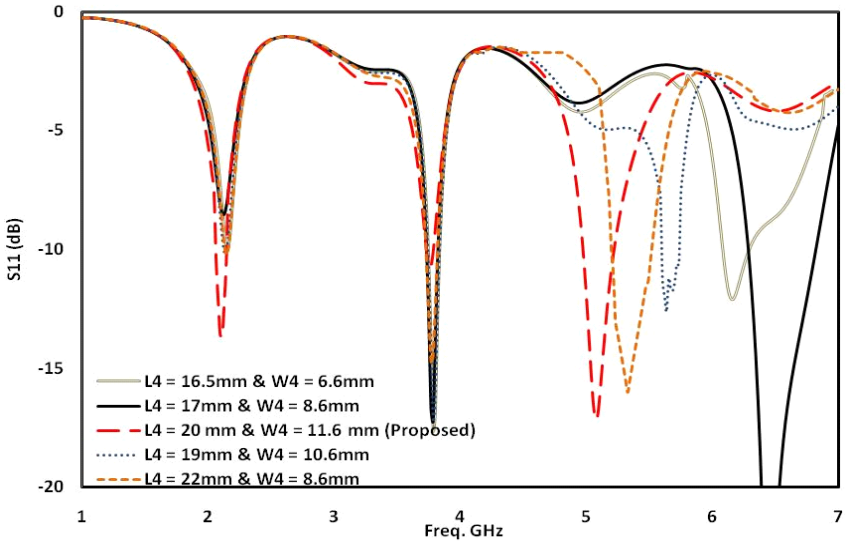

(c)

Figure 3-13: Parametric studies showing independent control for each band over wide range (a) 2.09 GHz band (b) 3.74 GHz band and (c) 5 GHz band

Table 3-3: Independent ontrol range in three bands

Frequency Band	2.09 GHz	3.74 GHz	5 GHz
Control Range (MHz)	1500 – 2090	3570 – 4188	5000 - 6800
Control Range (%)	33.33	15.76	30.50

3.3.5 Effect of Antenna Geometrical Parameters on the Antenna Performance

The effects of the ground plane size, the antenna location and the height of the PIFA on the performance of the antenna are examined and further elaborated in this section

3.3.5.1 Ground Plane Effect

The geometry of a ground plane in a PIFA are known to affect the antenna performance. In [15], slots were added to the ground plane to significantly improve the bandwidth performance of the antenna. In [12], it was shown that varying the ground plane size would affect S_{11}. An antenna can be designed to couple more energy to the ground plane, making the ground plane a radiating part and resulting in a wider impedance bandwidth. However,

this makes the ground plane quite sensitive. Since the proposed antenna is designed for use in the mobile phone systems which require a relatively narrow width, there is no need to use the ground plane to increase the bandwidth. Moreover, there are many advantages of having a less sensitive ground plane. For example, with an insensitive ground plane, the antenna performance will not be affected by other electronic components and circuits nearby. When multiple antennas are integrated together, there will be strong isolation between antennas, allowing easy optimization of antennas positions. The antenna can be used in mobile phones with different ground plane sizes without changing the performance. The user's hand will not affect the matching of the bands and also the radiation efficiency. For these reasons, we should design the antenna to have the ground plane as less sensitive as possible so that the performance mainly depends on the structure alone and not the surrounding elements [16]. For this antenna, results in Figure 3-14 (a) show that varying the length of the ground plane from 40 x 40 mm^2 to 40 x 100 mm^2 does not affect the matching or the bandwidth of the antenna, indicating that the ground plane effect is quite small. Similar observation was also reported in [6]. However, this will not be the case if the ground plane is used as part of the radiating part as in [12] and [15].

When the size of the ground plane changes the current distribution on the main radiator and the ground plane for the three bands do not significantly change. In addition, the gain and the radiation efficiency have been observed when changing the size of the ground plane. No significant changes in the gain and the radiation efficiency have been noticed at the three bands

3.3.5.2 Antenna Location with Respect to the Ground Plane

The location of the antenna can also affect the performances [6]. However, in the proposed antenna, results in Figure 3-14 (b) shows that changing the location of the proposed antenna along the substrate do not affect the matching or bandwidth of the bands. More results have also shown that this would not change the gain and the shape of the radiation pattern.

3.3.5.3 Height of the PIFA (h_2)

Figure 3-14 (c) shows the effects of the height (h_2) of the PIFA above the ground plane on the bandwidth of the antenna. It can be seen that, at a smaller value of h_2 = 1 mm, the

reflection coefficient is larger at the high frequency band and significantly lower at only 5 dB in the lower frequency band. This is because the radiator was too close to the substrate base to resonate at low frequency. At the heights of h_2 = 5, 6 and 9 mm, the return loss is larger than 10 dB (S_{11} <-10 dB) in the low frequency band, but less than 5 dB in the high frequency bands. With h_2 = 2 mm, the return losses of the three bands are larger than 10 dB which satisfies many applications. Since the objective of this research is to design a small antenna with a thin structure, we have selected the heights h_2 = 2 mm from the substrate and 3.57 mm from the ground plane for further studies. With these dimensions, the proposed antenna can operate in the UMTS, m-WiMAX and 5 GH WLAN bands with a bandwidth wide enough to cater for these applications. More results have also shown that changing h_2 does not alter the radiation efficiency and gain of the antenna significantly enough to affect the performance, except at 5 GHz for h_2 = 9 mm, where the efficiency changes slightly

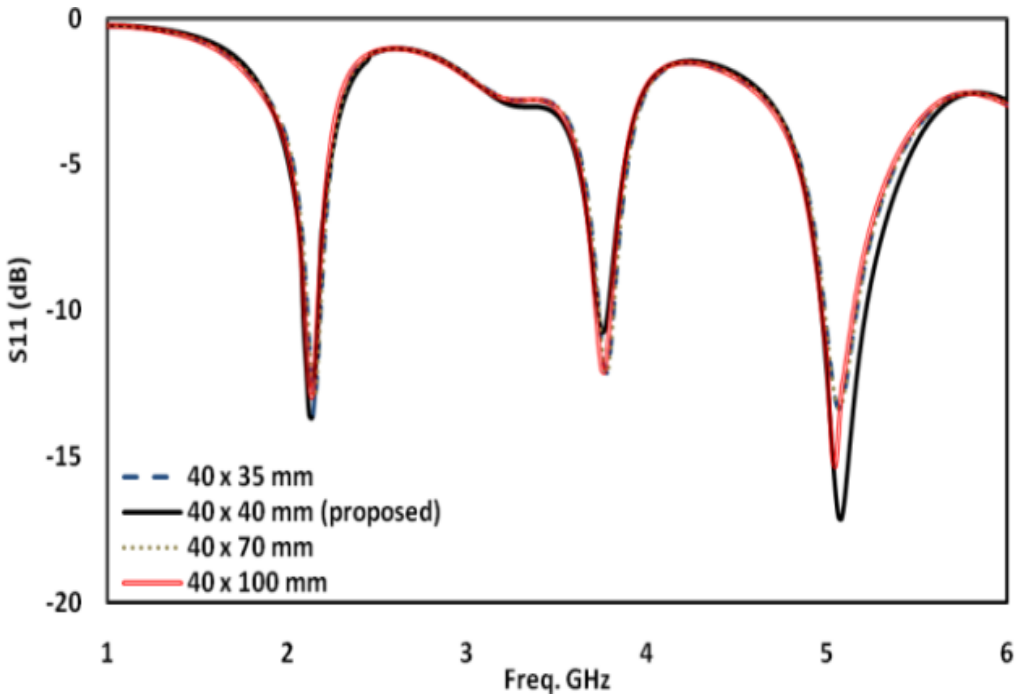

(a)

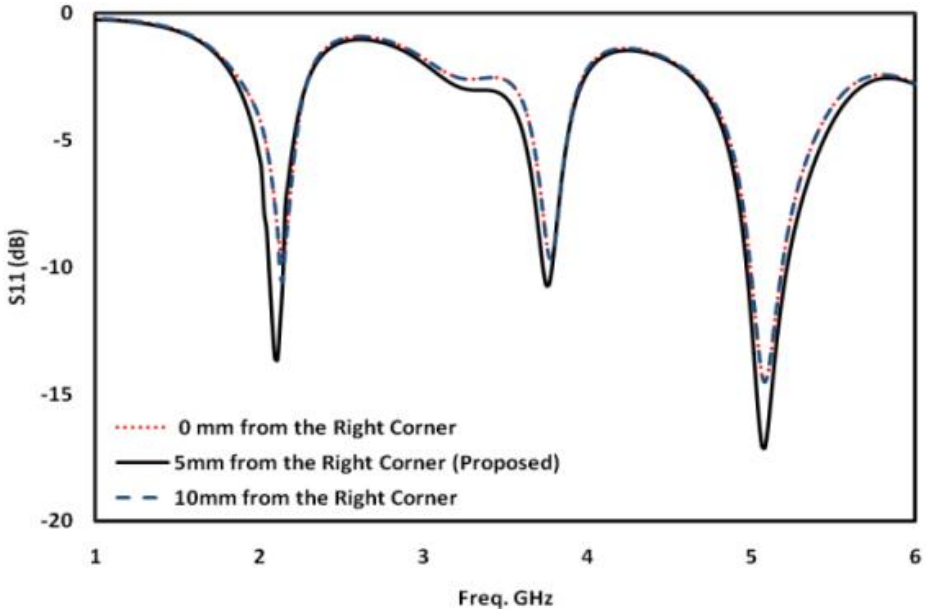

(b)

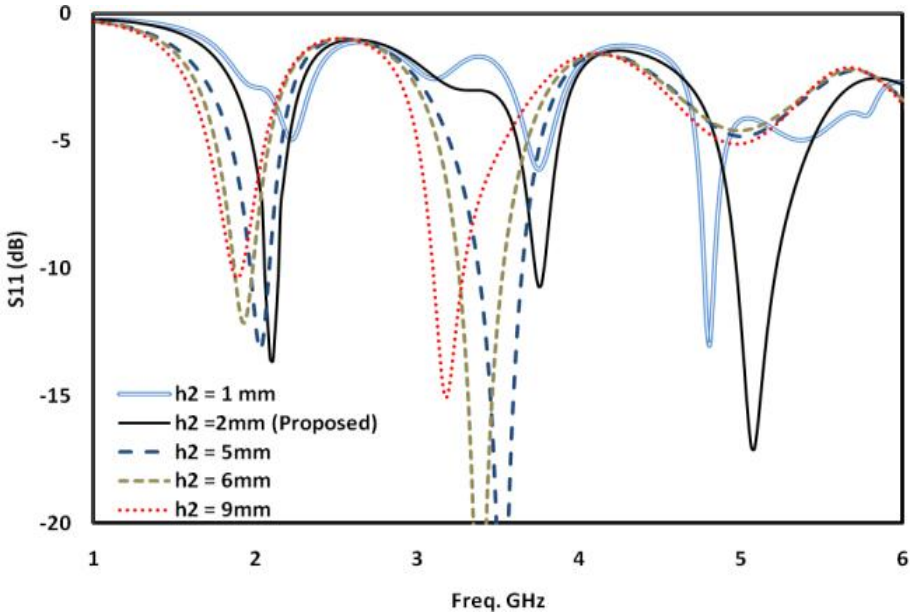

(c)

Figure 3-14: The effects of (a) ground plane size (b) antenna location and (c) physical height of the PIFA on S_{11} performance.

3.3.6 Simulation and Measurements

3.3.6.1 Measurement Setup

The antenna was measured using the antenna measurement equipment, StarLab, manufactured by Satimo [17]. The orientation of the antenna inside the Satimo is shown in Figure 3-15. Before any measurement was done, calibration was carried out by using the standard antennas provided. For radiation pattern and gain measurements, it is just like other antenna measurement equipment. For power efficiency measurement, the equipment first measures the gain, radiation intensity and reflection coefficient of the antenna and computes the directivity using the radiation intensity [8]. The efficiency of the antenna is then computed using equation (3-1):

$$Efficiency = \frac{G(\theta,j)}{D(\theta,j)}(1-|\Gamma|^2) \qquad (3\text{-}1)$$

where Γ is the voltage reflection coefficient, $G(\theta,f)$ and $D(\theta,f)$ are the gain and directivity, respectively, of the antenna and are functions of spherical coordinate angles θ and ϕ .

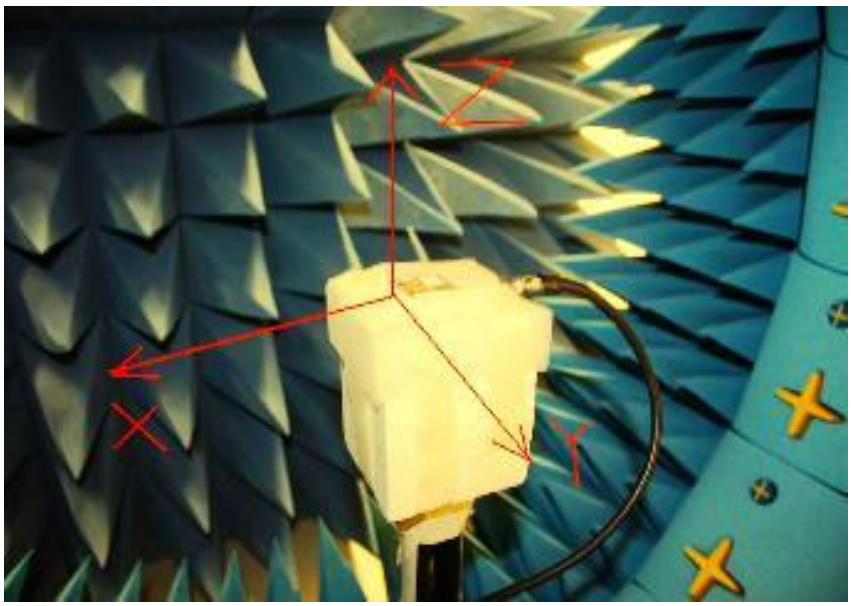

Figure 3-15: The orientation of the proposed antenna during the measurements of the radiation patterns, gain and radiation efficiency

3.3.6.2 Simulated and Measured Radiation Patterns and its Relation with the Current Distribution

The simulated and measured radiation patterns for co- and cross- polarizations in the E-plane and H-plane at the frequencies of 2.09, 3.74 and 5 GHz are shown in Figure 3-16 (b) - (d). It can be observed the radiation patterns are quite stable throughout the UMATS, m-WiMAX and WLAN bands. To relate the X-Y-Z orientation of the antenna in Figure 3-10 to the E- and H-planes in Figure 3-16, we use the current directions of Figure 3-12 (a) - (c) on the radiator in the individual frequency bands. Figure 3-12 (a) shows that the current direction for the first band at 2.09 GHz is in the X-direction, so the E- and H-planes in Figure 3-16 are the X-Z and Y-Z planes, respectively, in Figure 3-10. The current direction for the second band at 3.74 GHz is in the Y-direction as shown in Figure 3-12 (b), indicating that the E- and H-planes are the Y-Z and X-Z planes, respectively. Here, a high cross-polarization level is found at 3.74 GHz. This might be due to high current concentration around the bottom right corner of L_2, as shown in Figure 3-12 (b). Finally, the current direction for the 5 GHz band in Figure 3-12 (c) indicates that the E- and H-planes are the Y-Z and X-Z planes, respectively. To conclude this, at 3.74 GHz and 5 GHz, the currents have the same direction and their E-planes are the Y-Z plane, whereas at 2.09 GHz, the current has a different direction and the E-plane is the X-Z plane.

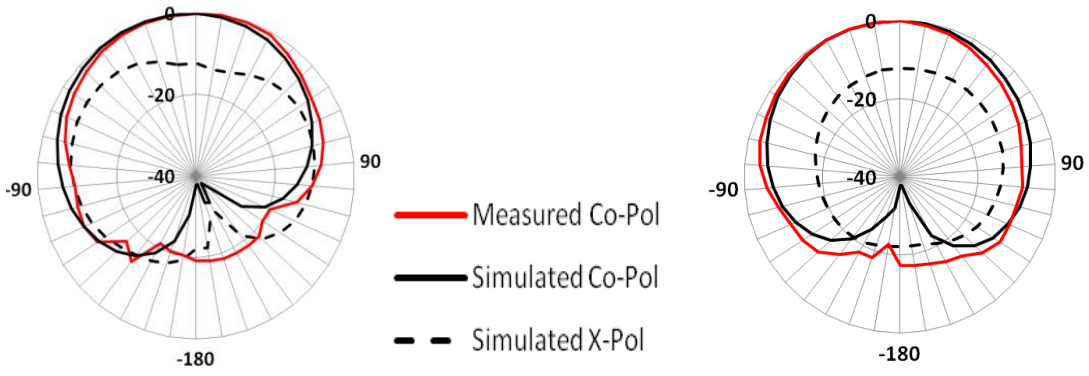

(X-Z) **(Y-Z)**

(a) 2.09 GHz

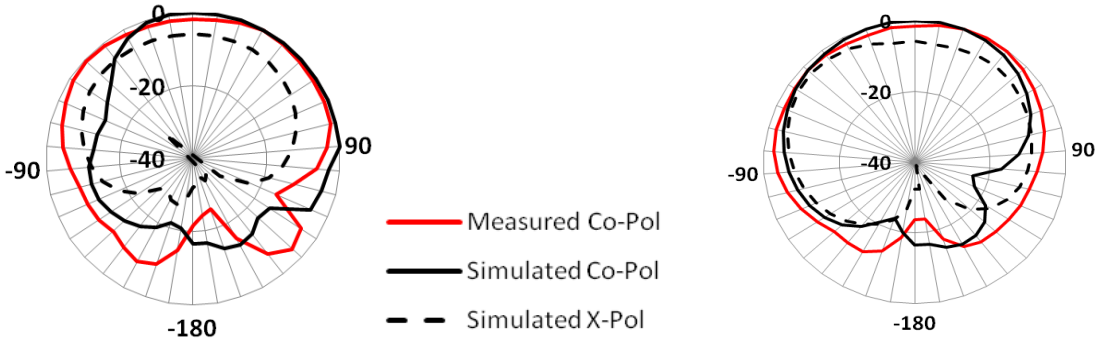

(X-Z) **(Y-Z)**

(b) 3.47 GHz

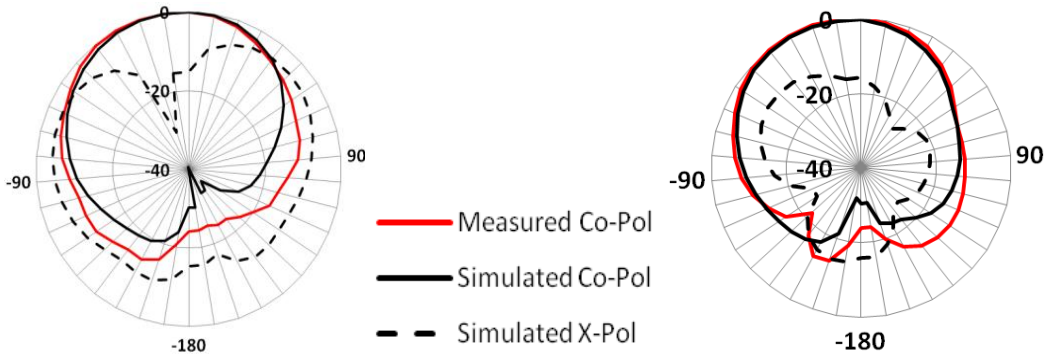

(X-Z) **(Y-Z)**

(c) 5 GHz

Figure 3-16: Simulated and measured Co and X-pol radiation patterns in E and H planes (a) 2.09 GHz (b) 3.74 GHz and (c) 5 GHz

3.3.6.3 Measured Gain and Radiation Efficiency

Simulations and measurements on the peak gain and radiation efficiency of the antenna have been carried out. Results have shown that, in the 2.09 GHz, 3.74 GHz and 5 GHz bands, the simulated peak gains are 2.14 dBi, 2.4 dBi and 5 dBi, respectively, and the corresponding measured peak gains 2.05 dBi, 2.32 dBi and 4.42 dBi, as shown in Figure 3-17. The measured radiation efficiencies for the three bands are 70.12 %, 60.29 % and 66.24 %, respectively, as shown in Figure 3-17. These results have taken into account the loss of the FR-4 substrate. If the loss is neglected, the gains and the radiation efficiencies in the three-band are higher, as shown in Table 3-4.

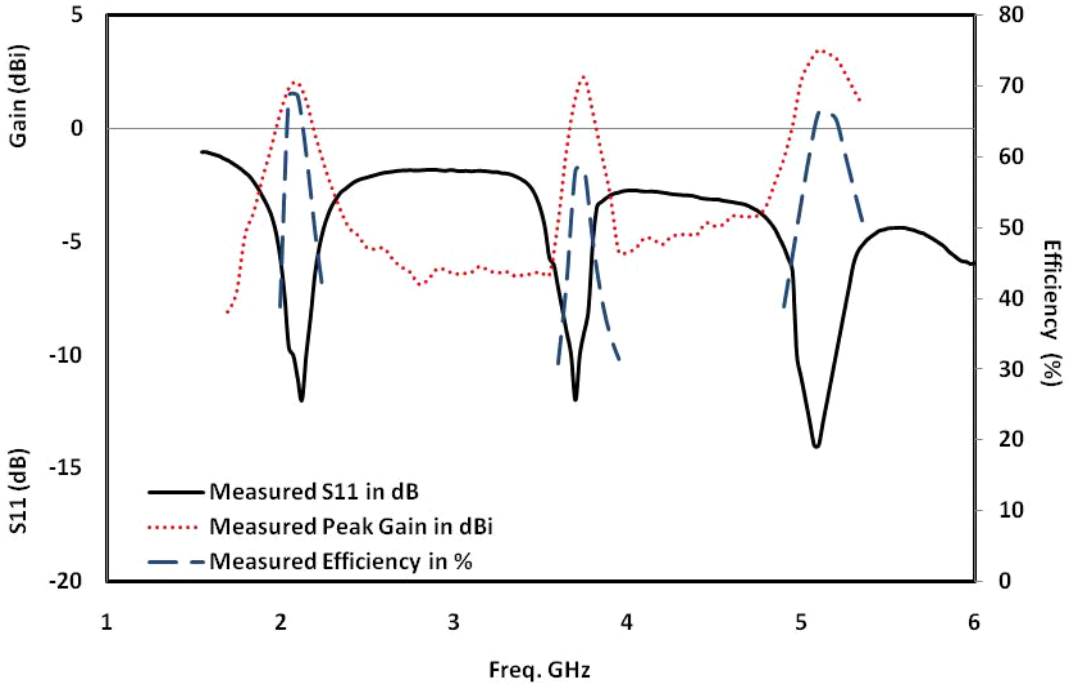

Figure 3-17: Measured S_{11}, peak gain and radiation efficiency

Table 3-4: Simulated and Measured gain and efficiency with and without the material losses

Parameters		**(f_1) 2.09 GHz**	**(f_2) 3.74 GHz**	**(f_3) 5 GHz**
Gain (dBi)	Measured with 0.02 FR-4 losses	2.05	2.32	4.47
	Simulated with Lossless material	2.24	3.70	5.53
Efficiency (%)	Measured with 0.02 FR-4 losses	70.12	60.29	66.24
	Simulated with Lossless material	99.8	96.5	99.6

3.3.7 Effects of Mobile Phone Housing and User's Hand on Antenna's Ground Plane

The effects of a human hand and mobile phone housing on the reflection coefficient S_{11}, radiation patterns, gain and efficiency of the antenna have also been investigated. Figure 3-18 (a) shows the simulation model of the antenna with the human hand model. The fingers and the palm are attached directly to the ground plane and the main substrate, respectively. In Figure 3-18 (b), the mobile phone housing model is in direct contact with the antenna and the hand model is then touching the housing of the mobile phone (the hand model is in direct touch the ground plane). The relative permittivity and conductivity of 3.5 and 0.02 S/m, respectively, for the mobile phone housing model [16] and of 54 and 1.45 S/m, respectively, for human hand model [18] have been used in simulations. The results in Figure 3-19 show that the human hand and mobile phone housing increase the S_{11} in the two lower frequency bands and slightly increase it in the higher frequency band.

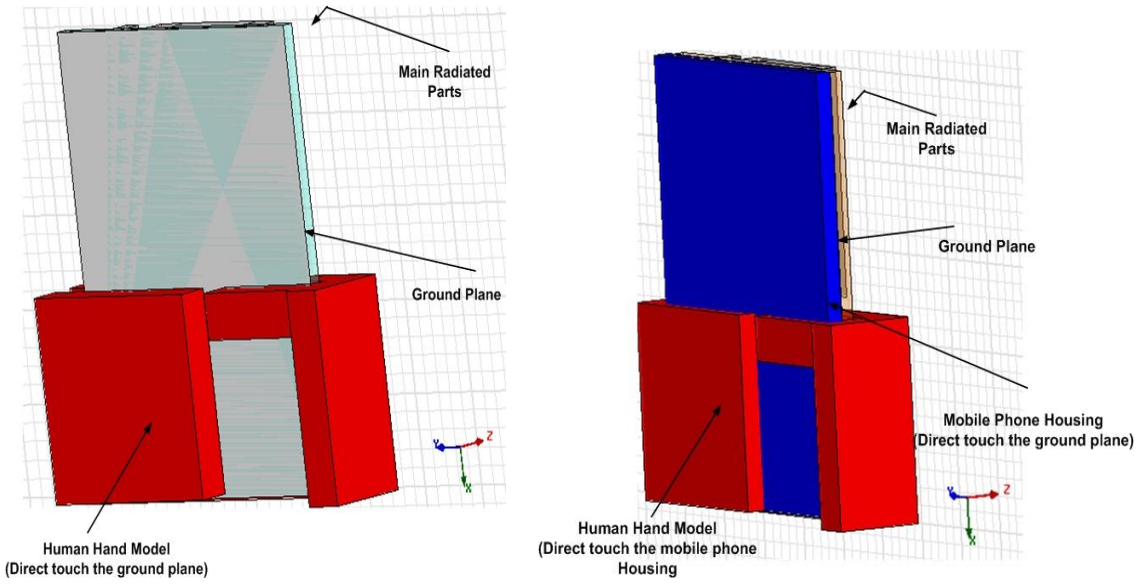

(a) **(b)**

Figure 3-18: The proposed antenna with (a) Hand (b) mobile phone housing and hand

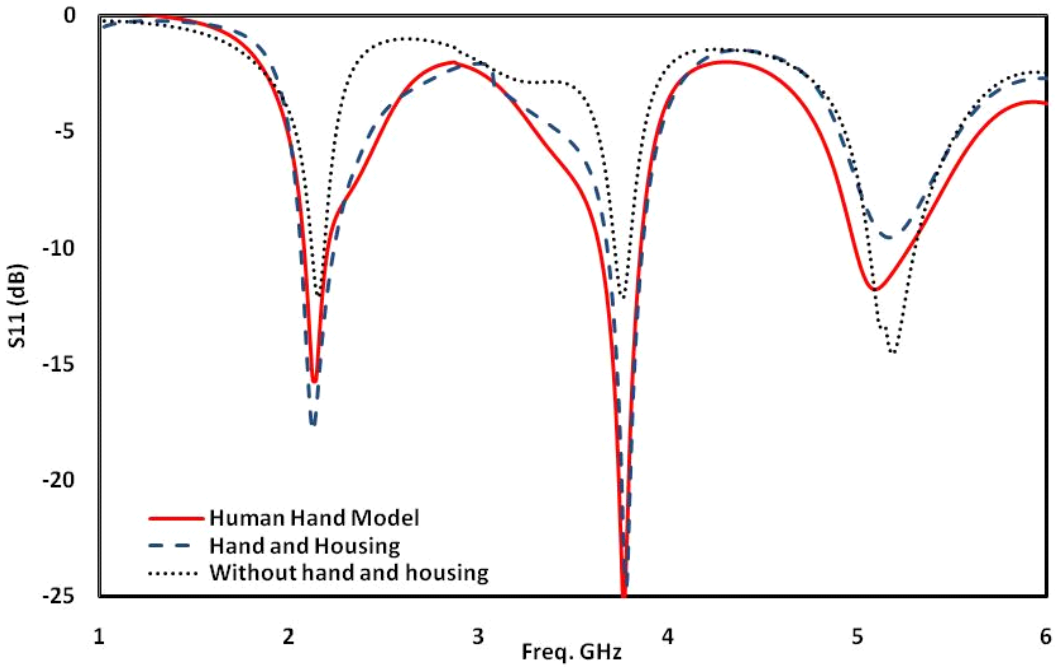

Figure 3-19: The effect of the human hand and the plastic housing of the mobile phone on S_{11}

With the human hand and mobile phone housing are in place, the radiation patterns at 2 GHz are shown in Figure 3-20. It can be seen that the shape of the radiation patterns does not change much. The simulated peak gain and radiation efficiency are shown in Figure 3-20. At 2 GHz, Figure 3-21(a) shows that the mobile phone housing and the hand increase the peak gain by 2 dB. However, if only the human hand is attached directly to the ground plane, the peak gain is decreased by almost 1 dB. This can also be observed in the radiation pattern of Figure 3-20 where the antenna loses some energy in the direction of the ground plane and gain from its maximum value. At 3.74 GHz and 5 GHz, the gains drop by approximately 1 dBi, yet maintaining the shape of the radiation patterns. There is no significant change in radiation efficiency when both the human hand model and mobile phone housing are present, as shown in Figure 3.21(b).

These results indicate that the ground plane of the proposed design is not too sensitive to the hand and mobile phone housing.

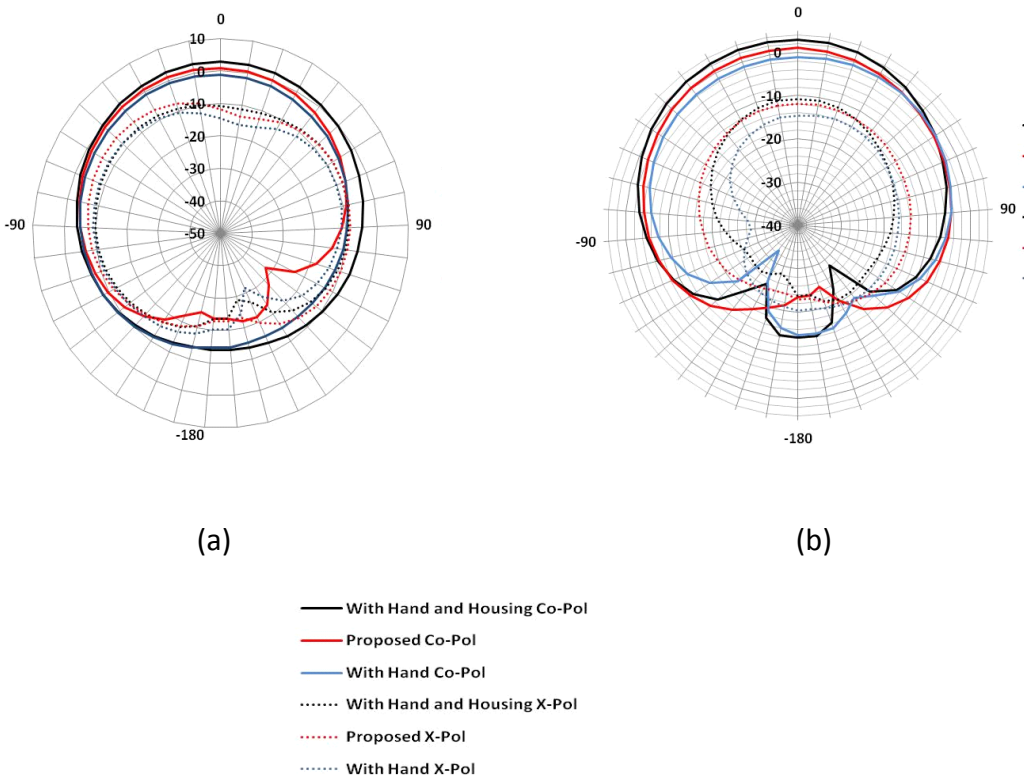

(a) (b)

Figure 3-20: Normalized Co-Pol and X-Pol radiation patterns at 2.09 GHz band in the presence of human hand model and the mobile phone housing in (a) X-Z Plane (b) Y-Z Plane

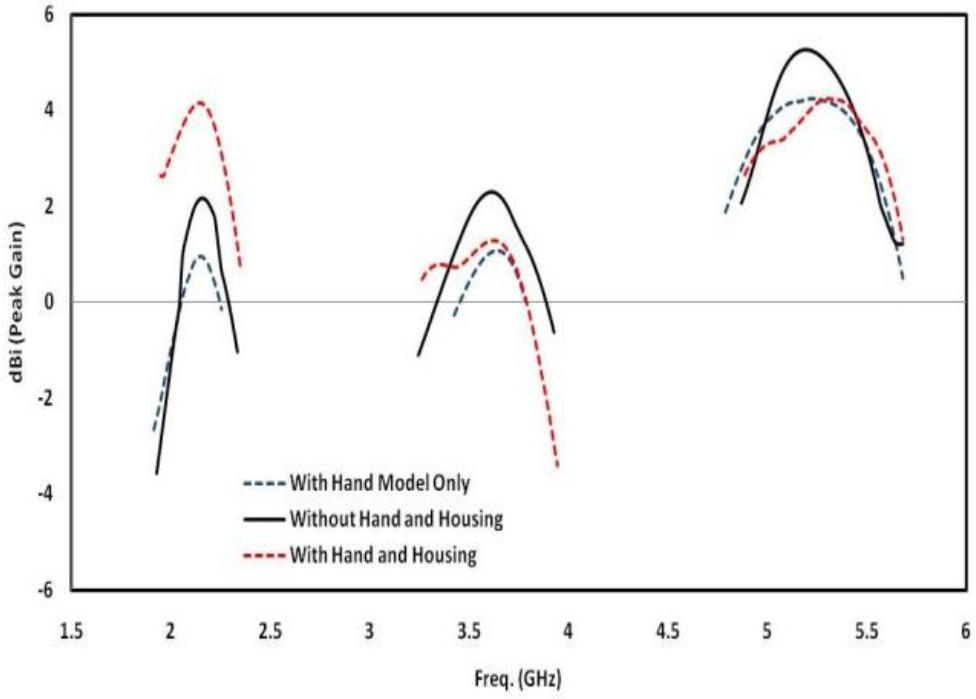

(a)

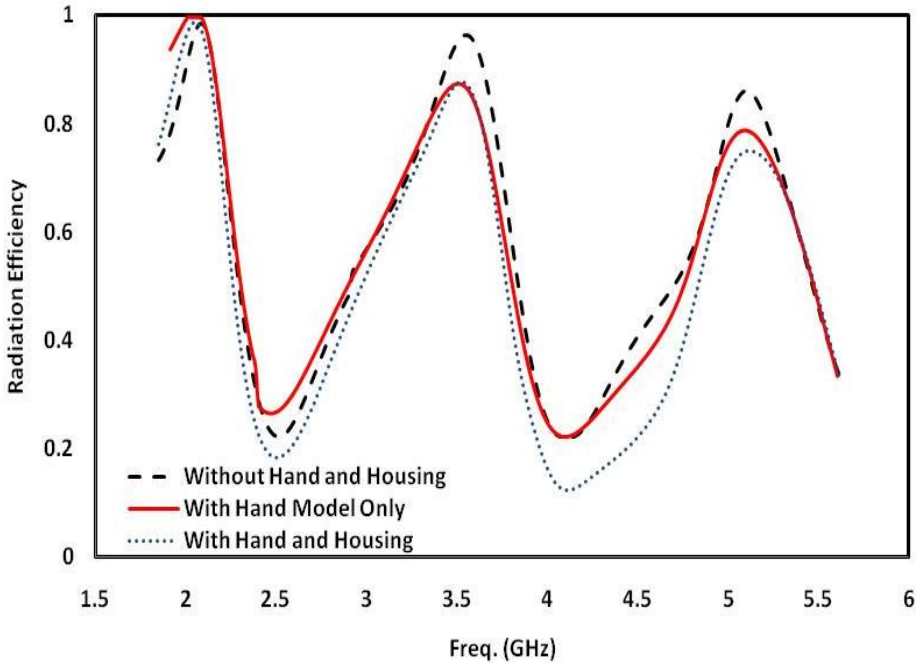

(b)

Figure 3-21: Simulated Results of the proposed antenna with human hand model and mobile phone housing (a) peak gain and (b) radiation efficiency

3.3.8 Effect of User's Hand at Different Positions on Antenna

It is also essential to examine the effects of the hand at different positions on the return loss, gain and efficiency of the antenna. In [19], results of studies showed a dual-band of the antenna was significantly affected by a hand placed on the top of the radiator with 1 cm gap between them. Here, the performances of the antenna with the hand in three different positions, positions 1, 2 and 3, as shown in Figure 3-22 (a) - (c), respectively, are studied. In position 1, the hand (palm) is placed 1 mm above the top of the radiator and the fingers are touching the ground plane on the other side. The results in Figure 3-23 (a) show that the first and the third resonances at 2.09 and 5 GHz remain about the same. The second resonance at 3.74 GHz slightly moves to 3.69 GHz. The S_{11} of the three bands are still greater than 6 dB (S_{11}<-6 dB), which is different from the results reported in [19]. In position 2, where the hand is at the centre of the antenna and the palm of the hand partially covering the radiator with 1 mm gap between them as shown in Figure 3-22 (b), the results in Figure 3-23 (a) show that the three resonant frequencies again remain about

the same. In position 3, where the hand model is relatively far from the radiator as shown in Figure 3-23 (c), the three resonances again remain about the same, as indicated in Figure 3-23 (a).

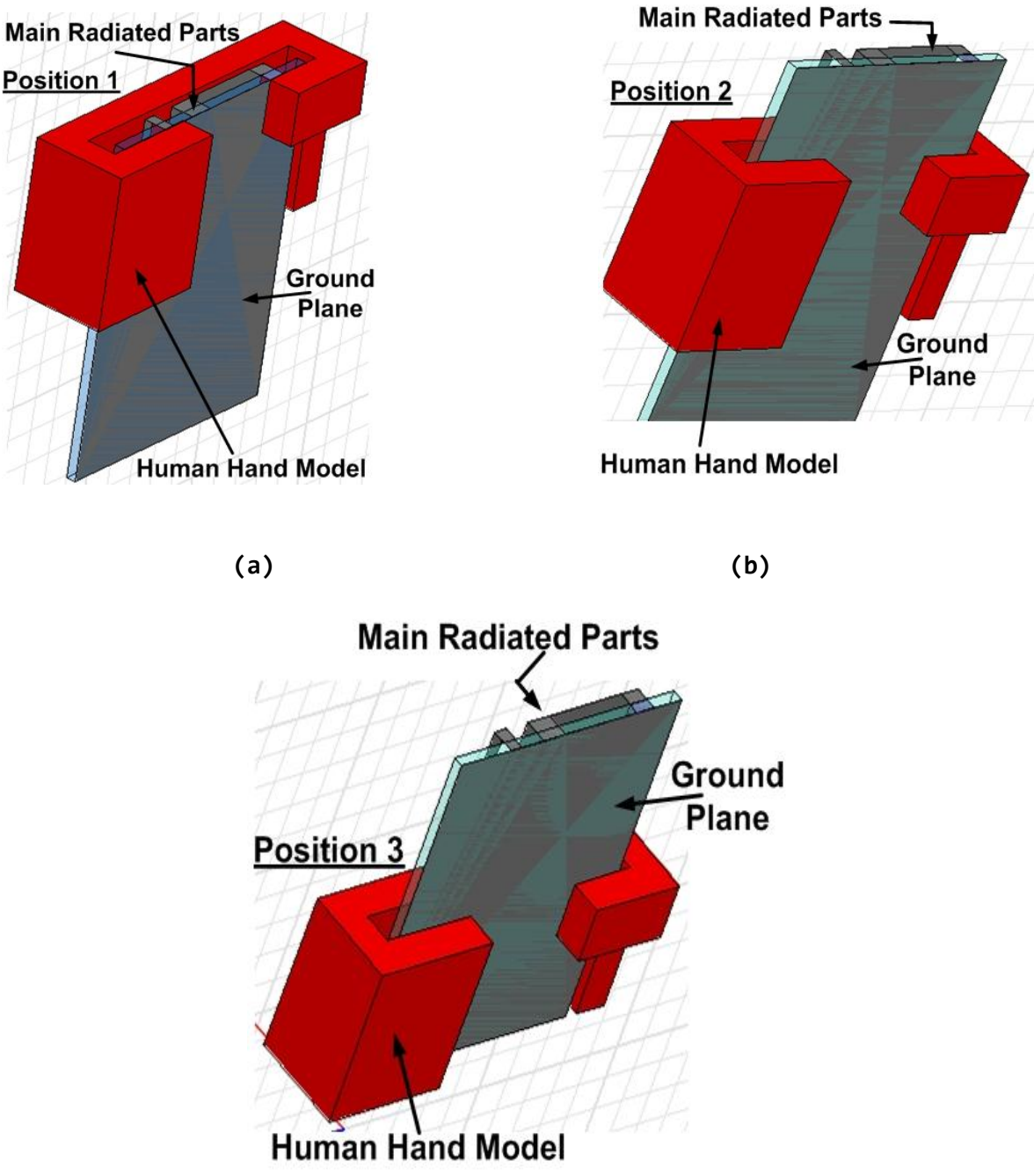

Figure 3-22: Simulation model for different positions of user's hand (a) User's hand covering radiator, (b) User's hand partly covering radiator and (c) User's hand not covering radiator of antenna.

The simulated results on the gain and radiation efficiency for the three different positions are shown in Figure 3-23 (b) - (c). It can be seen that, when the hand moves closer to the radiator, the gain drops by almost 0.7 dBi compared with that when the antenna in free space. The radiation efficiency drops to 63% when the hand moves closer to the radiator. These results indicate that, in these 3 positions, the performance of the antenna is not very much sensitive to the user's hand. The best position, in terms of maximum efficiency and gain, is when the user is holding the mobile phone from the bottom, i.e., position 3. When the user's hand gets closer to the radiator, the gain and the radiation efficiency drop slightly compared with the case when the antenna is in free space. Even for the worst case scenario where the user's hand is completely or partly covering the radiator with 1 mm gap between them, as in positions 1 and 2, the simulation results show that it still can attain above 60% efficiency which is considered quite acceptable for mobile phone applications unlike the design reported in [16] where the radiation efficiency is about 28% at 1795 MHz when the hand is covering the radiator. The gain only drops by 2.2 dBi in the first band of 2.09 GHz and by smaller amounts in the other bands.

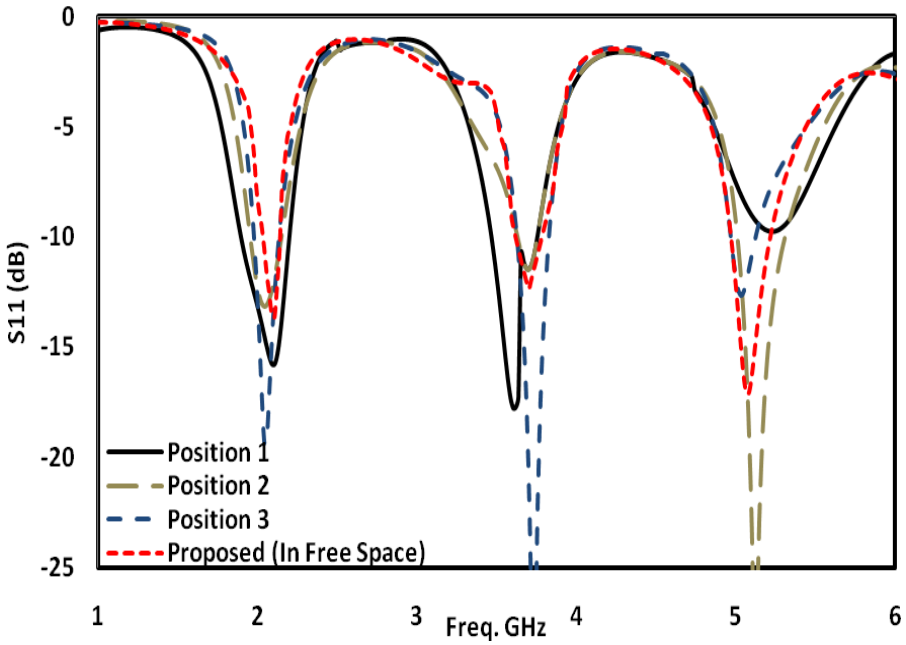

(a)

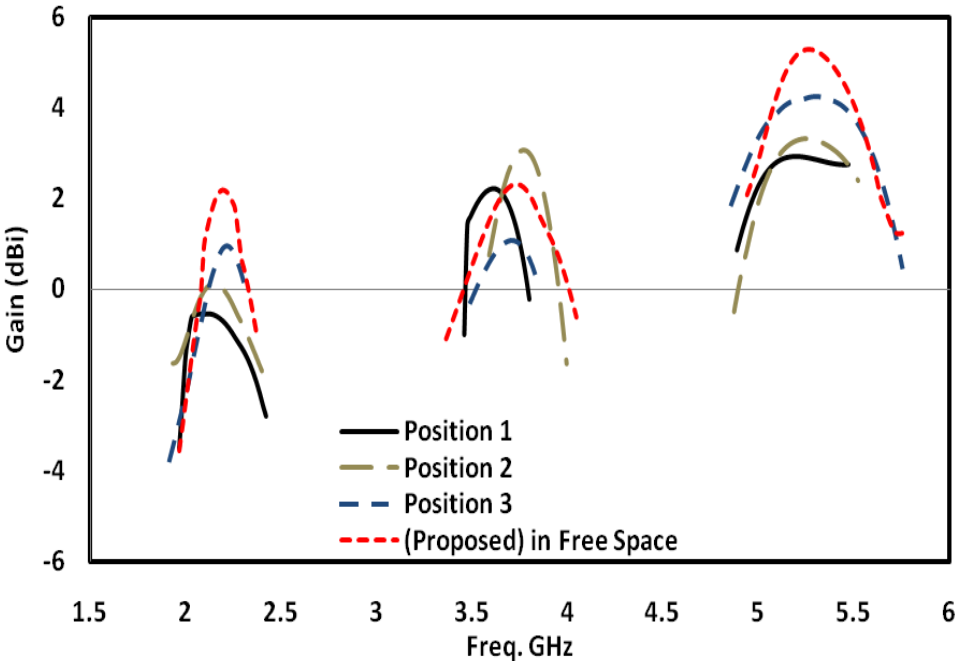

(b)

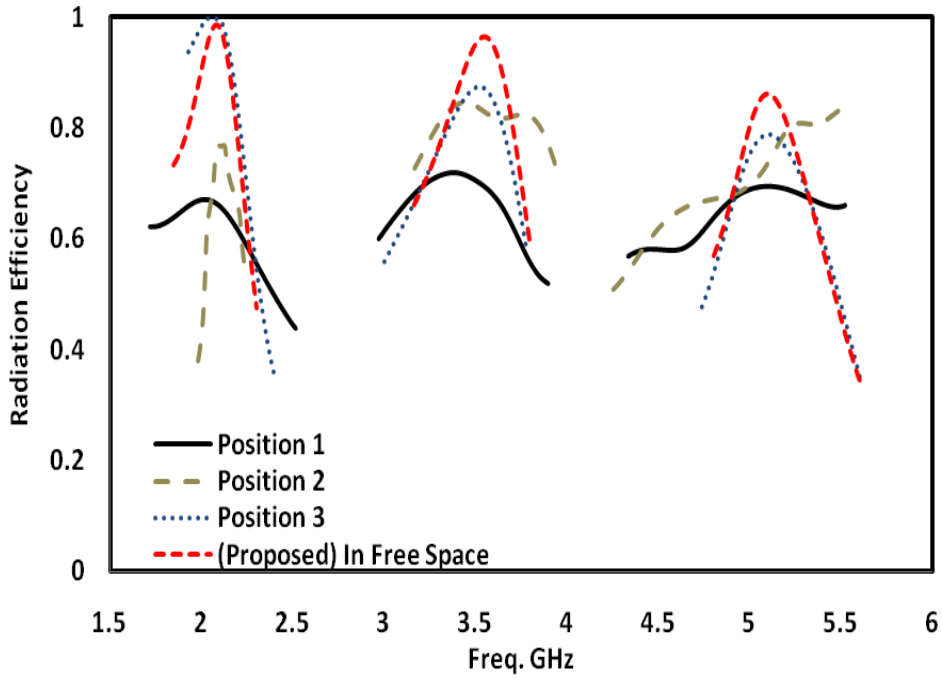

(c)

Figure 3-23: Effect of different positions of user's hand on (a) The reflection coefficient (S_{11}) (b) gain (c) radiation efficiency

3.4 Compact Printed Multiband Antenna with Independent-Control for Different Wireless Applications

3.4.1 Introduction

Based on the discussion in section 3.1, this section investigates the following points:

- Independent control over a wide range.
- Small size and simple design.
- Using sub-patches technique to generate multiple band operations.
- Targeting the lower frequency bands.

Therefore, a design of a low profile compact printed multiband antenna is presented. The antenna consists of a main patch, four sub-patches and a ground plane for generating five frequency bands, bands #1, #2, #3, #4 and #5 at 0.92, 1.73, 1.98, 2.4 and 2.9 GHz, respectively. In the proposed antenna, each of the frequencies in bands #1 to #5 can be adjusted and set independently over a wide range, i.e., 18.78%, 22.75%, 4.51%, 11% and 8.21%, respectively using just one parameter of the antennas.

3.4.2 Antenna Layout and Design Procedure

A simple and compact multiband antenna, having five frequency bands, bands #1, #2, #3, #4 and #5 at 0.92, 1.73, 1.98, 2.4 and 2.9 GHz, respectively, with the feature of independently setting on individual frequencies, is proposed here. The geometry of the proposed antenna is shown in Figure 3-24, with key parameters listed in Table 3-5. It consists of a main patch, four sub-patches (sub-patches #1, #2, #3 and #4), a ground plane and a 50-Ω feed line. The antenna is mounted on an FR-4 substrate with a thickness of 1.57 mm and a relative permittivity of 4.4. The structure occupies a total area of 45.6 × 50 mm and has a ground plane of 50 × 50 mm on the other side of the substrate. Computer simulation using the HFSS is employed to design the antenna. In the design procedure, the main patch is first designed and the four sub-patches, sub-patches #1, #2, #3 and #4, are then designed and added one-by-one to the main patch to generate the five desirable frequency bands required for the other standards and applications.

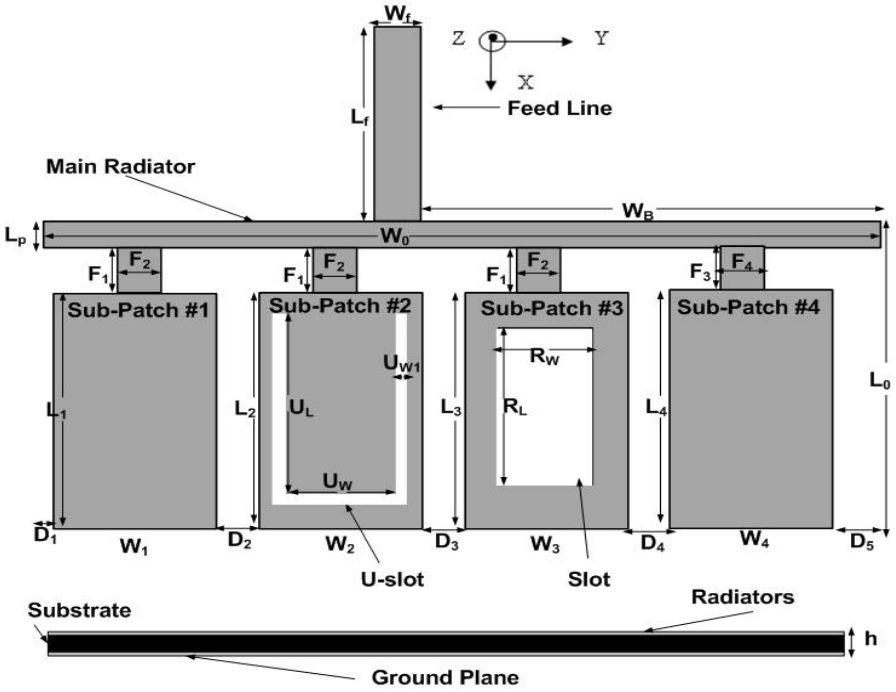

Figure 3-24: Structure of the proposed fixed design

Table 3-5: Dimensions of the proposed printed antenna (in mm)

L_o	L_1	L_2	L_3	L_4	L_f	L_P
31	24	24	24	24	14.6	4
W_o	W_1	W_2	W_3	W_4	W_f	W_B
50	8	10	10	12	3	27
F_1	F_2	F_3	F_4	D_1	D_2	D_3
3	2	3	2.5	1	2	2
D_4	D_5	h	U_L	U_W	R_L	R_W
3	2	1.57	19	7	14	6
Ground Plane						
50 x 50						

3.4.3 Design Methodology

The design steps can be easily described with the aids of Figure 3-25(a) - (e) as follows.

Step 1: The main patch, with an area of 50 mm × 30 mm (length × width), is designed to generate operate band #4 at 2.4 GHz for the Wireless Local Area Network (WLAN) band and optimised in terms of minimizing the reflection coefficient s_{11} across the band by computer simulation. Figure 3-25(b) shows the layout and the optimised s_{11} for the main radiation patch. At 2.4 GHz, s_{11} = -18 dB.

Step 2: Sub-patch #1 is added to the main patch as shown in Figure 3-25(b) and designed to generate the resonant frequency for band #1 at 0.92 GHz with s_{11} = -7 dB. To make room for adding the sub-patch without increasing the antenna size, the width of the main radiator is reduced to 4 mm, so the main patch in Figure 3-25(b). looks like a strip line. It can be seen that adding sub-patch #1 and reducing the width of the main patch increases the s11 for band #4 at 2.4 GHz from -18 dB to about -7 dB which is undesirable.

Step 3: Sub-patch #2, with layout shown in Figure 3-25(c), is added to the main patch. A U-Slot cut on sub-patch #2 is used to generate band #2 at 1.73 GHz. The dimensions of sub-patch #2 are optimised in terms of minimizing s_{11} at the resonant bands. It can be seen that sub-patch #2 does not alter the frequencies for bands #2 and #4 generated by the main patch and sub-patch #1, respectively, but lowering down their s_{11} values. Sub-patch #2 also generates an unwanted band at 1 GHz which will become insignificant in the final design (in Step 5). Note that, without the U-Slot, band #2 disappears, as can be seen in Figure 3-25(c).

Step 4: Sub-patch #3 is added to the main radiation patch as shown in Figure 3-25(d). A rectangular slot is cut on the sub-patch to generate a band #5 at 2.9 GHz. The dimensions of the sub-patch are optimised and the simulated s_{11} is shown in Figure 3-25(d). It can be seen that all the bands generated are not affected by adding sub-patch #3, except band #1 at 0.92 GHz which is slightly detuned by sub-patch #3. However, adding sub-patch #4 in Step 5 will tune the resonant frequency back to 0.92 GHz as seen later. Note that, without the rectangular slot, band #5 disappears, as can be seen in Figure 3-25(d).

Step 5: Sub-patch #4 is added to generate band #3 at 1.98 GHz as shown in Figure 3-25(e), resulting in five different bands, at 0.92, 1.73, 1.98, 2.4 and 2.9 GHz, for serving different applications. The dimensions of the sub-patch are optimised in terms of minimizing the s_{11} in all bands, so the s_{11} values in these five bands are much lower than those without having

sub-patch #4. For example, when sub-patch #1 is added to the main patch in Step 1, the s_{11} in band #1 is only about -7 dB. When all the sub-patches are added, the s11 in band #1 is reduced to more than -10 dB. Thus sub-patch #4 plays a major role in matching. The key parameters of the antenna are listed in Table I. The final design of the five-band antenna is fabricated on a substrate, as shown in Figure 3-25(f), with the same parameters used for simulation. The s_{11} of the prototyped antenna is measured using an Agilent N5230A network analyzer and shown in Figure 3-25(e) for comparison. It can be seen that the simulated and measured s_{11} are in good agreements.

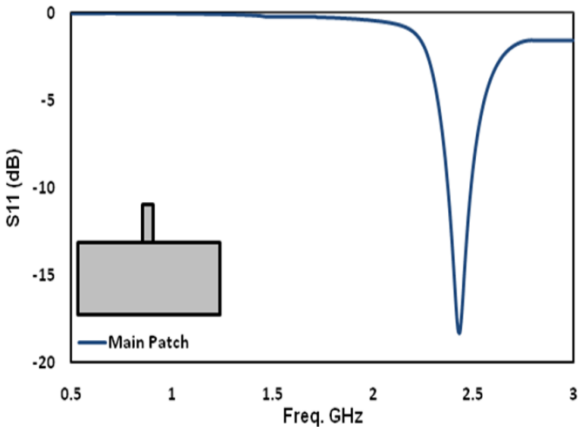

(a)

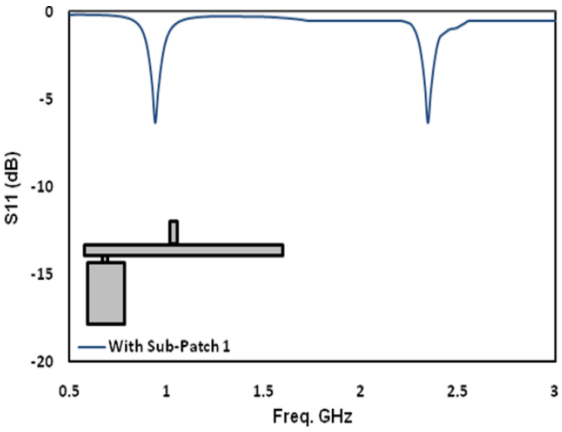

(b)

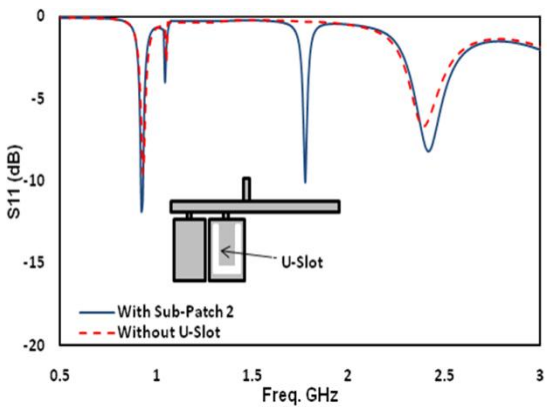

(c)

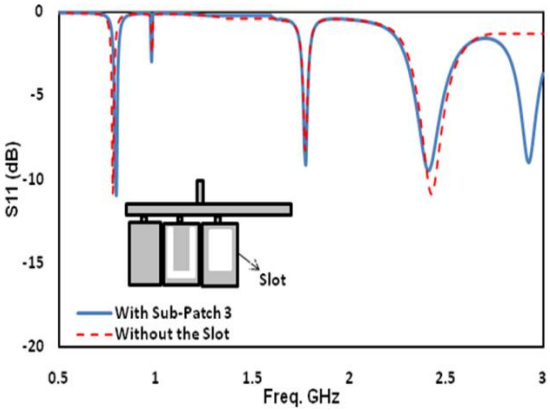

(d)

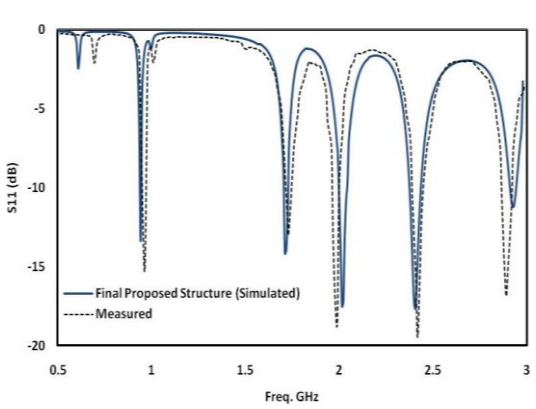

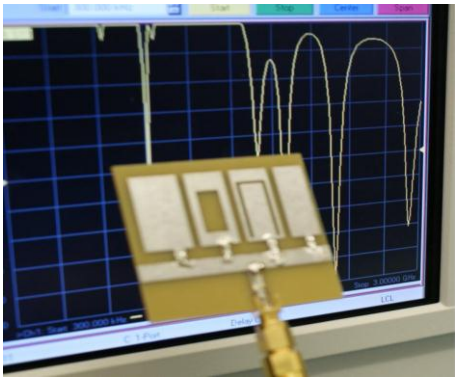

(e) **(f)**

Figure 3-25: The steps involved in designing the proposed antenna (a) Main patch (b) Main Patch and Sub-Patch 1 (c) Main patch and sub-patch 1 & 2 with and without U-slot (d) Main patch and sub-patch 1, 2 & 3 with and without rectangular slot (e) Simulated and measured results

3.4.4 Current Distributions

The operation of the five-band antenna is further studied using surface current distributions at the five resonant frequencies and simulated results are shown in Figure 3-26. For band #1 at 0.92 GHz, Figure 3-26(a) shows that the current mainly flows on the main radiator and sub-patch #1 which contribute to most radiation. The other sub-patches simply help improve matching. This explains the reason that when all sub-patches are added to the main patch, the s_{11} at 0.92 GHz is reduced from -7 dB to more than -10 dB. For band #2 at 1.73 GHz, Figure 3-26(b) shows that the current is mainly concentrating on sub-patch #2 which contributes most radiation. Similarly, for bands #5 and #3 at 2.9 and 1.98 GHz, respectively, sub-patches #3 and #4 have the highest current densities and so are responsible for the corresponding radiations. The current paths indicated in Figure 3-26(a) - (d) where λ is the wavelength at the resonant frequency of the respective band and given by $\lambda = \lambda_0 / \sqrt{(\varepsilon_r + 1)/2}$, with λ_0 being the free space wavelength.

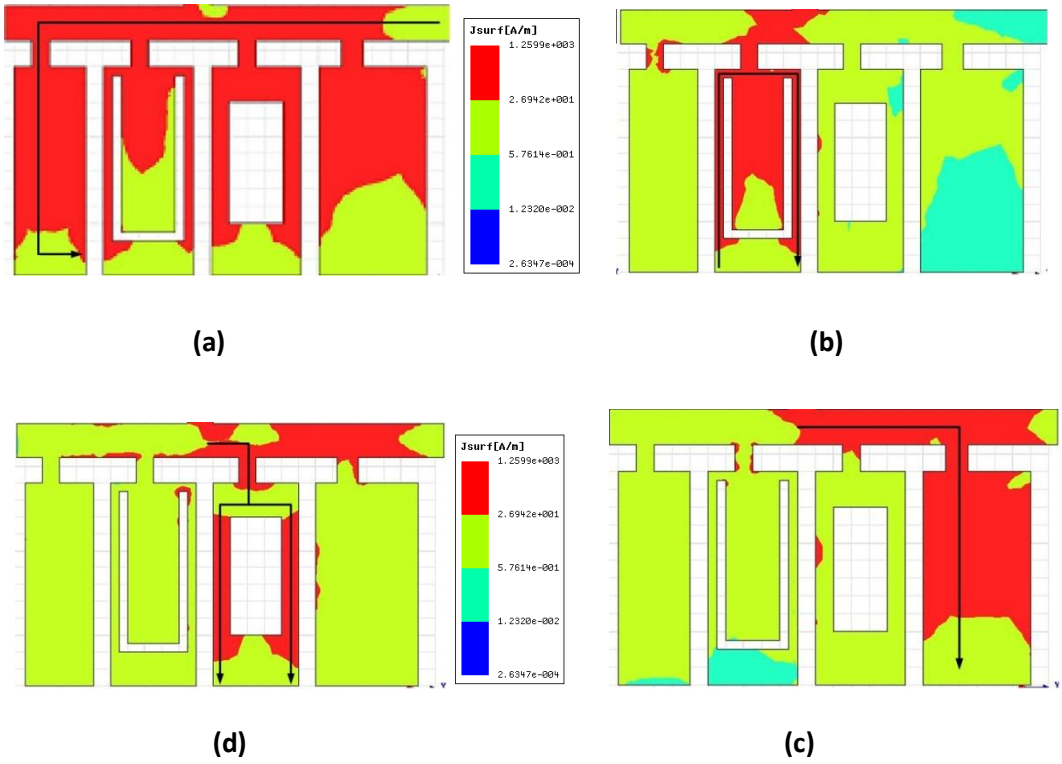

Figure 3-26: Simulated surface current distributions at (a) 0.92 GHz, (b) 1.73 GHz, (c) 2.9 GHz and (d) 1.98 GHz

3.5 Independent Control Concept

In this proposed antenna, we can independently set the individual frequency bands, one-by-one, without affecting other bands. In the previous results in section 3.4.4, The current paths responsible for radiations at different resonant frequencies were identified. Thus, those antenna parameters can be change, which in turn alter the lengths of the current paths and set the resonant frequencies independently. For example, at 0.92 GHz band, Figure 3-27(a) shows that the current travels along sub-patch #1 in the Y-direction, thus changing the width W_1 of sub-patch #1 alters the resonant frequency 0.92 GHz but without affecting other bands. Applying this same principle to Figure 3-27 (b)-(d), it can be shown that the lengths L_2, L_3, and L_4 in sub-patches #2, #3 and #4, respectively, can be used to independently set the corresponding frequencies 1.73, 2.9 and 1.98 GHz to other values. The simulation results on the effects of varying the parameters W_1, L_2, L_3, and L_4 on the frequency bands are shown in Figure 3-27. It is can be seen from Figures 3-27(a)-(d) that, the parameters , W_1, L_2, L_3, and L_4 can be used to independently adjust the frequency bands

at 0.92, 1.73, 1.98, and 2.9 GHz over the wide ranges of 18.78%, 22.75%, 4.51%, and 8.21% respectively. Table 3-6 summaries these results.

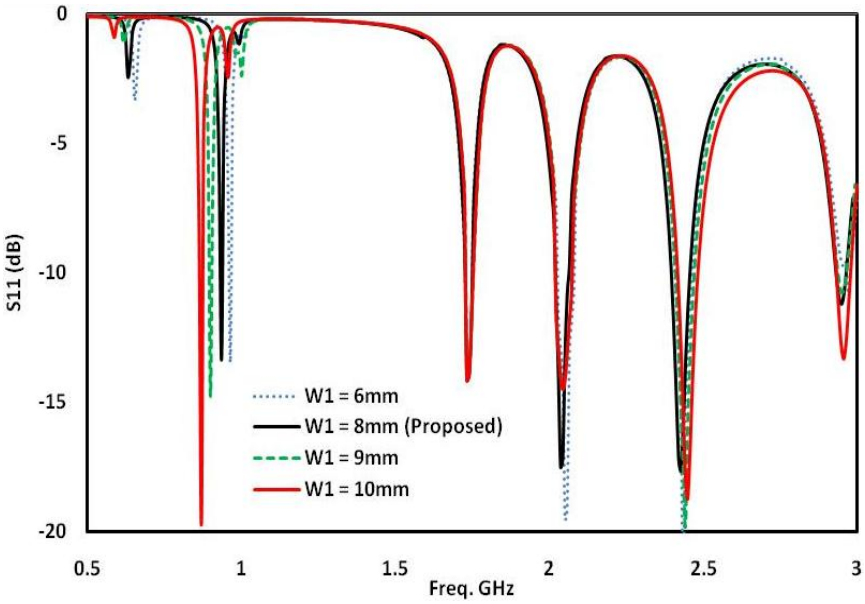

(a)

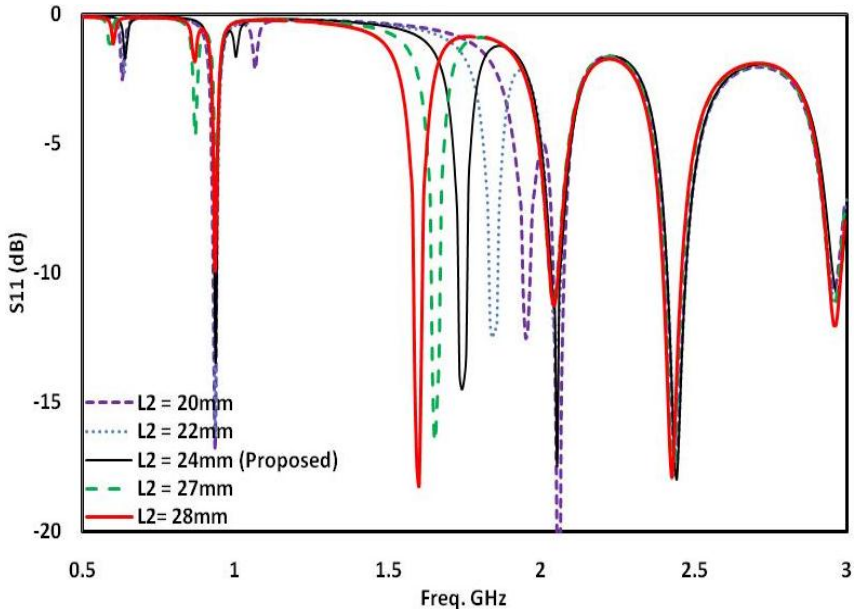

(b)

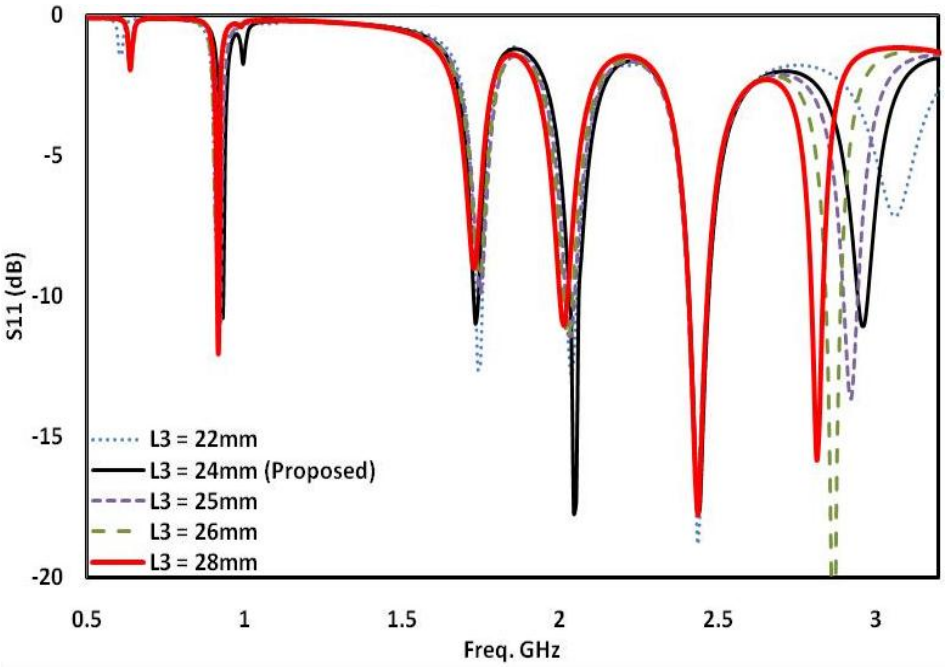

(c)

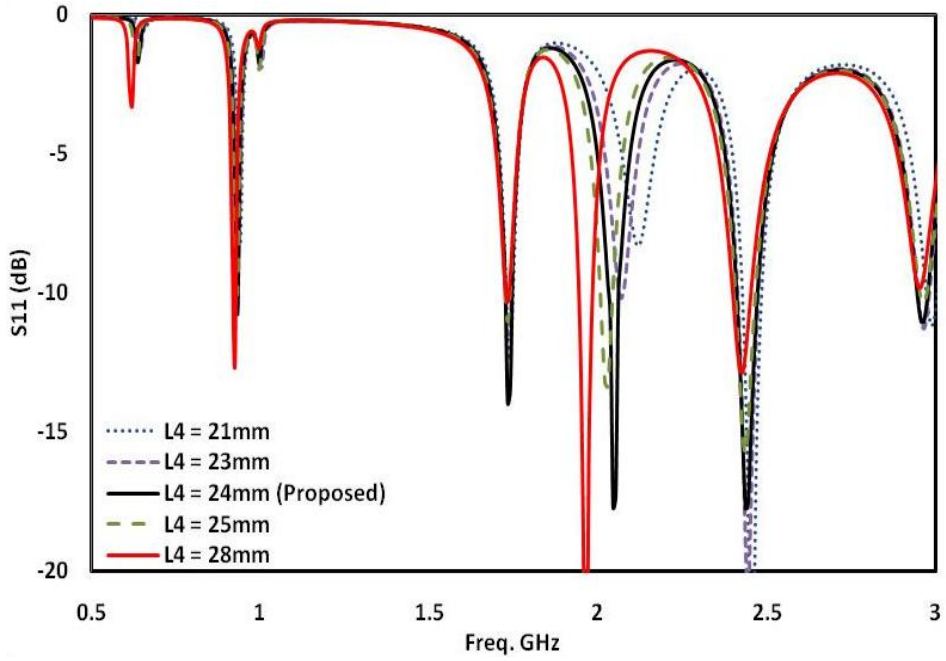

(d)

Figure 3-27: Parametric study on the fixed design showing the independent control at (a) 0.92 GHz band (b) 1.7 GHz band (c) 2.9 GHz band and (e) 1.98 GHz band

Table 3-6: Effects Of Changing W_1, L_2, L_4, and L_3, On S_{11}

Parameters	0.92 GHz	1.73 GHz	1.98 GHz	2.4 GHZ	2.9 GHz
W_1	820-990 MHz 18.78%	Fixed	Fixed	Fixed	Fixed
L_2	Fixed	1550-1948 MHz 22.75%	Fixed	Fixed	Fixed
L_3	Fixed	Fixed	1952-2044 MHz 4.51%	Fixed	Fixed
L_4	Fixed	Fixed	Fixed	Fixed	2800-3044 MHz 8.21%

3.5.1 Simulated and Measured radiation patterns

The measurements were conducted at the Small Antenna Radiated Testing Range (SMART) of the National Physical Laboratory (NPL). After measuring the co and cross polar patterns, the results were normalized with the maximum value. The normalized measured and simulated radiation patterns for the co- and cross polar far field E-plane (X-Z plane) and H-plane (Y-Z plane) at 0.92, 1.73, 1.98, 2.4 and 2.9 GHz are shown in Figure 3-28 (a) - (e) respectively. An example of measured 3D pattern is shown in Figure 3-28 (f) for 0.92 GHz.

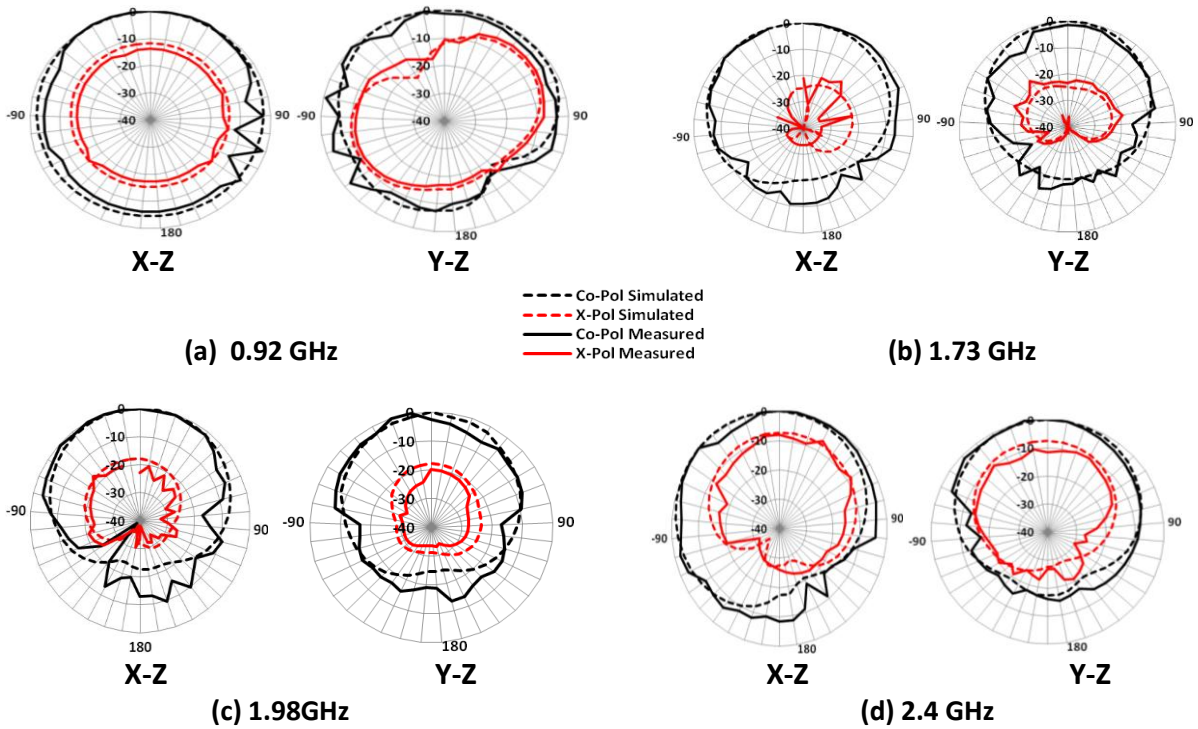

(a) 0.92 GHz (b) 1.73 GHz

(c) 1.98GHz (d) 2.4 GHz

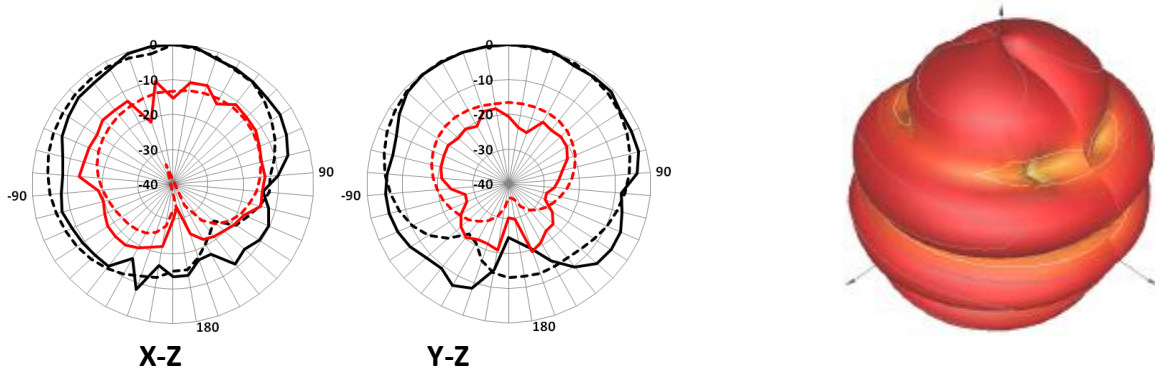

(e) 2.9 GHz (f) 2.9 GHz

Figure 3-28 Measured versus simulated Co-Pol and X-Pol radiation patterns for X-Z and Y-Z planes at (a) 0.92 GHz (b) 1.73 GHz (c) 1.98 GHz (d) 2.4 GHz (e) 2.9 GHz and (f) 3D measured patterns at 2.9 GHz.

3.6 Summary

Small and ultra-slim multiband antennas for wireless and mobile applications have been investigated in this chapter. Tackling the challenge of limited space in modern small and slim device was one of the main motivations of this chapter. The multiplicity of bands and the size reduction have been achieved by the use of different methods including different shapes of slots and sub-patches. The capabilities of Planar Inverted-F Antenna (PIFA) and patch antenna have been extended to include independent control over a wide range. The effect of user's hand and housing of mobile phone have been discussed and taken into account to minimise their effects in real applications.

In section 3.2, U-Slots technique has been used to minimise the size of the antenna and to create multiple band operations. The antenna is optimised for WiMAX applications. Other applications are also possible. In section 3.3, an ultra-slim PIFA for mobile handsets has been designed. The effect of the feed location and the sensitivity of the ground plane have been studied. In addition, the ground plane of the antenna has minimal effects on the antenna performance and the performance is not too sensitive to the human hand and the mobile phone housing used in the studies. This feature allows the nearby electronic components to be placed closed to the antenna, making the overall size the mobile phones even more compact and thin.

In section 3.4, Sub-patches technique has been used to allow the antenna to operate in five-band. Some sub-patches had U-slot and rectangular shape to disturb the current path on the sub-patch.

All the presented antennas in this chapter have the independent control feature which was obtained by studying the key controlling parameters of each band. This feature allow the antennas to cover the major wireless and mobile applications and standards such as the Global System for Mobile Communications (GSM900 and 800), Personal Communication System (PCS 1800 and 1900), Digital Communication Systems (DCS), Global Position System (GPS), Universal Mobile Telecommunications System (UMTS), Wireless Local Area Networks / Bluetooth (WLAN) and Worldwide Interoperability for Microwave Access (WiMAX), etc.

Finally, the designed antennas have been fabricated and tested to verify the results from HFSS software. The measured and simulated results showed very good agreement.

3.7 References

[1] M.C. Huynh, and W. Stutzman, "Ground Plane Effects on Planar Inverted-F Antenna (PIFA) Performance", lEE Proceeding Microwave Antennas Propagation, Vol. 150, no. 4, pp. 209-213, August 2003.

[2] Y. Chi, and K. Wong, "Internal Compact Dual-Band Printed Loop Antenna for Mobile Phone Application", IEEE Transactions on Antennas and Propagation, vol. 55, no. 5, pp. 1457-1462, May 2007.

[3] Yi Huang, and Kevin Boyle, "Antennas: From Theory to Practice", John Wiley & Sons, ISBN: 978-0-470-510'''t28-5, 2008.

[4] K. Wong, S. Su, C. Tang, and S. Yeh, "Internal shorted patch antenna for a UMTS folder-type mobile phone", IEEE Transactions on Antennas and Propagation, vol. 53, no. 10, pp. 3391- 3394, Oct. 2005.

[5] Z. Chen, Terence S. See, and X. Qing, "Small Printed Ultrawideband Antenna with Reduced Ground Plane Effect", IEEE Transactions on Antennas and Propagation, vol. 55, no. 2, pp. 383-388, Feb. 2007.

[6] Steven R. Best, "The Significance of Ground-Plane Size and Antenna Location in Establishing the Performance of Ground-Plane-Dependent Antennas", IEEE Antennas and Propagation Magazine, vol. 51, no. 6, pp. 29-43, Dec. 2009.

[7] W. Stutzman and G. Thiele, Antenna Theory and Design, 2nd ed. New York: Wiley, 1998

[8] C.A. Balanis, “Antenna Theory Analysis and Design” Wiley & Sons, (3rd Edition), 2005.

[9] www.wimax.com/commentary/wimax_weekly/2-3-3-ofdm-parameters-in-wimax-cont

[10] T. H. Loh, M. Alexander, F. Widmer, P. Miller, D. Knight, "Validation of a New Small-Antenna Radiated Testing Range", 3rd European Conference on Antennas and Propagation, Berlin, Germany, pp.699–703, Mar. 2009.

[11] M. Alexander, T. H. Loh, A. L. Betancort, "Measurement of electrically small antennas via optical fibre," Loughborough Antennas & Propagation Conference, LAPC 2009, pp.653-656, Nov. 2009.

[12] D. Kim, J. Lee, C. Cho, and T. Lee, "Design of a Compact Tri-Band PIFA Based on Independent Control of the Resonant Frequencies", IEEE Transactions on Antennas and Propagation, vol. 56, pp. 1428-1436, 2008.

[13] J.H. Lim, G.T. Back, Y.I. Ko, C.W. Song, T.Y. Yun, "A Reconfigurable PIFA Using a Switchable PIN-Diode and a Fine-Tuning Varactor for USPCS / WCDMA / m-WiMAX / WLAN", IEEE Transactions on Antennas and Propagation, vol.58, no.7, pp.2404-2411, July 2010.

[14] H. F. AbuTarboush, R. Nilavalan, D. Budimir, and H.S. Al-Raweshidy, "Double U-slots patch antenna for tri-band wireless systems", International Journal of RF and Microwave Computer-Aided Engineering, vol. 20, no. 3, pp. 279-285, 2010.

[15] M. Abedin, M. Ali, "Modifying the ground plane and its effect on planar inverted-F antennas (PIFAs) for mobile phone handsets", IEEE Antennas and Wireless Propagation Letters, vol. 2, pp. 226- 229, 2003.

[16] Y. Chi, and K. Wong, "Internal Compact Dual-Band Printed Loop Antenna for Mobile Phone Application", IEEE Transactions on Antennas and Propagation, vol. 55, no. 5, pp. 1457-1462, May 2007.

[17] http://www.satimo.com/

[18] D. Zhou, R.A Abd-Alhameed, C.H. See, A.G. Alhaddad, and P.S. Excell, "Compact Wideband Balanced Antenna for Mobile Handsets", IET Microwave Antennas and Propagation Journal, vol. 4, pp. 600 - 608, 2010.

[19] Zi Dong Liu, P.S Hall, D. Wake, "Dual-frequency planar inverted-F antenna," IEEE Transactions on Antennas and Propagation, vol.45, no.10, pp.1451-1458, Oct 1997.

Chapter 4

Switchable Multiband Antennas

4.1 Introduction

Future cognitive communication systems will require reconfigurable antennas (Switchable) capable of operating over a wide range and over multiple wireless standards [1]. Therefore, the antenna should be designed to have multiple band and wideband operation to cover multiple standards at the same time. This requirement can be achieved by using switchable antenna (coarse tuning) capable of operating in wideband and multiband operations to cover different standards.

It is a well known that patch antennas have narrow bandwidth, which can limit their uses in any applications requiring wideband antennas. A variety of studies has come up with different techniques to achieve wideband operation for printed antennas. Some of the techniques employed are changing the physical size of the antenna, modifying the radiator shape (which sometime increases antenna size) and adding additional parts such as multi layers or gaps (which again make the antenna large and of a high profile). Other techniques include using U-slot array [2], shorting wall [3], folded shorting wall [4], Y-V Slot [5], slots form [6], stacked patch [7], pair of slits on the patch (with total size of the antenna 150 x 150 x 14.3 mm^2) [8], E-shaped patch on thick substrates with ground plane size of 140 x 210 mm^2 [9] and using circular arc shaped slot on thick substrate [10]. The designs in [2]-[10] can achieve wide impedance bandwidths. However, these antennas are larger in sizes and difficult to fit into small and slim devices.

A reconfigurable (switchable) antenna is another solution to achieve a wide impedance bandwidth by switching ON and OFF some parts of the antenna. In literature, few papers were found to use this approach for switching between wideband and narrowband operations. For example in [11], studies were done on switching between dual ports, one port for Ultra Wideband (UWB) and the other port for a single narrowband. In [12]-[13], switching between UWB and a single narrowband was reported. However, the use of an UWB antenna for multiband applications could result in unwanted emissions in the transmission mode.

Therefore, in section 4.2, a single feed switchable wideband and multiband antenna using two patch elements on a planar structure is proposed. Dual-band modes are achieved by switching "ON" either one of the two patch elements, while the wideband mode with an impedance bandwidth of 33.52% is obtained by switching "ON" both patch elements. The antenna occupies a compact volume of 50 x 50 x 1.57 (3925mm^3), including the ground plane. The frequencies in the dual-band modes can be independently controlled over a wide range without affecting the wideband mode. This approach help to overcome the need for increasing the surface area normally incurred when designing wideband patch antennas.

Moreover, several studies on switchable multiband-antenna designs for different wireless applications using H-shape [14]-[17] and T-shape antennas [18]-[21] have been reported. Although fixed multiband antennas can be used in different wireless systems, they lack the flexibility to accommodate new services when compared with reconfigurable antennas which can be considered as one of the key advances for future wireless communication transceivers. In the past few years, there has been a significant interest in the field of reconfigurable-multiband antennas. Different techniques used for reconfigurable antennas were reported in [22]. One of the advantages of reconfigurable antenna is to use the same antenna for multiband operation, thus the total antenna volume can be reduced when compared with those of having fixed multiband, leading to a reduction in the overall volume of wireless device and more space for integrating with other electronic components.

An independent-multiband Planer Inverted-F Antenna (PIFA) was studied in [23], where three resonant frequencies were generated and controlled by employing additional parts in the main radiating patch.

Multiband antennas can cover multiple frequencies using a single antenna and so are very desirable for wireless applications. However, fixed multiband antenna usually requires complicated filters with inflexible requirements to improve their out-of-band noise rejection. The filters are bulky and can add complexity to the communication systems [22]. As a solution to these problems, reconfigurable antenna can achieve a better out-of-band noise rejection. Some designs from the literature review on switchable antennas are given in Table 4-1.

Table 4-1 Some related work in switchable antennas

Reference	Antenna Type	Bands	Switches	Size	Remarks
24	PIFA	2	2	70 x 30	Switching between 2 bands
25	Monopole	1	4	120 x 120 x 7.8	switching between 8 bands (1.8 - 2.4)
26	Quasi-Yagi Dipole	1	3	102 x 87	Switching between 4 bands
27	PIFA	1	4	40 x 100 x 8	Switching between 5 bands
28	Patch	1	3	24 x 25 x 1.524	Switching between 4 bands
29	PIFA	2	2	100 x 42	Switching between 4 bands
30	Annular Slot	1	3	40 x 40	Switching between 2.4 and 5.2 GHz bands
31	Branched	Up to 6	3	96 x 9 x 3	Switching between a group of 6 bands
32	Patch	2	10	38 x 25 x 1.524	Selected dual frequencies (4.8 and 7.6 GHz)

From Table 4-1 and the literature on switchable antennas, the following points can be observed:

- When using more than one switch, the antenna can offer additional features. However, the switches will add complexity to the communication system as the biasing will be more complicated. Therefore, to achieve reconfigurable behaviour, less switches should be used as much as possible.
- The number of bands increases with the increase in size. However, in modern wireless devices or systems, the size of the devices are getting smaller while many different services have to be offered in one device. The challenge is not only to reduce the size of the antenna but also to make the antenna capable of operating in different wireless and mobile applications.

Therefore, in section 4.3, the design of a planar antenna with frequency reconfigurability is proposed. The antenna has an H-shaped radiator, a CPW and a varactor diode connecting the upper and lower arms of the H-shape radiator. Through the use of DC bias voltage across the varactor diode, the antenna can be operated in three different modes, a single-band mode covering the Global System for Mobile communications 1900 (GSM1900) system, a dual-band mode at 1.88 and 2.4 GHz to cover GSM1900 and Bluetooth or Wireless Local Area Network (WLAN) systems, respectively, and a tri-band mode at 1.57, 1.88 and 2.4 GHz to cover the GSM1900, WLAN and Global Positioning System (GPS), respectively. The frequency bands in these modes can also be controlled by the varactor diode and the widths of the arms in the H-shape radiator. Detailed simulation studies on the reflection coefficient, current density, antenna pattern and gain are carried out to investigate the behaviour of the antenna at each resonant frequency. Results are validated by measurements using the Small Antenna Radiated Testing Range (SMART) at the National Physical Laboratory (NPL).

4.2 Reconfigurable wideband and multiband patch antenna for Cognitive Radio

4.2.1 Introduction

Cognitive radio communication is envisaged to be a new/unconventional paradigm of methodologies for enhancing the performance of radio communication systems through the efficient utilization of radio spectrum. The driving force behind the idea of cognitive communication is the motivation of efficient and intelligent utilization of the radio spectrum. Owing to a number of possible methodologies for achieving the objectives associated with cognitive radio communication, it is very difficult to restrict its definition to a particular system specification. However, there are common traits of cognitive communication systems, for instance, according to [33], a cognitive communication system is an intelligent communication system, capable of learning from its radio environment and accordingly adapting its operational parameters for reliable communication and efficient utilization of radio spectrum. In order for a communication system to be intelligent, capable of learning, adaptive, and reliable (thus cognitive) there is a need of joint cooperation between several protocols across the layers. Learning from the environment constitutes an important part of a cognitive radio communication system. The learning phase employs many (hard and soft) parameters; for instance, a cognitive radio should be capable of sensing the spectrum over a wide range of frequencies and then combining the information gathered from sensing (hard parameters), with (optionally) using various soft-parameters (e.g. user preference, protocols' interaction).The hard and soft parameters of the learning stage work as an input to the decision making module. Such a decision- making module is deemed to be intelligent so that it can take an appropriate decision according to the input parameters. The behaviour of the communication system in terms of its operational parameters has to be adaptive in order to support the decisions of a decision making module. Increasing the adaptability of the overall communication system comes at the price of higher protocol/hardware complexity; nevertheless, higher adaptability would imply the possibility of higher degrees of cognition in the system.

It is important to notice that a key enabler for realization of the learning phase, more specifically for gathering the hard-parameters, is the capability of re-configurability in the

underlying hardware and the associated protocol suite [34]. For accomplishing the spectrum sensing the underlying hardware (antenna) should be capable of operating over a wide range of frequencies. The decision making module may then direct the actual transmitter to operate at a particular frequency band. As the 'cognitive communication' is still in its evolutionary research phases, there is no specification for the underlying hardware which should conform to the specification of a Cognitive communication system.

In this section, C-Slots are employed on two patch elements to allow the antenna to generate dual-band and wideband modes. Two PIN diode switches are placed on the connecting lines of a simple feed network to the patch elements. Dual-band and wideband-mode operations are obtained by switching "ON/OFF" the two patch elements. The antenna can be used for narrowband applications such as the WLAN and WiMAX and wideband operations in the frequency range of 5 GHz to 7 GHz for other wireless standards. The design eliminates the need for using two ports as proposed in [12]-[13] and increases the number of possible frequency bands from one to four. The volume of the proposed antenna, including the ground plane and the substrate, is 50 mm x 50 mm x 1.57 mm.

4.2.2 Antenna Configuration and Design Procedure

Figure 4-1(a) shows the schematic diagram of the proposed reconfigurable antenna which consists of two patch elements with a simple feed network, two PIN-diode switches and two chip capacitors on one side of the substrate and a ground plane on the other side of the substrate. The complete antenna is designed using the EM simulator, HFSS V.11.2, based on Finite Elements Modelling (FEM) and fabricated on an FR-4 substrate with thickness of 1.57 mm and a relative permittivity of 4.4. The key antenna parameters of the antenna are shown in Table 4-2.

The dimensions of the patch elements of the antenna are computed to operate at the 5.5-GHz WLAN band using the equations given in [35]. Since cutting a slot on the radiator can change the current distribution and the current path, and hence improve the impedance matching especially at higher frequencies, as discussed in [36], in this design, two C-Slots are used on the two patch elements, as shown in Figure 4-1(a), to generate a wide impedance bandwidth and to create multiple resonant frequencies. The feed network has a main 50-Ω feed line and two connecting lines which have been optimized, in terms of impedance bandwidth, to have a line impedance of 63 Ω. Two PIN diodes are placed on the

connecting lines to the patch elements and used as switches. Just to prove the design concept, practical PIN diodes, SMP1320-079 from Skyworks Solutions Inc, were used with a size of 1.5 x 0.7 mm^2, as the switches. In computer simulation, these two diodes are modelled using the Resistance, Inductance and Capacitance (RLC) boundary sheet which gives 0.9 Ω as the impedance value of the PIN diode in the ON state and 0.3 pF as the capacitance value in the OFF state. These PIN diodes are turned "ON/OFF" using a DC biased signal, so two DC block chip capacitors (C_1 and C_2) each with 10 pF are used to prevent the DC signal from flowing to the main feed line but allow the RF current to pass through. The bias network for the diodes is shown in Figure 4-1(b), where the inductors L_1, L_2, L_3 and L_4, all with 12 nH, are used as radio-frequency (RF) chokes to provide low impedance for DC signal and high impedance for RF signals. The resistors R_1, R_2, R_3 and R_4, each with 10 kΩ, are used to control the biasing current to the PIN diodes. Results in the following section show that the antenna has a wide impedance bandwidth from 5 to 7 GHz band and so can cover many applications in this frequency range.

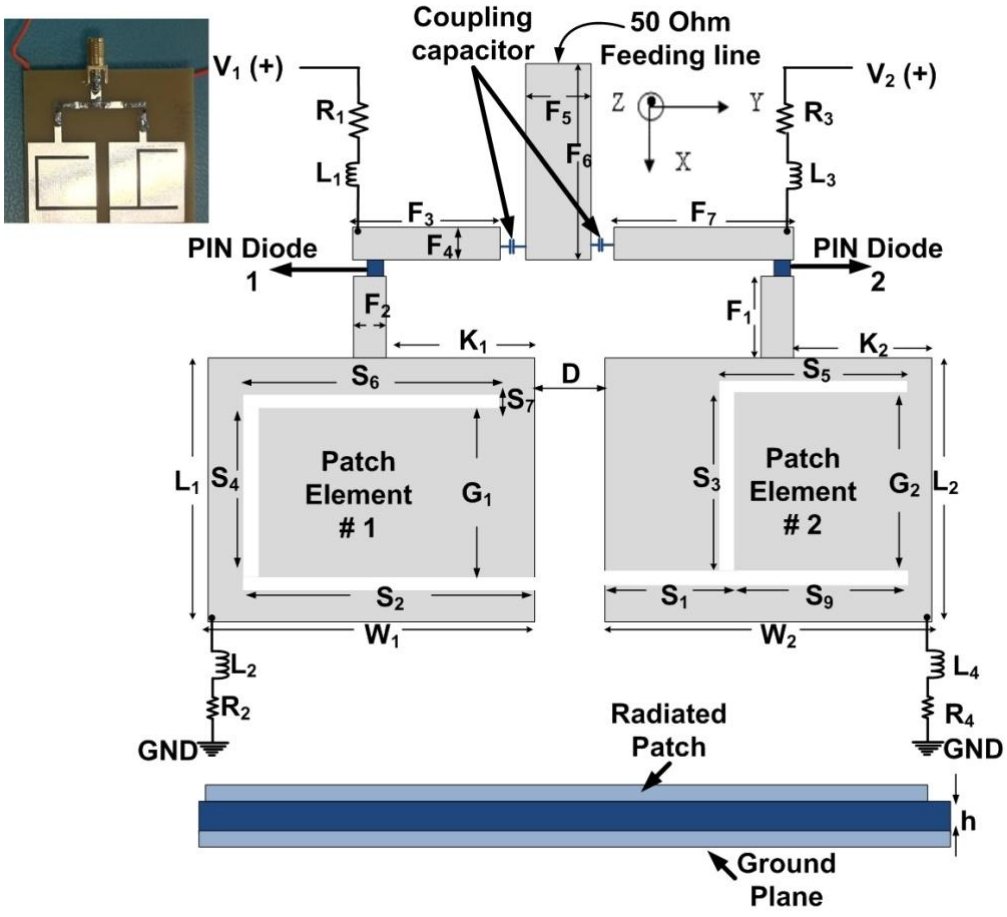

(a)

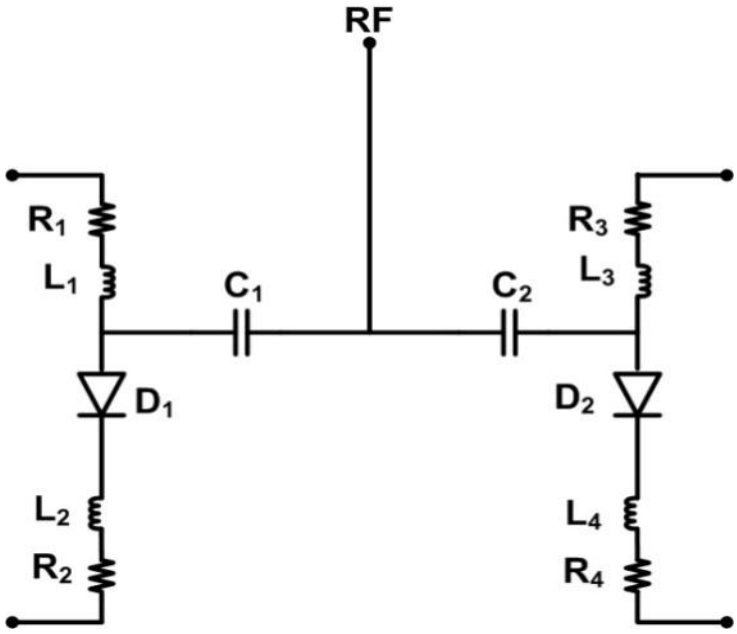

(b)

Figure 4-1: (a) Configuration of proposed antenna (b) Bias network

Table 4-2: Detailed dimensions for the proposed antenna (unit in millimetres)

L_1	W_1	L_2	W_2	S_1	S_2	S_3	S_4
24	20	24	22	9	16	16	14
S_5	S_6	S_7	S_9	F_1	F_2	F_3	F_4
12	16	1	11	9	2	9	2
F_5	F_6	F_7	D	R_1	R_2	G_1	G_2
3	11.6	12	4	**9**	11	14	16
h	Ground PlaneArea			Antenna Area			
1.57	50 x 50			46.6 x 46			

4.2.3 Simulated and Experimental Results

4.2.3.1 Impedance Bandwidth for S_{11}<-10 dB

The two diodes provide three possible and useful switching states, i.e., ON-OFF, OFF-ON and ON-ON states (note that the OFF-OFF state is no practical use). Simulation tests using the HFSS have been carried out on the impedance bandwidth (for S_{11}<-10 dB) of the antenna in different states. In the OFF-ON state, only patch element #2 is ON and functioning. Simulation results in Figure 4-2(a) show that the dual-band is obtained at 5.6 GHz and 6.2 GHz, with the respective bandwidths of 5.2% and 4.85%. In the ON-OFF state, only patch element #1 of the antenna is ON and radiating. The results in Figure 4-2(b) show that a dual-band mode is obtained at 5 GHz and 5.7 GHz, with the corresponding impedance bandwidth of 4.2% and 2.4%. In the ON-ON state, both patch elements are radiating. A wide bandwidth of 33.52%, covering the frequency range from 4.99 GHz to 7 GHz, is obtained as shown in Figure 4-2(c). To validate the simulation results, the proposed antenna has also been fabricated and the S_{11} in the ON-OFF, OFF-ON and ON-ON states have been measured using Agilent N5230A vector network analyzer. Results are shown in Figure 4-2(a) - 2(c) for comparison. It can be seen that the simulated and measured results are in good agreement. The small discrepancies between the simulated and measured results could be attributed to the fabrication accuracy of the prototype.

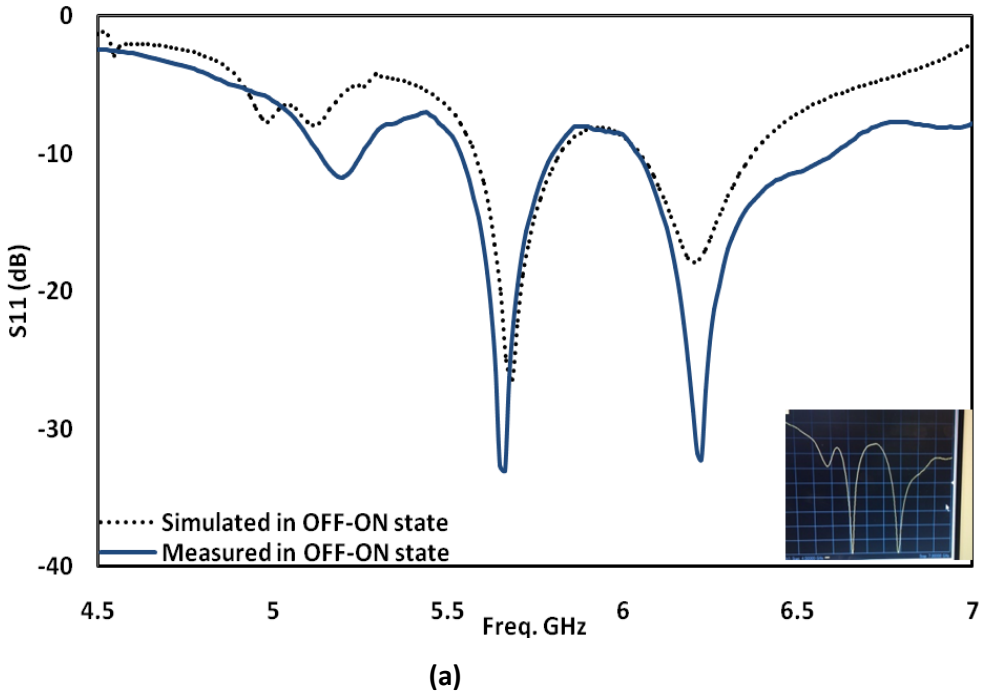

(a)

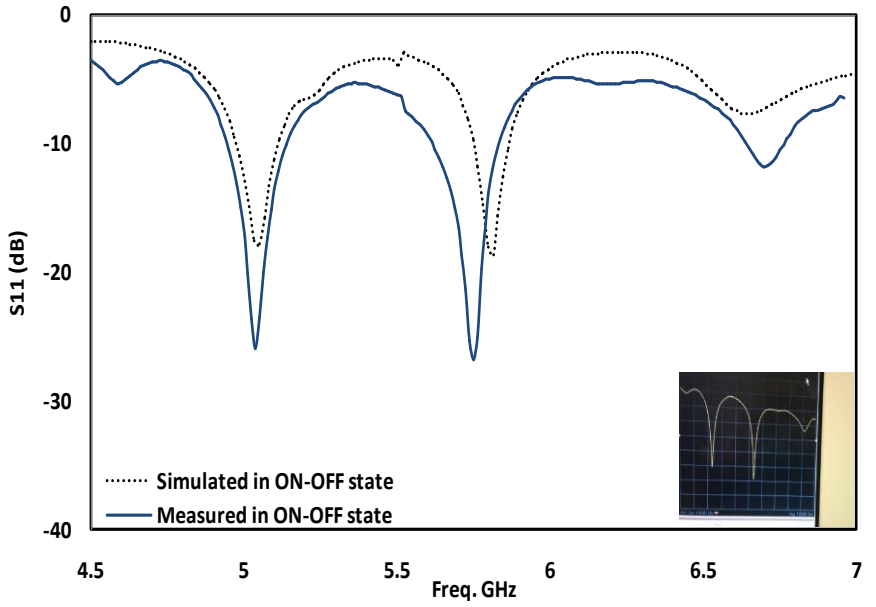

(b)

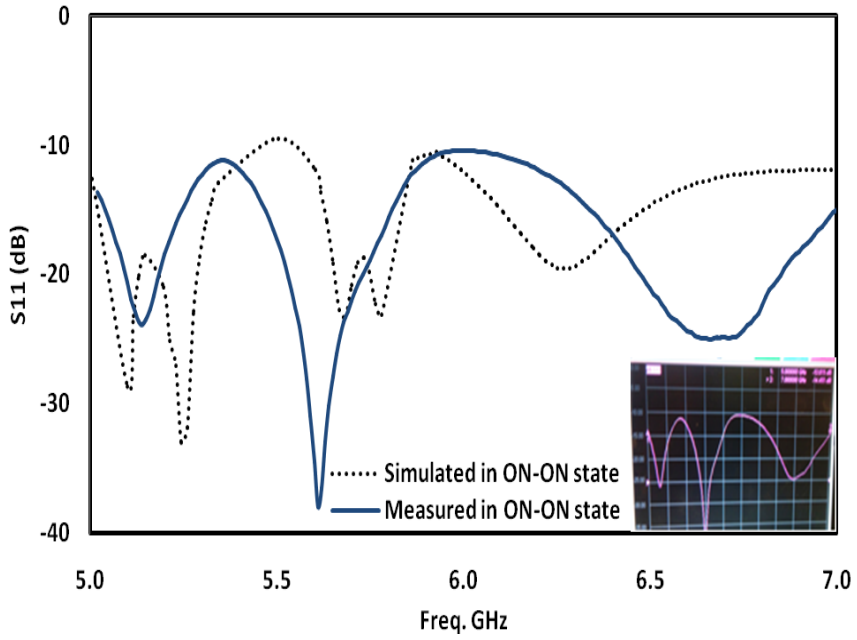

(C)

Figure 4-2 Simulated and measured S_{11} in (a) OFF-ON (b) ON-OFF and (c) ON-ON states

4.2.3.2 Effect of C-Slots

Multiband operation of the antenna is achieved mainly by the C-Slots on the patch elements. Simulation tests have been carried out to study the reflection coefficient S_{11} of the antenna without the C-Slots in the ON-OFF and OFF-ON states. Figure 3 compares the S_{11} with and without the C-Slots in the patch elements. In the ON-OFF state when patch element #1 is active and patch element #2 is OFF, Figure 4-3(a) shows that, without the C-

Slots, the antenna has a resonant frequency at 5.6 GHz. While with the C-Slots, a dual-band is generated at 5 GHz and at 5.7 GHz. In the OFF-ON state when patch element #2 is turned ON and patch element #2 is OFF, Figure 4-3(b) shows that the antenna without the C-Slots has a single band at 5.55 GHz. While with the C-Slots on the patch elements, a dual-band is generated at 5.6 GHz and at 6.2 GHz. Therefore, the C-Slots on the patch elements help generate a dual band. Moreover, simulation results have also shown that the widths and the lengths of the patch elements determine the centre frequencies in the single band cases. While the positions and dimensions of the C-Slots on the patch elements determine the centre frequencies in the dual-band cases. The simulated-frequency bands generated with and without the C-Slots are summarised in Table 4-3.

Table 4-3: Bands generated in ON-OFF, OFF-ON and ON-ON states with and without C-Slots

`	Without Slots	With C-Slots
ON-OFF	5.6 GHz	5 GHz and 5.7 GHz
OFF-ON	5.55 GHz	5.6 GHz and 6.2 GHz
ON-ON	5.55 GHz and 5.65 GHz	Wideband 5 GHz to 7 GHz

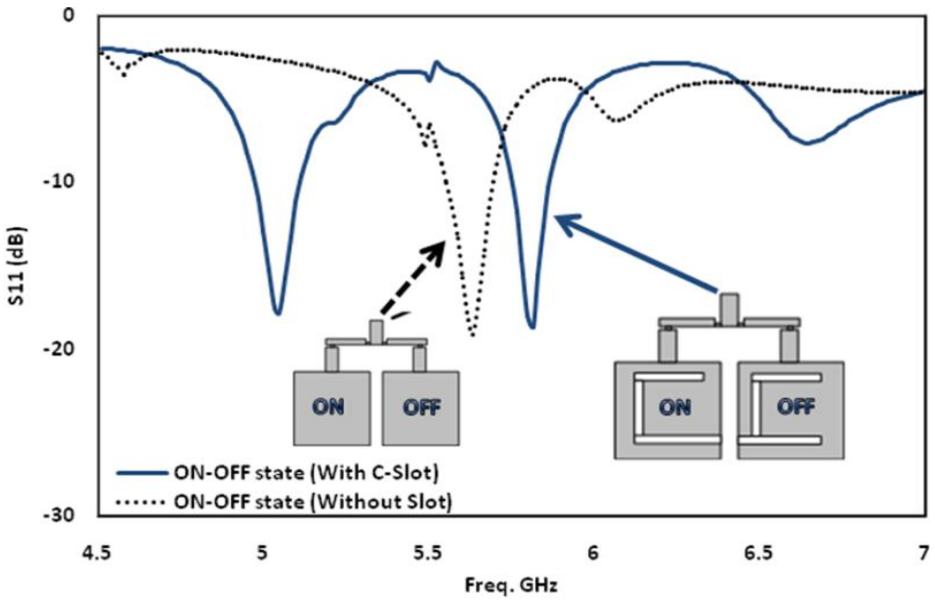

(a)

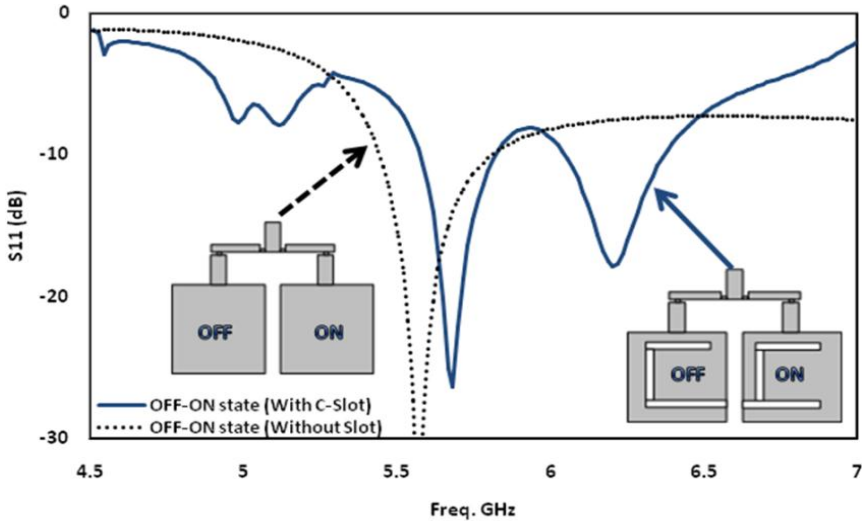

(b)

Figure 4-3 Effects of introducing the C-Slots on the radiated patch when switches are (a) ON-OFF and (b) OFF-ON states

4.2.3.3 Current distributions

Cutting slots on the radiator of an antenna can change the current path and so can be used to generate dual-band or even multiple-bands operations. In this antenna, if the slots are absent, the antenna will have only one major current path on each of the patch elements. However, in the presence of the two C-slots, the current path on each of the patch elements is disturbed, hence creating the dual-band operation. Figures 4-4(a) and (b) shows the simulated current distributions on the patch elements in different switching states. In the OFF-ON state, patch element #2 is radiating and patch element #1 is OFF. Figure 4-4(a) shows that the current travels around the C-Slot on patch element #2, as expected, generating the resonant frequencies at 5.6 and 6.2 GHz as shown in Figure 4-2(a) for the WLAN 802.11a/h/j/n applications. In the ON-OFF state, only patch element #1 is ON and radiating and patch element #2 is OFF. Figure 4-4(b) shows that the current travels around the C-Slot on patch element #1, generating the dual band at 5 and 5.7 GHz as shown in Figure 4-2(b), for the WLAN 802.11a/h/j/n applications. The dominate current paths for OFF-ON and ON-OFF states are shown in Figure 4-4. These paths correspond to approximately 0.5λ, where λ is the wavelength at the resonant frequency of the respective band and given by $\lambda = \lambda_0 / \sqrt{(\varepsilon_r + 1)/2}$, with λ being the free space wavelength. The 6.2-GHz band in the OFF-ON case is generated from a higher order mode. In the ON-ON

state where both patch elements are ON, the wideband operation is obtained by coupling which will be explained later.

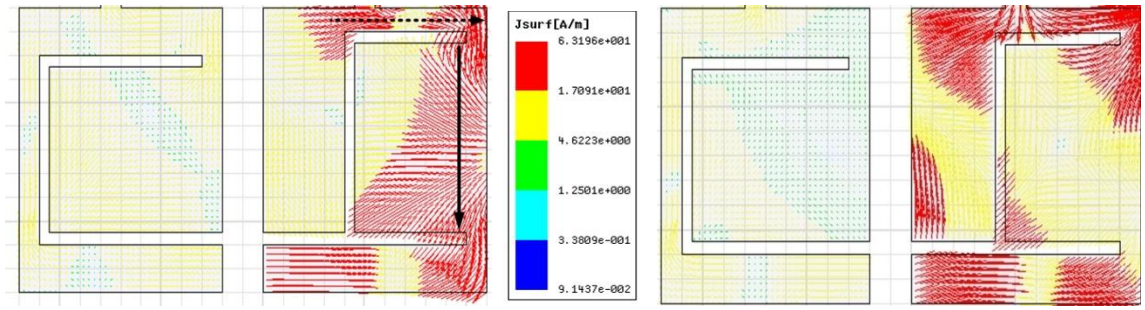

5.6 GHz 6.2 GHz

(a) OFF ON

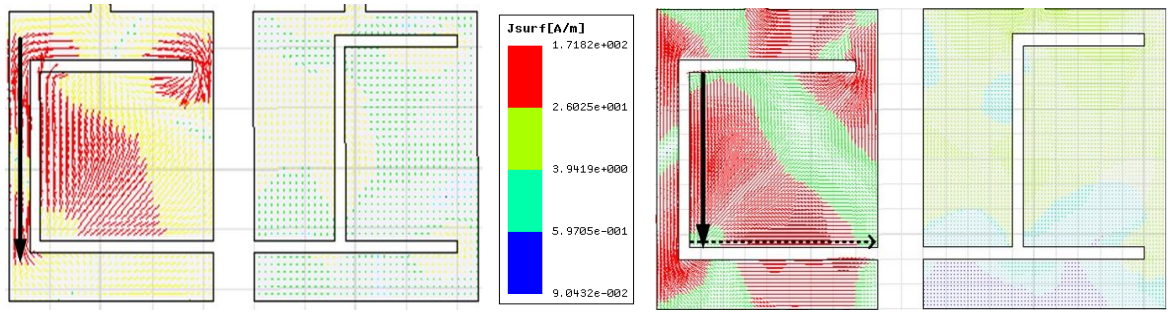

5GHz 5.7 GHz

(b) ON OFF

Figure 4-4 Simulated current distribution in (a) OFF-ON and (b) ON-OFF

4.2.4 Radiation patterns and gain measurements

The radiation patterns of the antenna have been measured using the Small Antenna Radiated Testing Range (SMART) at the National Physical Laboratory (NPL), with results normalized to the maximum values. Figures 4-5 to 4-7 show the measured and simulated co- and cross-polarization patterns of the antenna in different switch states at several frequencies across the operating bandwidth. In OFF-ON, ON-OFF and ON-ON states, the radiation patterns at resonant frequencies of 5.6 and 6.2 GHz, 5 and 5.7 GHz, and 5.2 and 6.5 GHz, respectively, are used for comparison. Since the directions of the dominant current paths at all these frequencies, as shown in Figure 4-4, are mainly in the X-direction, the Y-Z and X-Z planes are the H- and E-planes, respectively. As expected, the co-polarization patterns in Figures 4-5 to 4-7 are all unidirectional to the Z-direction with some back radiation due to the finite ground plane size. There is no major change in the radiation patterns in the three switch states of OFF-ON, ON-OFF and ON-ON. Some minor

discrepancies occur between the simulated and measured results, which could be due to the effect of the coaxial cable connected to the antenna during measurements. Better results could be obtained by using a fibre optic cable instead [37]. The peak gains at different frequencies are between 3 to 5 dBi in different switching states. The simulated radiation efficiency of the antenna in the ON-ON state ranges from 60% to 70%.

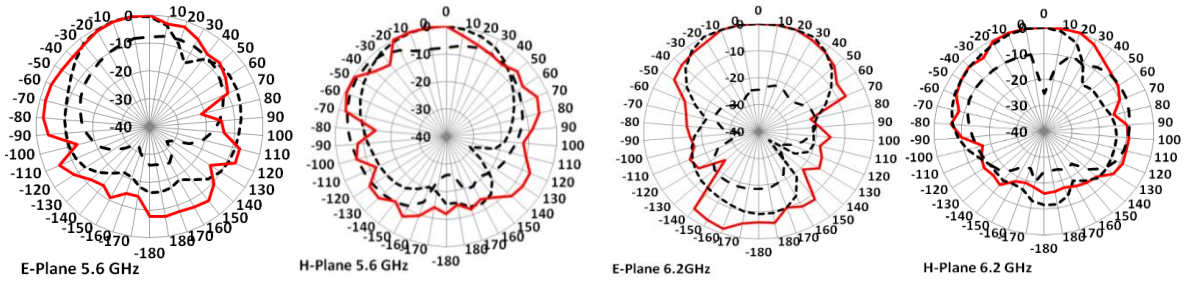

Figure 4-5 Simulated and measured Co and X-pol in E and H-planes in OFF-ON state at (a) 5.6 GHz and (b) 6.2 GHz

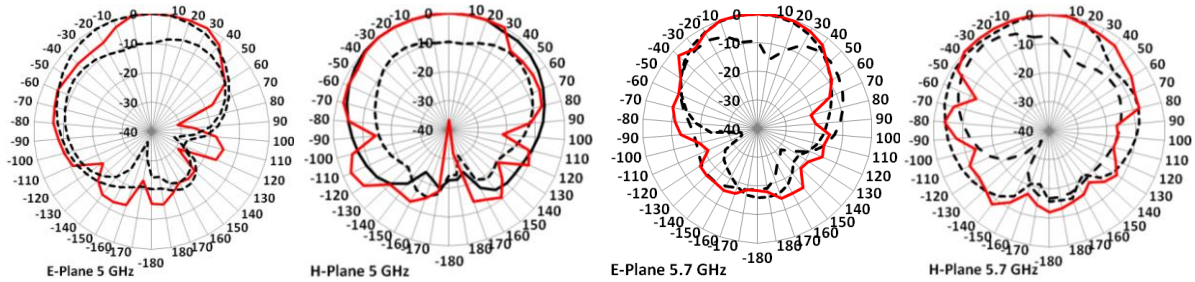

Figure 4-6 Simulated and measured Co and X-pol in E and H-planes in ON-OFF state at (a) 5 GHz and (b) 5.7 GHz

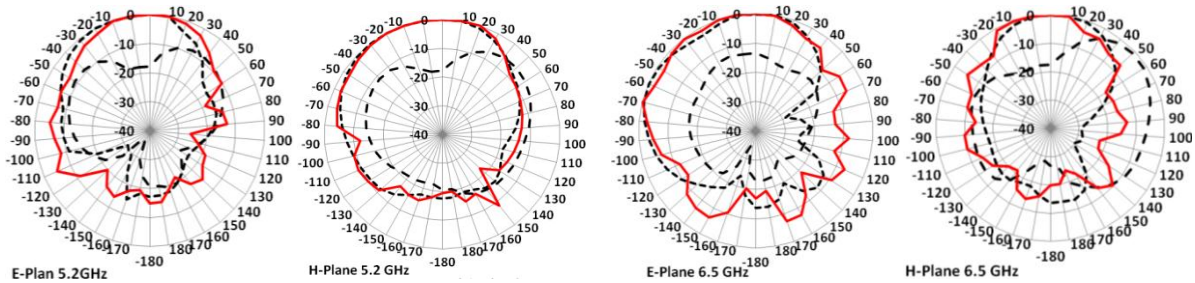

Figure 4-7 Simulated and measured Co and X-pol in E and H-planes in ON-ON state at (a) 5.2 GHz and (b) 6.5 GHz

4.2.5 Independent Control of Each Band

To design antennas with multiple band operations, it is desirable to have independent frequency controls on the frequencies as mentioned in section 2.2.

Previous results have shown that, in the ON-OFF and OFF-ON states, the C-Slots on the patch elements of the antenna can be used to generate two frequency bands for dual-band operation. How to use the C-Slots to independently control the frequency bands for dual-band operation without affecting the wideband operation is shown here.

In the ON-OFF state, the simulation results in Figure 4-8 (a) shows the effects of changing the length S_4 in the slot of patch element #1 on the lower band of the dual band. It can be seen that increasing S_4 can move the 5-GHz band lower while keeping the 5.7-GHz band fixed. Figure 4-8 (b) shows that the effect of changing W_1 and S_2 together on the higher band of the dual band. It can be seen that reducing W_1 and S_2 together can move the 5.7-GHz band to a higher frequency band, yet the 5-GHz band remains unchanged.

In the OFF-ON state, Figure 4-9 (a) shows the effects of changing the position of the whole C-Slot up and down on patch element #2. It can be seen that the position of the C-Slot can be used to move the lower band (at around 5.6 GHz) while keeping the 6.2-GHz band fixed. Finally, Figure 4-9(b) shows that changing the distance G_2 (i.e., moving S_1 & S_9 together closer or further from S_5 while keeping S_3 the same) can shift the higher band (at around 6.2 GHz) to a higher or lower frequency band, yet maintaining the 5.6-GHz band. It should be noted that, in some cases, after moving the frequency of the band, we may need to optimize the other parameters of the antenna to achieve the desirable S_{11}.

These results show that we can independently control the frequencies of the dual bands by using the C-Slots on the radiators. Simulation results have also shown that the wideband performance in the ON-ON state is not affected when these narrow bands are moved to other bands. This degree of freedom further enhances the antenna capability.

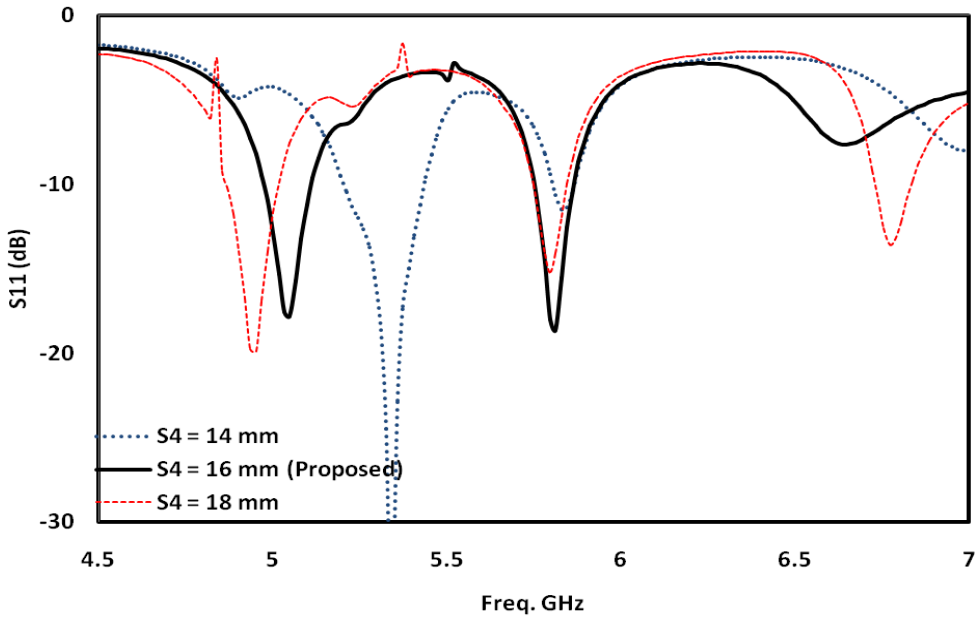

(a)

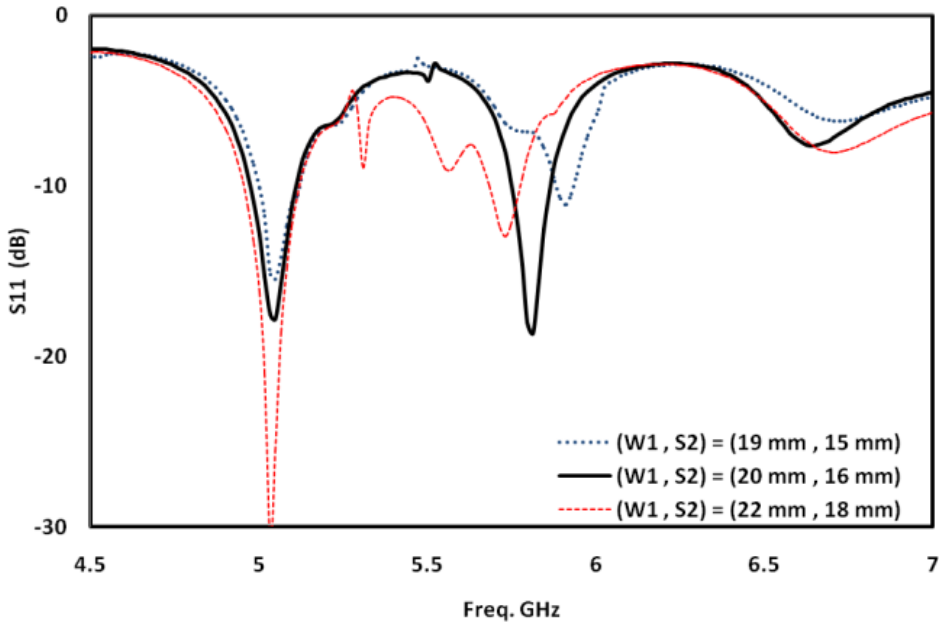

(b)

Figure 4-8: In ON-OFF state: (a) effects of S_4 on lower band of dual band and (b) effects of W_1 and S_2 together on higher band of dual band

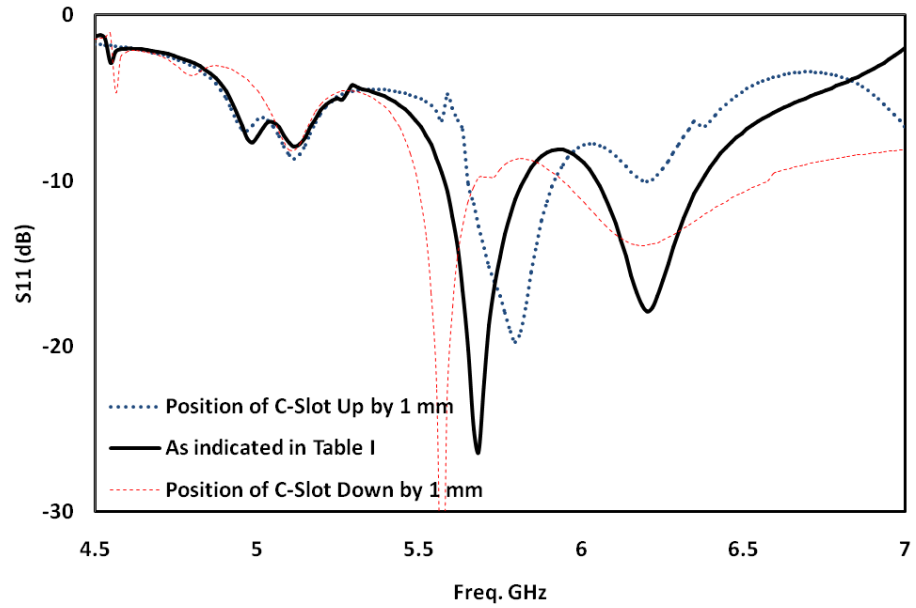

(a)

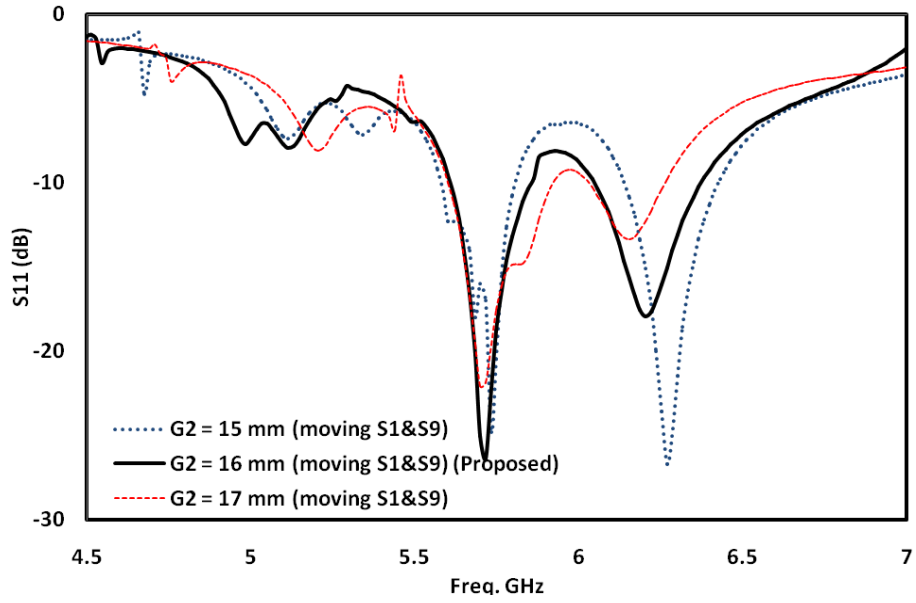

(b)

Figure 4-9: In OFF-ON state, (a) effects of C-Slot position on lower band of dual band and (b) effects of G_2 on higher band of dual band.

4.2.6 Effect of Coupling

It has been shown that when both patch elements are ON, the antenna has a wide bandwidth. Mutual coupling between the patch elements must have played an important part for these characteristic and it is analysed here.

To study the coupling effects between the 2 patch elements, we place an EM wave absorber (high lost material) between the 2 patch elements in the simulation model as shown in Figure 4-10 (a) - (b) to remove the coupling effects and impedance bandwidth was simulated using the reflection coefficient S_{11} in the ON-OFF, OFF-ON and ON-ON states.

With patch element #1 turned ON, patch element #2 turned OFF, and the coupling effect from element #2 to element #1 removed by the absorber, the simulated S_{11} is shown in Figure 4-11(a). For comparison, the simulated S_{11} without the absorber, i.e. with coupling, is also shown in the same figure. It can be seen that the differences in S_{11}, particularly near the dual frequency bands, are quite insignificant, indicating that the coupling between the two patch elements is very small. With patch element #1 turned OFF and patch element #2 turned ON, the simulated S_{11} with and without the absorber are shown in Figure 4-11(b). The differences in S_{11} near the dual frequency bands are slightly noticeable. Nevertheless, it is insignificant and so the coupling between the two patch elements is still very small. With both patch elements #1 and #2 are ON, i.e. in the ON-ON state, the simulated S_{11} with and without the absorber are shown in Figure 4-11 (c). It can be seen that the mutual coupling between the 2 elements are much stronger and significantly reduces the reflection coefficient S_{11} to less than –10 dB across the whole frequency band. As a result, the operation bandwidth of the antenna is much wider.

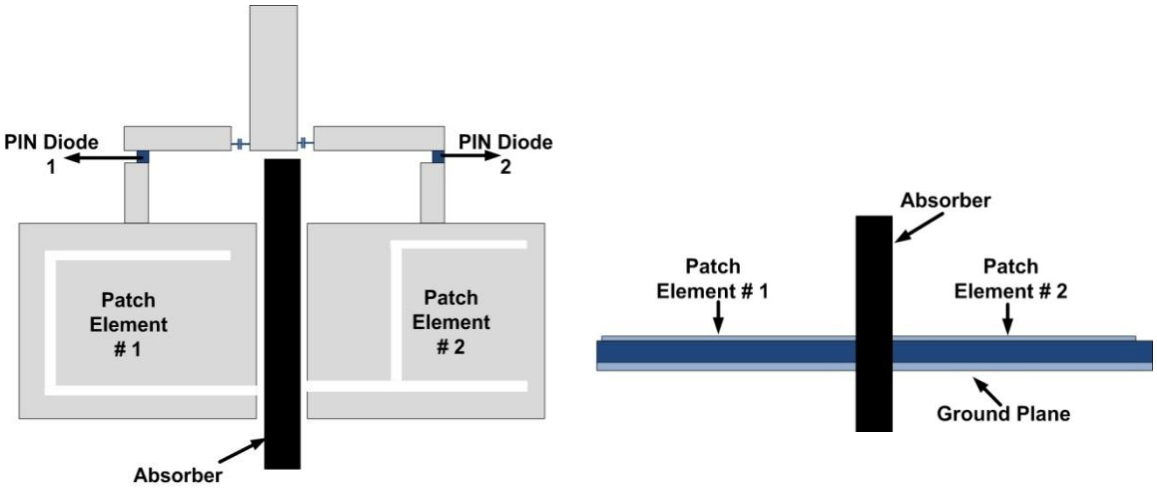

Figure 4-10 Antenna with absorber to remove coupling effects (a) Top view and (b) side view

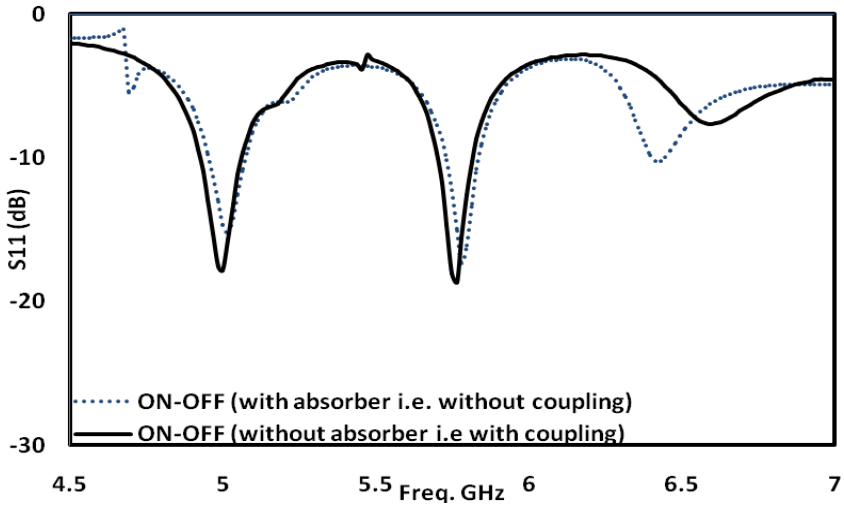

(a)

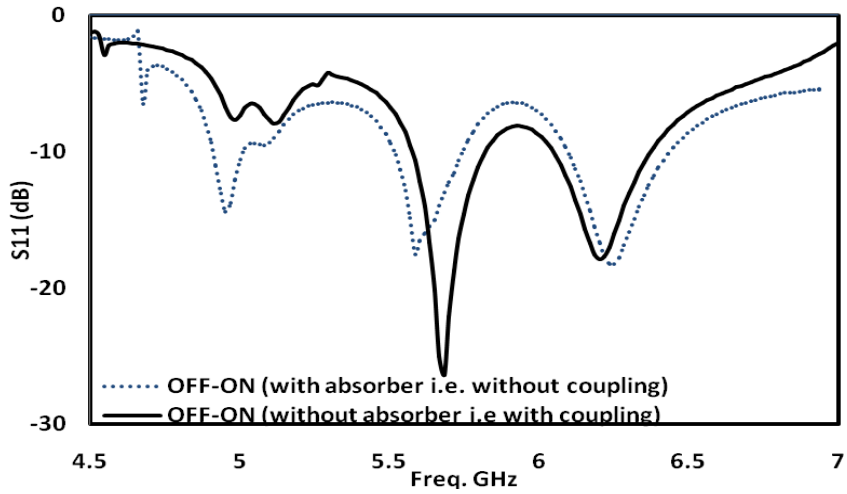

(b)

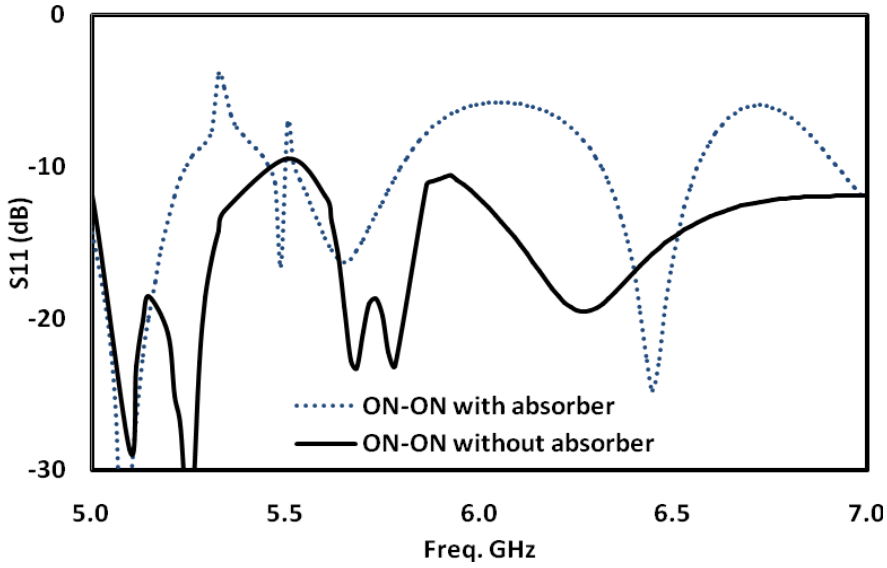

(c)

Figure 4-11 Reflection coefficient (S_{11}) with absorber in (a) ON-OFF (b) OFF-ON and (c) ON-ON states.

4.3 A CPW Antenna with Frequency Selectivity Feature

4.3.1 Introduction

From the extensive literature in switchable multiband antenna, this section tackle some important issues which needs to be addressed such as the size, thickness and the number of switches. Therefore, the antenna in this section consists of an H-shape radiator and a CPW printed on a PCB and a varactor diode connecting the upper and lower arms of the H-shape radiator for reconfigurability. The uniqueness of the antenna lies on the ability to select the operating mode and frequencies electronically using a varactor diode. By selecting the DC bias voltages of 11.5, 10 and 8 V across the varactor diode, which in turn selecting the corresponding varactor capacitances of 2, 4 and 6 pF, the antenna can be controlled to operate in three different modes, namely, a single-band mode to cover the Global System for Mobile communications 1900 (GSM1900) system, a dual-band mode at 1.88 and 2.4 GHz to cover the GSM1900 and Bluetooth or Wireless Local Area Network (WLAN) systems, respectively, and a tri-band mode at 1.57, 1.88 and 2.4 GHz to cover the GSM1900, WLAN and Global Position System (GPS), respectively. Furthermore, by varying the varactor capacitance from 7 to 13 pF, the GPS and WLAN bands can be tuned by 11.44 % (1.57 - 1.4 GHz) and 6.46 % (2.4 - 2.25 GHz), respectively, yet keeping the 1.88-GHz band unchanged. Thus the proposed single antenna can be used to support different wireless standards. Detailed studies on the reflection coefficient, current density, antenna pattern and gain are carried out using simulations and measurements to investigate the behaviour of the antenna at each resonant frequency in each operating mode.

4.3.2 Antenna Configuration

The structure of the proposed reconfigurable antenna is shown in Figure 4-12, which is optimised using the HFSS software version 11.2 with the main optimized dimensions listed in Table 4-4. The antenna has an overall area of 43.6 mm x 50 mm, suitable for compact wireless devices. The antenna consists of an H-shape radiator; a CPW feed line and a varactor diode connecting the two horizontal arms of the H-shape radiator as shown in Figure 4-15. The antenna is designed on an FR-4 substrate with a thickness of 1.57 mm and a dielectric constant of 4.4. The CPW has a characteristic impedance of 50 Ω. The varactor diode used in this design is BB184 from NXP. From its data sheet, the varactor diode has a

capacitance *C* ranging from 16 to 1 pF, depending on the DC bias voltage, as shown in Figure 4-16, an inductance of 0.6 nH, a resistance of 0.65 Ω and physical dimension of 0.6 mm x 0.9 mm. The location of the varactor diode on the antenna is optimized to provide the desirable frequency bands for the antenna.

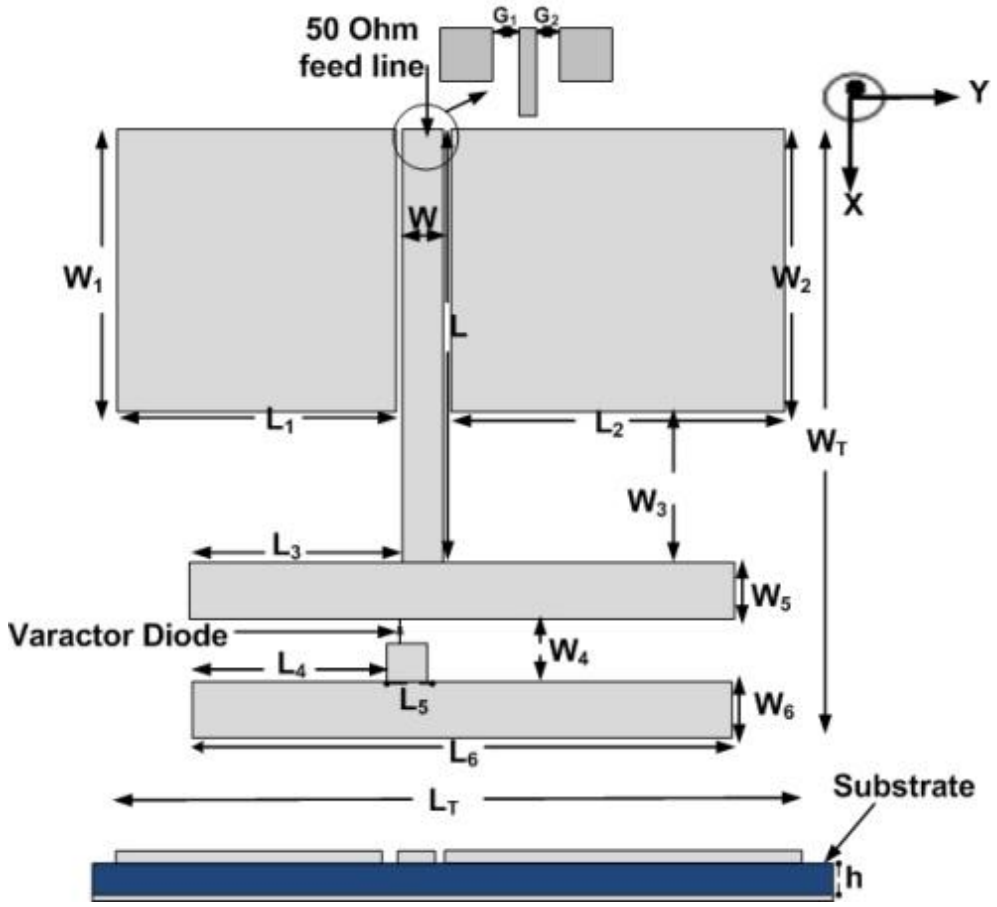

Figure 4-12 Layout of the proposed antenna

Table 4-4: Dimensions of the proposed CPW antenna (In mm)

W	W_1	W_2	W_3	W_4	W_5	W_6	W_T	L	L_1
3	20	20	10.6	5	4	4	43.6	30.6	19.5
L_2	L_3	L_4	L_5	L_6	L_T	h	G_1	G_2	
26.5	15	14	2.5	40	50	1.57	0.5	0.5	

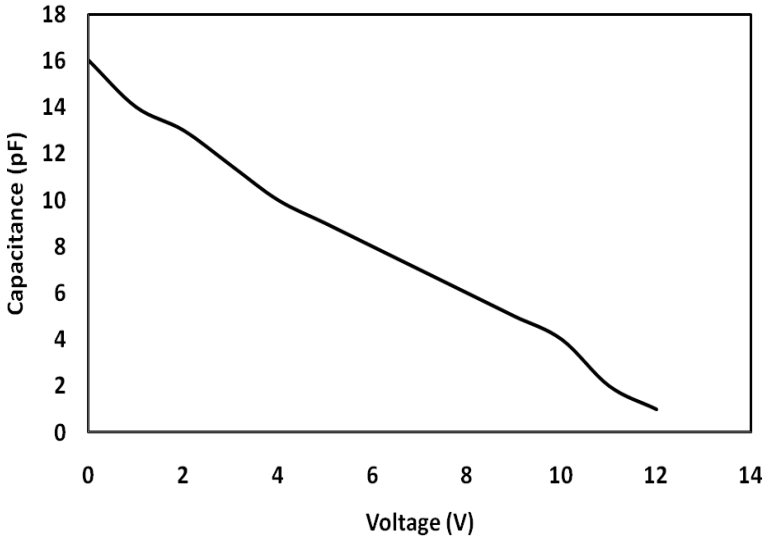

Figure 4-13 Capacitance versus DC bias voltage for the varactor Diode (BB184 data sheet)

4.3.3 Simulations and Measured Results

The performances of the proposed antenna, in terms of return losses, radiation patterns and gains, with different DC bias voltages across the varactor diode, have been studied using computer simulation. In the simulation tests, the varactor diode is modelled as a capacitance using the characteristic of Figure 4-13. The proposed antenna has also been fabricated as shown in Figure 4-14 (a) and measured using the Small Antenna Radiated Testing Range (SMART) at the National Physical Laboratory (NPL) shown in Figure 4-14 (b).

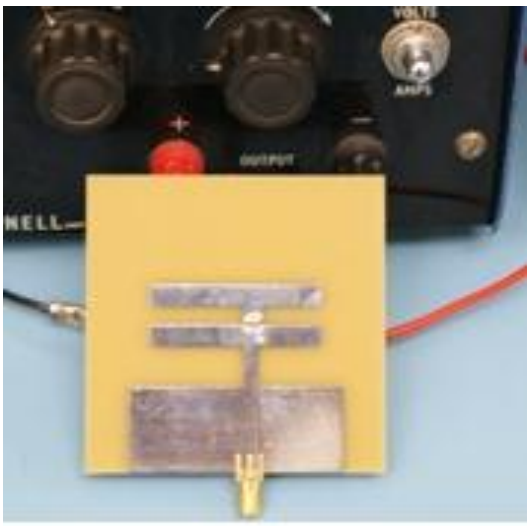

(a)

(b)

Figure 4-14: (a) Fabricated prototype and (b) proposed antenna mounted on receiving mast at NPL smart anechoic chamber

4.3.3.1 Single, Dual- and Triple-Frequency Bands

The simulated and measured reflection coefficients S_{11} of the proposed antenna, for the DC bias voltages of 8, 10 and 11.5 V across the varactor diode, corresponding to the varactor capacitances C = 2, 4 and 6 pF, are presented in Figure 4-15. The measurements were performed using a network analyzer Agilent N5230A. It can be seen that the measured and simulated results are in good agreements. The differences can be attributed to the fabrication tolerance and measurement errors. The results in Figure 4-15 (a)-(c) show that the antenna can operate in three different modes, a single-band, dual-band and tri-band modes, depending upon the DC bias voltage across the varactor diode. With C = 2 pF, Figure 4-15 (a) shows that the antenna generates a single band at 1.88 GHz with a bandwidth from 1.850–1.910 GHz, which is suitable for the GSM1900 applications. With C = 4 pF, Figure 4-15 (b) shows that the antenna has a dual-band at 1.88 and 2.4 GHz. Here, the antenna generates another band at 2.4 GHz with a bandwidth from 2.4–2.46 GHz, which can be used for the IEEE802.11b/g WLAN and Bluetooth applications, yet the frequency band for

GSM1900 remaining unchanged. While with *C* = 6 pF, Figure 4-15 (c) shows that the antenna generates a tri-band at 1.575, 1.88 and 2.4 GHz. The additional band at 1.575 GHz can be used for the GPS applications. In this mode, same as in the dual-band mode, the GSM1900 band at 1.88 GHz and the WLAN/Bluetooth bands at 2.4 GHz remain unchanged. The bandwidths for the GSM1900, WLAN and GPS bands are 3.17%, 2.8%, and 2.6%, respectively. The DC bias voltages with the corresponding capacitances in these three operation modes for different applications are shown in Table 4-5.

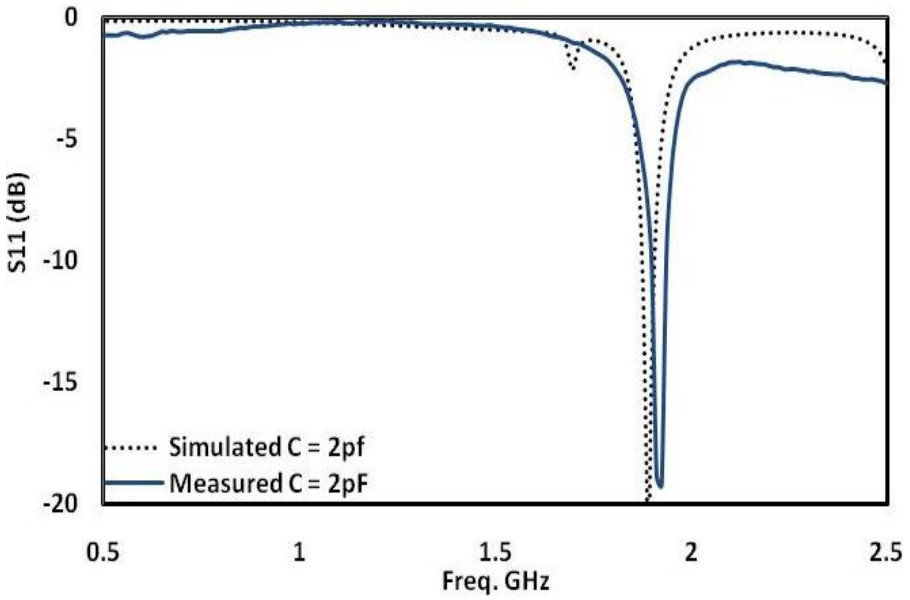

(a)

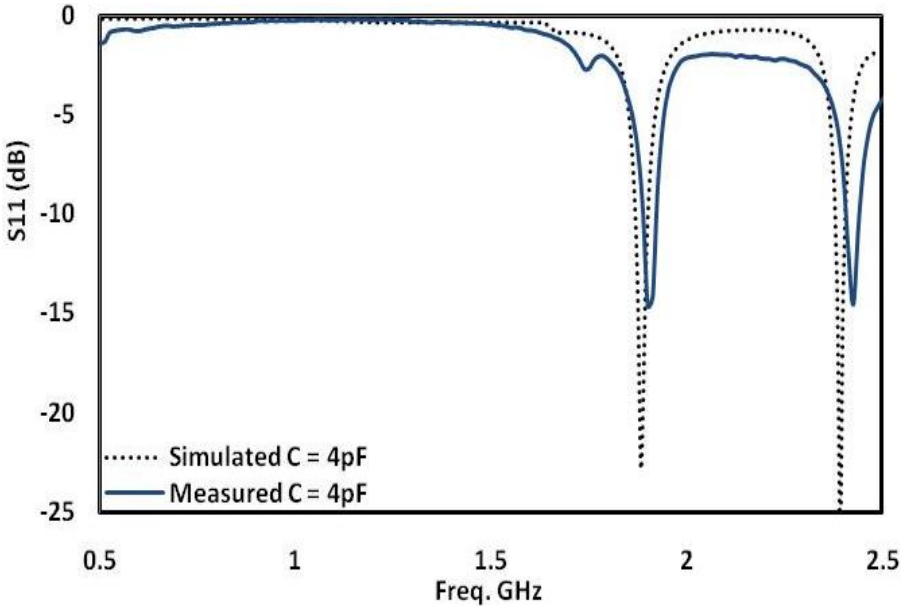

(b)

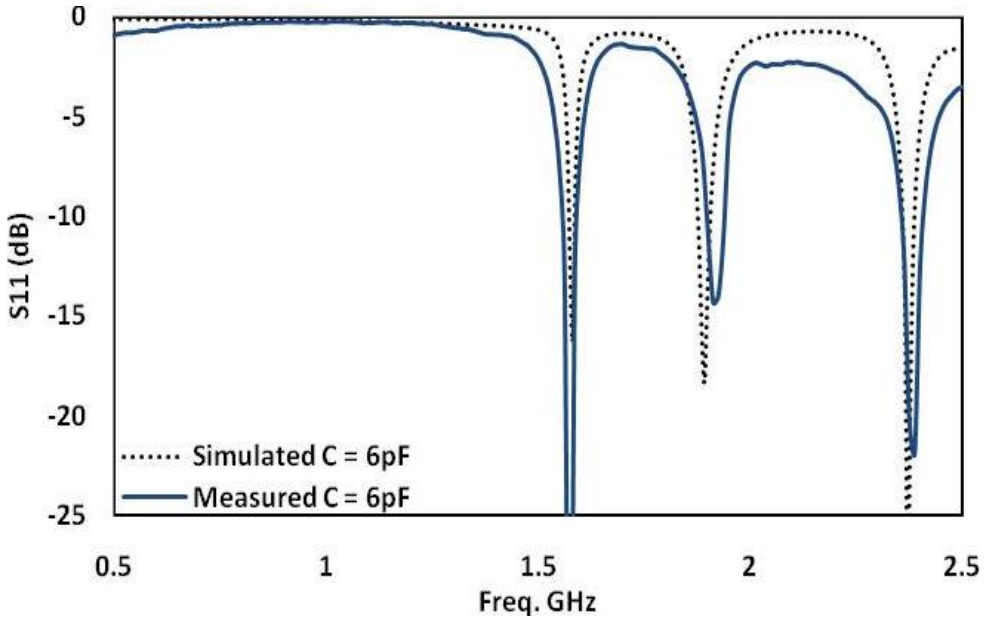

(c)

Figure 4-15 Simulated and measured return loss for the three resonant frequencies at (a) Single band when c = 2pF (b) Dual band when c = 4pF and (c) Tri-band when c = 6 pF.

Table 4-5: DC bias voltages with corresponding capacitances in three operation modes for different applications

Bias voltage	C	Frequency Mode	Frequency bands	Application
11.5 V	2 pF	Single-band	1.88 GHz	GSM1900
10 V	4 pF	Dual-band	1.88 & 2.4 GHz	GSM1900 & WLAN/Bluetooth
8 V	6 pF	Tri-band	1.57, 1.88 & 2.4 GHz	GPS, GSM1900 & WLAN/Bluetooth

The GPS system uses circular polarization and the antenna has linear polarization. However, linearly polarized antennas can also be useful for GPS system in many practical multipath scenarios. According to the investigations carried out in [38], a linearly polarized PIFA antenna can reach relatively high performance, comparable with that of right hand circularly polarized antennas.

In [23], a multiple-band antenna was designed by adding additional parts and folded parts to the radiators which resulted in a larger dimension, higher profile and very complicated structure which are difficult to manufacture. The Double-T antenna (or is called H-shape

antenna) reported in [20] is similar to the proposed antenna's shape in this section. The antenna could operate only in a dual-band mode at the higher frequencies 2.4 and 5.2 GHz. Switchable techniques using three or more switches were proposed in [25, 28 and 32]. These techniques had limitations in terms of the number of switches required to reconfigure the antennas to a single-band or dual-band modes. In addition to increased complexity and space required, the multitude of switches also increases the power consumption and fabrication cost. However, the proposed antenna employs a simple varactor diode to select three operation modes, i.e., the single-band, dual-band and tri-band modes, yet without requiring to incorporate with any additional parts to the antenna, yet having more flexibility with smaller size.

It should be noted that the selectivity of the bands proposed here could be extended to a more complicated structure to generate more bands. For example, by using multiple H-shape structures, it is possible to design antennas to operate more than three frequency bands. Since the target is for small wireless devices applications, we have limited the antenna structure to just a single H-shape.

4.3.3.2 Radiation Patterns

The simulated and measured co- and cross-polarization radiation patterns in the E- and H-planes for the single-band, dual-band and Tri-band modes are shown in Figure 4-16 (a) - (c), respectively. The measured radiation patterns have been normalized to the maximum values. It can be seen good agreements between measured and simulated patterns. The differences in some cases are due to the fabrication tolerance, measurements accuracy and the effects of the coaxial cable used for measurements. Figure 4-16 shows that the radiation patterns at a given bias condition remain nearly constant. The cross polarization is below -15 dB in most of the cases. More studies have also shown that the length of the CPW feed line affects the cross polarization level. Figure 4-17 shows the radiation patterns in the H-plane at 2.4 GHz with different lengths used for the CPW-feed line. It can be seen that a shorter feed line leads to a lower cross polarization. The measured 3D patterns in the three bands with C = 6 pF are shown in Figure 4-18.

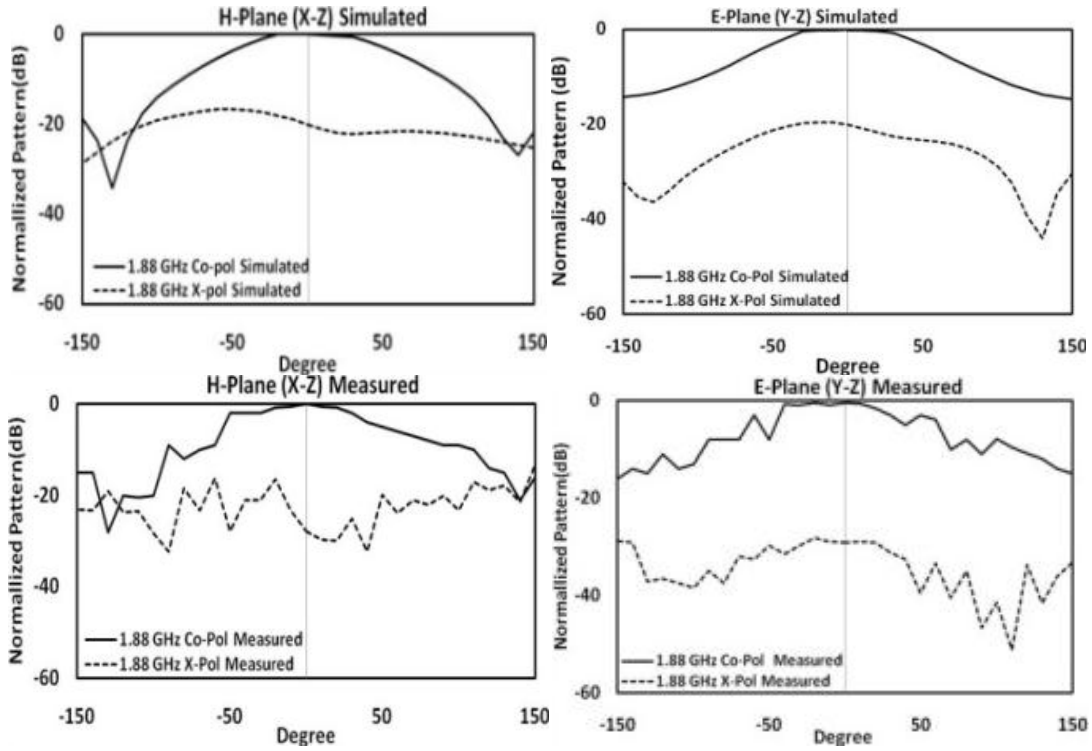
H-Plane (X-Z) Simulated
Normallized Pattern(dB)
0
-20
-40
-60
1.88 GHz Co-pol Simulated
1.88 GHz X-pol Simulated
-150
-50
50
150
Degree
E-Plane (Y-Z) Simulated
Normalized Pattern (dB)
1.88 GHz Co-Pol Simulated
1.88 GHz X-Pol Simulated
H-Plane (X-Z) Measured
1.88 GHz Co-Pol Measured
1.88 GHz X-Pol Measured
E-Plane (Y-Z) Measured
1.88 GHz Co-Pol Measured
1.88 GHz X-Pol Measured

(a)

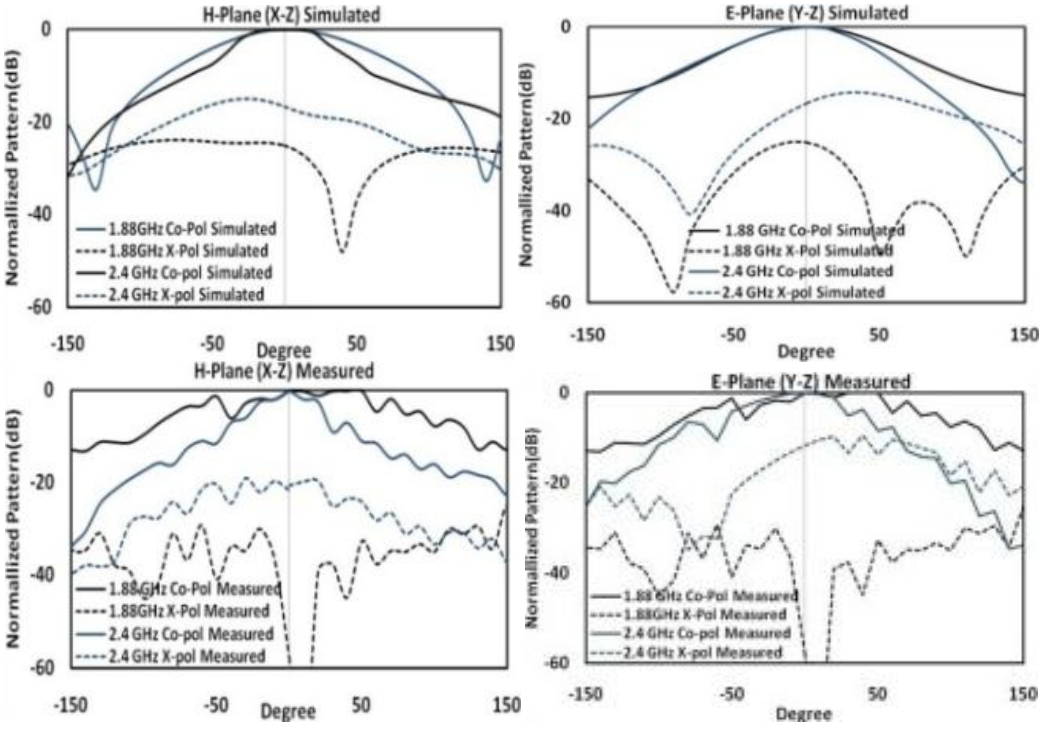
H-Plane (X-Z) Simulated
Normallized Pattern(dB)
0
-20
-40
-60
1.88GHz Co-Pol Simulated
1.88GHz X-Pol Simulated
2.4 GHz Co-pol Simulated
2.4 GHz X-pol Simulated
-150
-50
Degree
50
150
E-Plane (Y-Z) Simulated
1.88 GHz Co-Pol Simulated
1.88 GHz X-Pol Simulated
2.4 GHz Co-pol Simulated
2.4 GHz X-pol Simulated
H-Plane (X-Z) Measured
1.88GHz Co-Pol Measured
1.88GHz X-Pol Measured
2.4 GHz Co-pol Measured
2.4 GHz X-pol Measured
E-Plane (Y-Z) Measured
1.88 GHz Co-Pol Measured
1.88GHz X-Pol Measured
2.4 GHz Co-pol Measured
2.4 GHz X-pol Measured

(b)

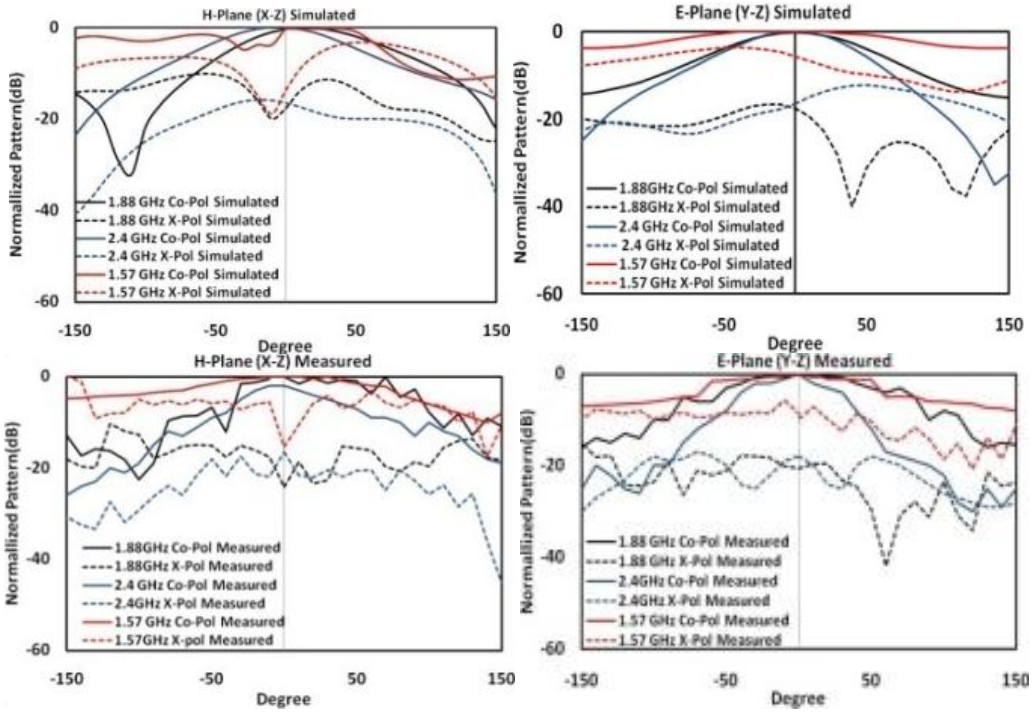

(c)

Figure 4-16: Simulated and measured Co- and X-pol radiation patterns in E- and H-plane for (a) single-band, (b) dual-band and (c) Tri-band modes.

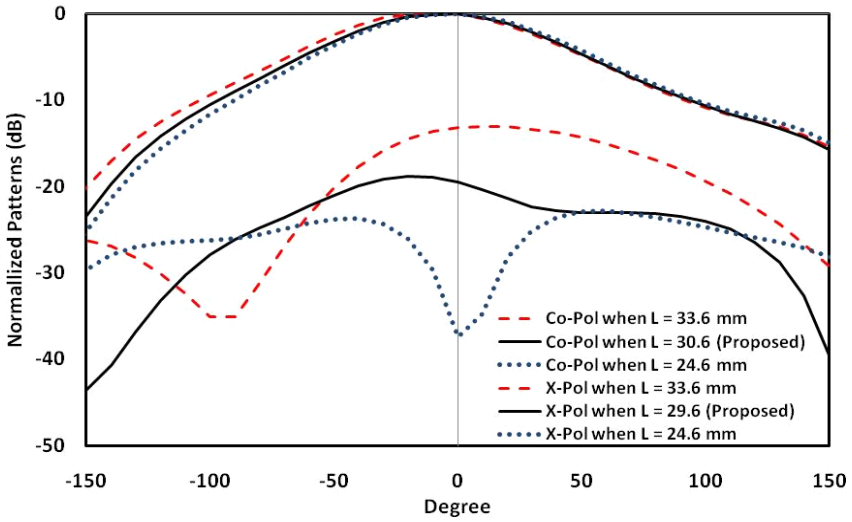

Figure 4-17: Effect of feed-line length on radiation patterns in H-plane at 2.4 GHz with C = 6 pF.

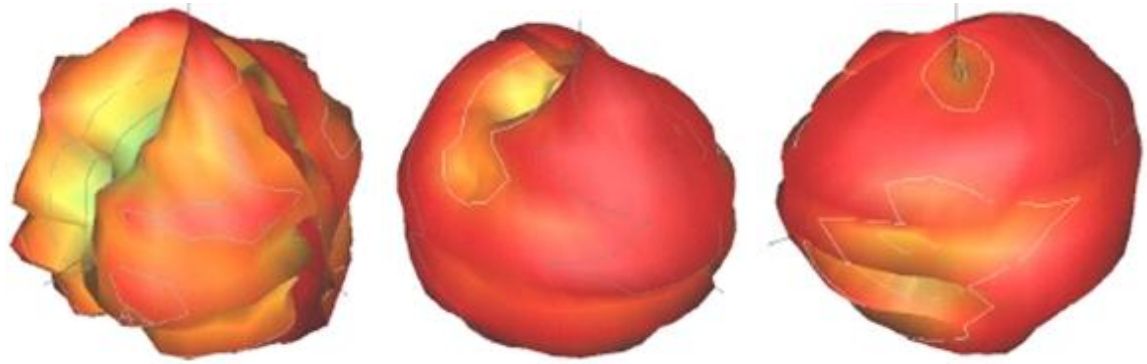

(a) 1.57GHz (b) 1.88 GHz (c) 2.4 GHz

Figure 4-18: Measured 3D patterns at (a) 1.57, (b) 1.88 and (c) 2.4 GHz

4.3.3.3 Control of Frequency Bands

Although the three frequencies 1.57, 1.88 and 2.4 GHz are used for studies here, other combinations of frequency bands can also be generated by using different arm widths, W_5 & W_6, in the H-shape radiator. The previous results in Figure 4-15 (c) show that, with *C* = 6 pF, W_5 = W_6 = 4 mm, the antenna generates a tri-band at 1.575, 1.88 and 2.4 GHz. If different values of W_5 & W_6 are used, the antenna can generate different frequency bands as shown in Figure 4-19, which indicates that increasing the widths of both arms simultaneously shifts the bands to the higher frequencies, and vice versa. Thus the arm widths of the H-shape radiator can also be used to generate other combinations of frequency bands. Some simulation results are shown in Table 4-6. With W_5 = W_6 = 0.5 mm, a single UMTS band can be generated by using *C* = 2 pF. A dual band for the UMTS and WiMAX systems can be created by increasing *C* to 4 pF and a tri-band for the DCS, UMTS and WiMAX systems can be generated by increasing *C* further to 6 pF.

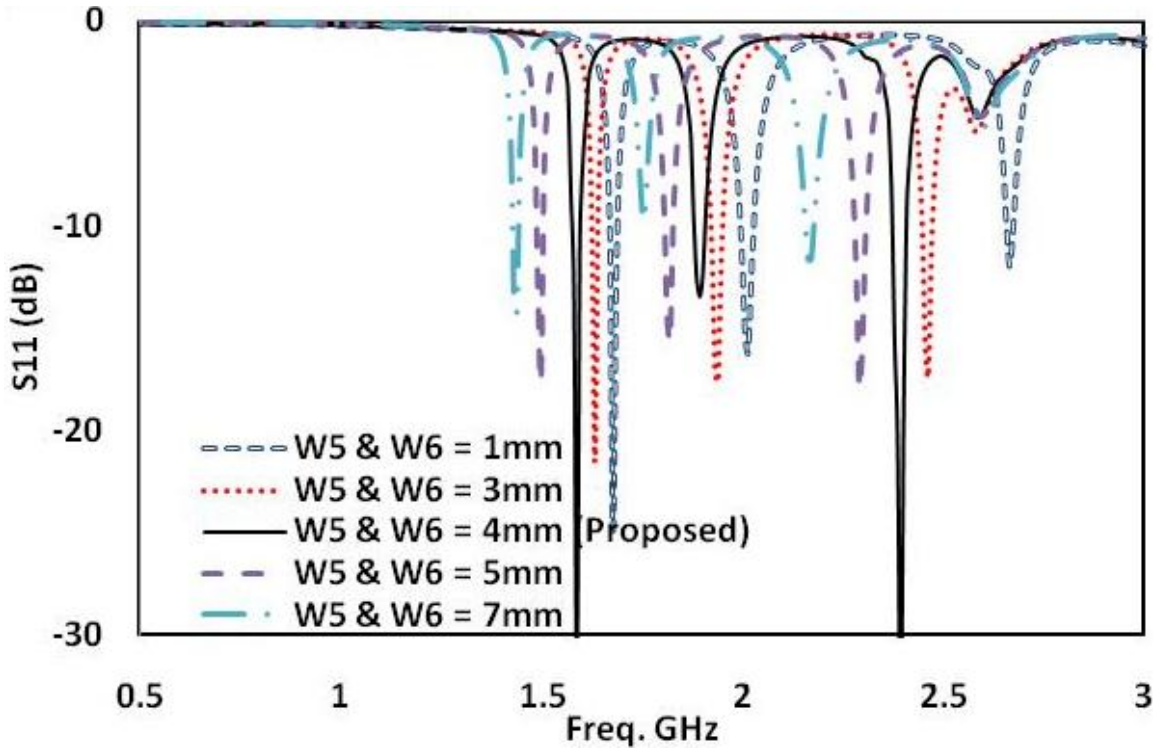

Figure 4-19: Effect of widths W_5 and W_6 on frequency bands

Table 4-6: Frequency bands (GHz) Using Different widths W5 and W6 and Capaciatnce C

W_5 & W_6 (mm)	Tri-band (6pF)		
		Dual band (4pF)	
		Single band (2pF)	
0.5	1.75	2.06	2.78
1	1.72	2.01	2.60
3	1.62	1.95	2.45
4 (Proposed)	1.57	1.88	2.4
5	1.49	1.81	2.3
7	1.39	1.79	2.1
10	1.29	1.61	1.89

More studies have shown that, apart from the arm widths W_5 & W_6 of the H-shape radiator, the varactor capacitance *C* can also be used to shift the frequency bands to other frequencies. The varactor diode used in this study here has a capacitance ranging from 1 to 14 pF and Figure 4-15 (c) shows that, with *C* = 6 pF and W_5 = W_6 = 4 mm, the antenna generates a tri-band at 1.575, 1.88 and 2.4 GHz. With the varactor capacitance *C* increased from 7 to 13 pF at a step of 1 pF, simulation results in Figure 4-20 shows that the higher and lower frequency bands of the tri-band move to the lower frequencies. The tuning range for the lower band is 11.44 % (from 1.57 to 1.4 GHz) and for the higher band is 6.46 % (from 2.4 to 2.25 GHz). The middle band at 1.88 GHz is not affected by the varactor capacitance. This tuning capability of the proposed antenna can give designers more flexibility in designing reconfigurable antennas for uses in different systems and environments.

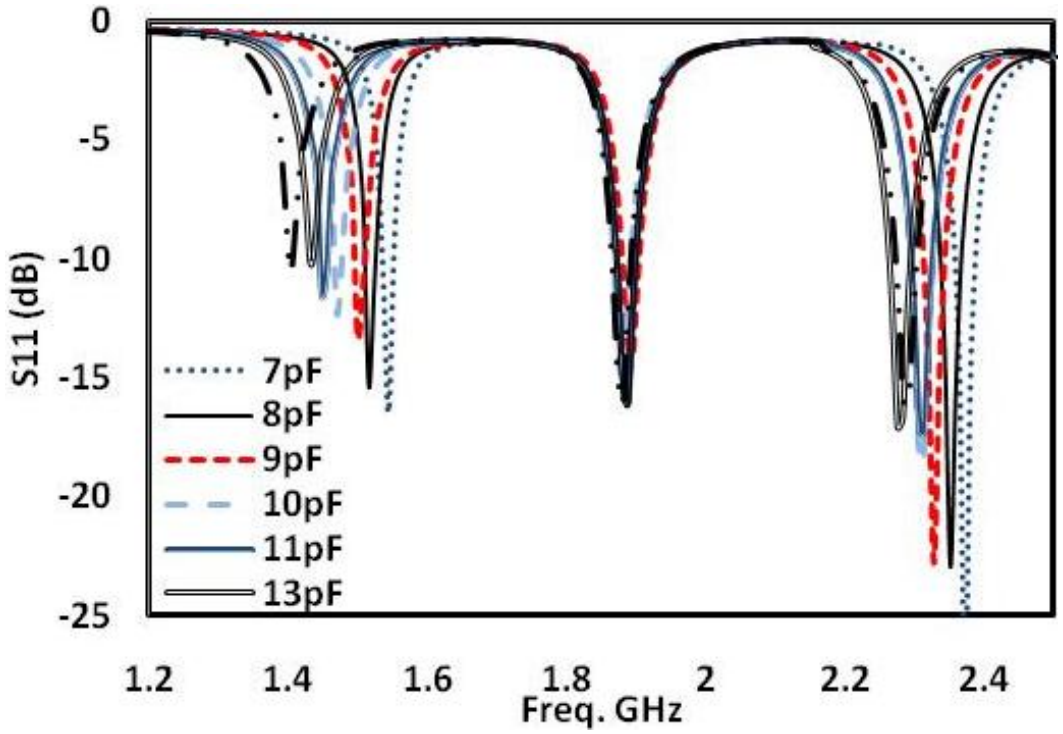

Figure 4-20: Effect of varactor capacitance on frequency bands

4.3.4 Studies on H-Shaped Radiators

4.3.4.1 Full H-Shape Radiator

The previous results show that a single-band, dual-band or tri-band mode can be generated using the varactor diode through the applied DC bias voltage. The operating modes using the Smith chart is studied in here.

Figure 4-21 shows the S_{11} with the varactor capacitance *C* = 2, 4 and 6 pF. With C = 2 pF, Figure 4-21 shows that S_{11} is less than -10 dB for the frequency band from 1.86 to 1.91 GHz and minimum at 1.88 GHz, generating the single-band mode. With *C* increased to 4 pF, Figure 4-15 (b) shows that the 1.88-GHz band remains unchanged, but a higher frequency band is created from 2.37 to 2.44 GHz with S_{11} < -10 dB and minimum at 2.4 GHz. This generates the dual-band mode. With C further increased to 6 pF, Figure 4-21 (c) shows that the 1.88-GHz and 2.4-GHz bands remain about the same, but a lower band at 1.57 GHz is created, resulting in a tri-band mode.

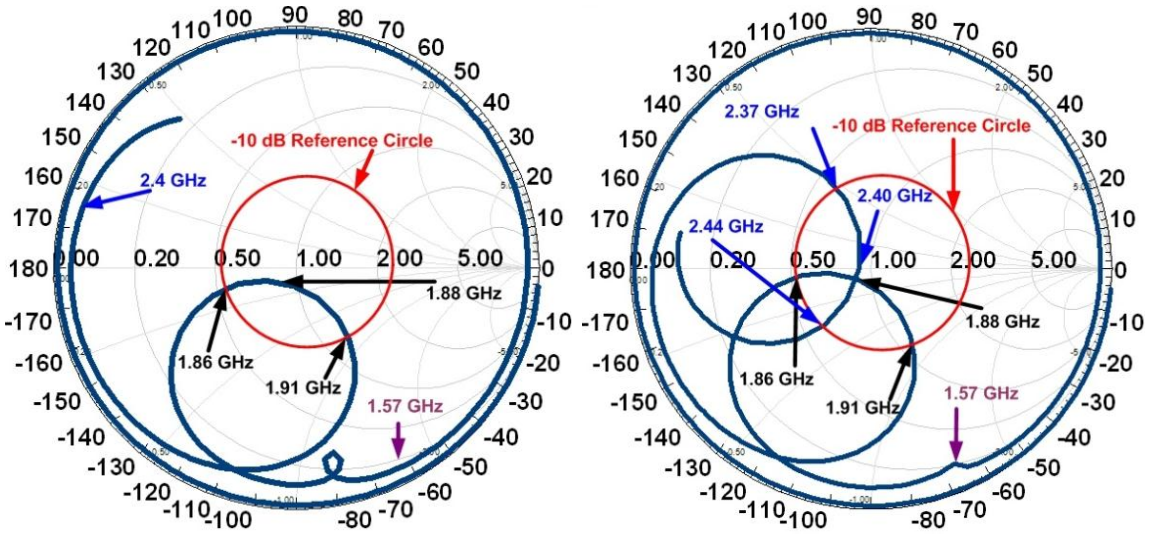

(a) **(b)**

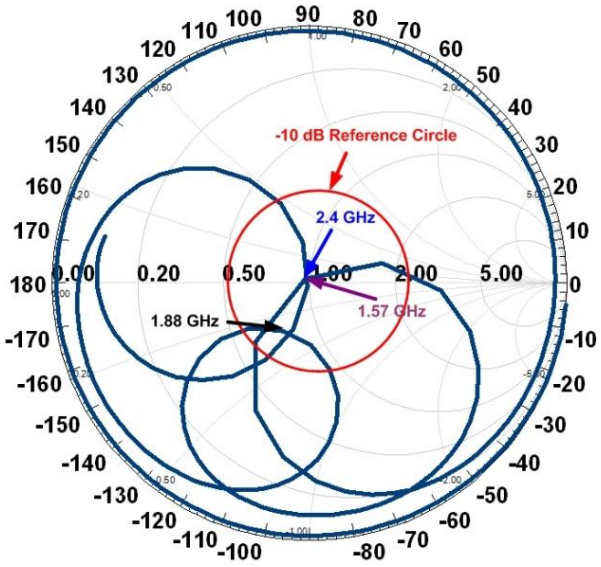

(c)

Figure 4-17: Simulated Smith Charts with varactor capacitance C of (a) 2 pF, (b) 4 pF and (C) 6 pF

To further understand the antenna behaviour, the current distribution for the three resonant frequencies at 1.88, 2.4 and 1.57 GHz have been studied by simulation and results are shown in Figure 4-22 (a)-(c), respectively. The current density in Figure 4-22 (a) shows that the CPW feed line and the H-shape radiator have the highest densities and so generate the resonant bands at 1.88 GHz as shown in Figure 4-15 (a). Figure 4-22 (b) shows that the highest current density is on the left-hand side (LHS) of the H-shape, which generates the 2.4-GHZ band in Figure 4-15 (b), while Figure 4-22 (c) shows that the current concentrates most in the right-hand side (RHS) of the H-shape radiator, generating the 1.57-GHz band in Figure 4-15 (c). So different parts of the H-shape radiator are responsible for generating different frequency bands and are further studied in the following section.

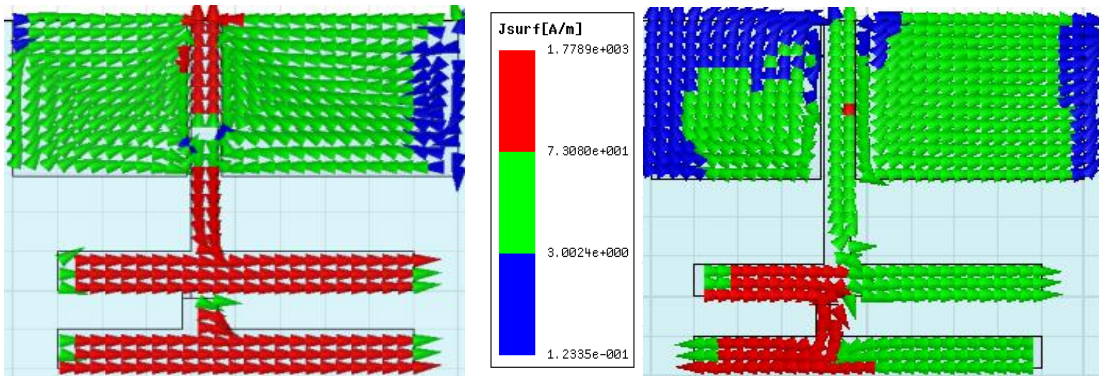

(a) (b)

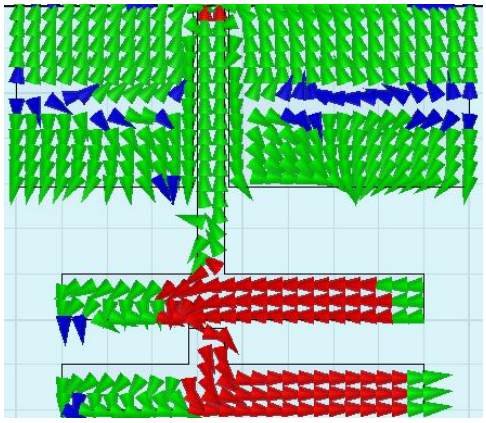

(c)

Figure 4-18: Simulated current distributions at (a) 1.88GHz, (b) 2.4GHz and (c) 1.57GHz with C=6pF

4.3.4.2 Partial H-shape radiator

Figures 4-23 (a) - (c) shows the simulated results with only the upper arm, the LHS of the H-shape radiator and only the RHS of the H-shape radiator. Figure 23 (a) shows that, a 1.88-GHz band with a return loss of less than 10 dB (S_{11} > -10 dB) can be generated by the upper arm of the H-shape. The lower arm with *C* = 2 pF increases the return loss to more than 10 dB. The 2.4-GHz band as shown in Figure 4-26 (b) is mainly generated by the LHS of the H-shape with *C* = 4 or 6 pF, while the 1.57-GHz band is generated by the RHS of the H-shape with *C* = 6 pF as shown in Figure 4-23 (c).

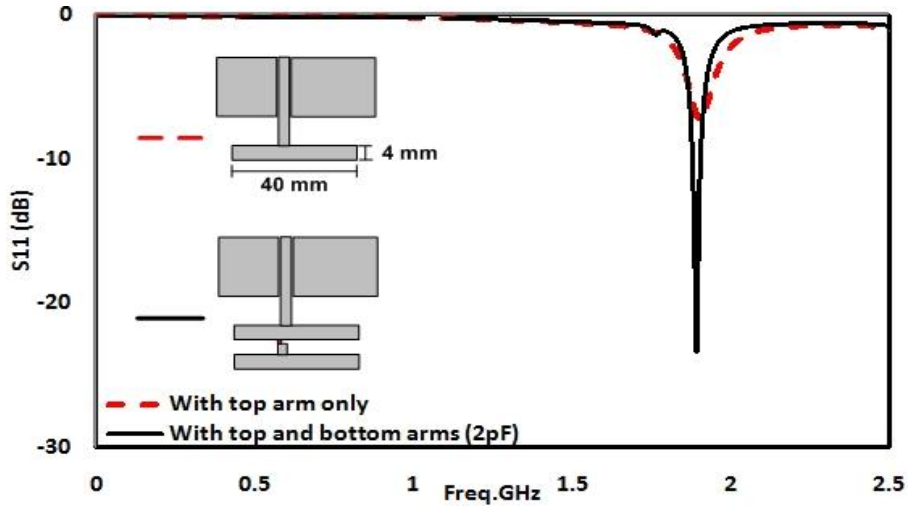

(a)

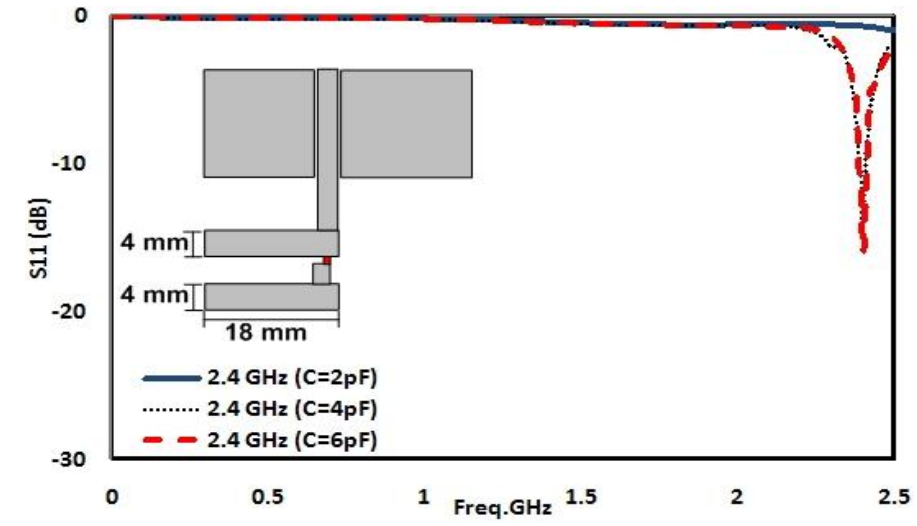

(b)

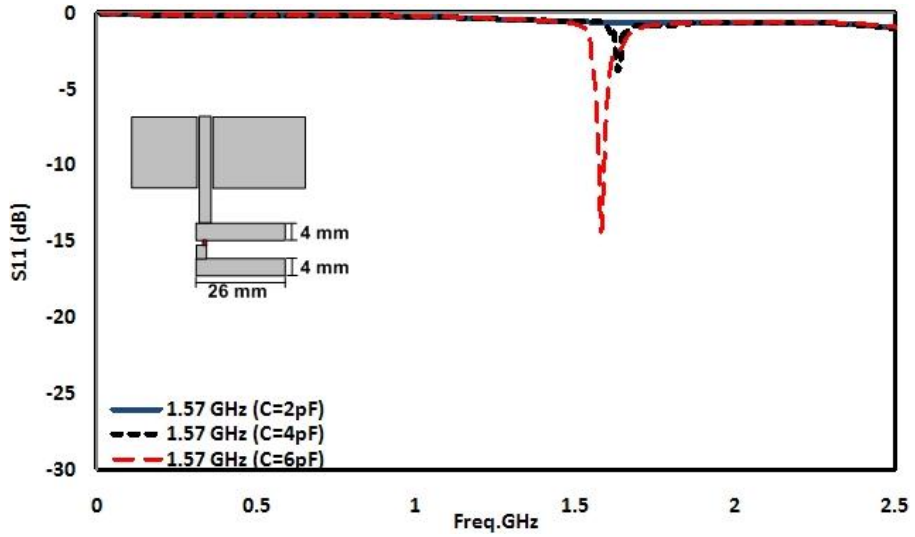

(c)

Figure 4-19: Simulated S_{11} with (a) upper arm only and two arms with C = 2 pF, (b) LHS arms and C = 2, 4, and 6 pF and (c) RHS arms with C = 2, 4 and 6 pF.

The resonant behaviours of the antenna in these three conditions are also studied using the Smith charts in Figure 4-24. With the use of only the upper arm in the H-shape, Figure 4-24 (a) shows that the return loss cannot be larger than 10 dB (i.e., cannot reach inside the -10-dB circle). With *C* = 2, 4, or 6 pF, the antenna with only the LHS of the H-shape generates a frequency band centred at 2.4 GHz as can be seen in Figure 4-24 (b), while the antenna with only the RHS of the H-shape generate the bands all centred at 1.88 GHz as shown in Figure 4-24 (c). Figures 4-23 and 4-24 indicate that different parts of the H-shape are used to generated different frequency bands. However, it should be noted that the role of the varactor diode is simply to help achieve the required matching at these frequencies.

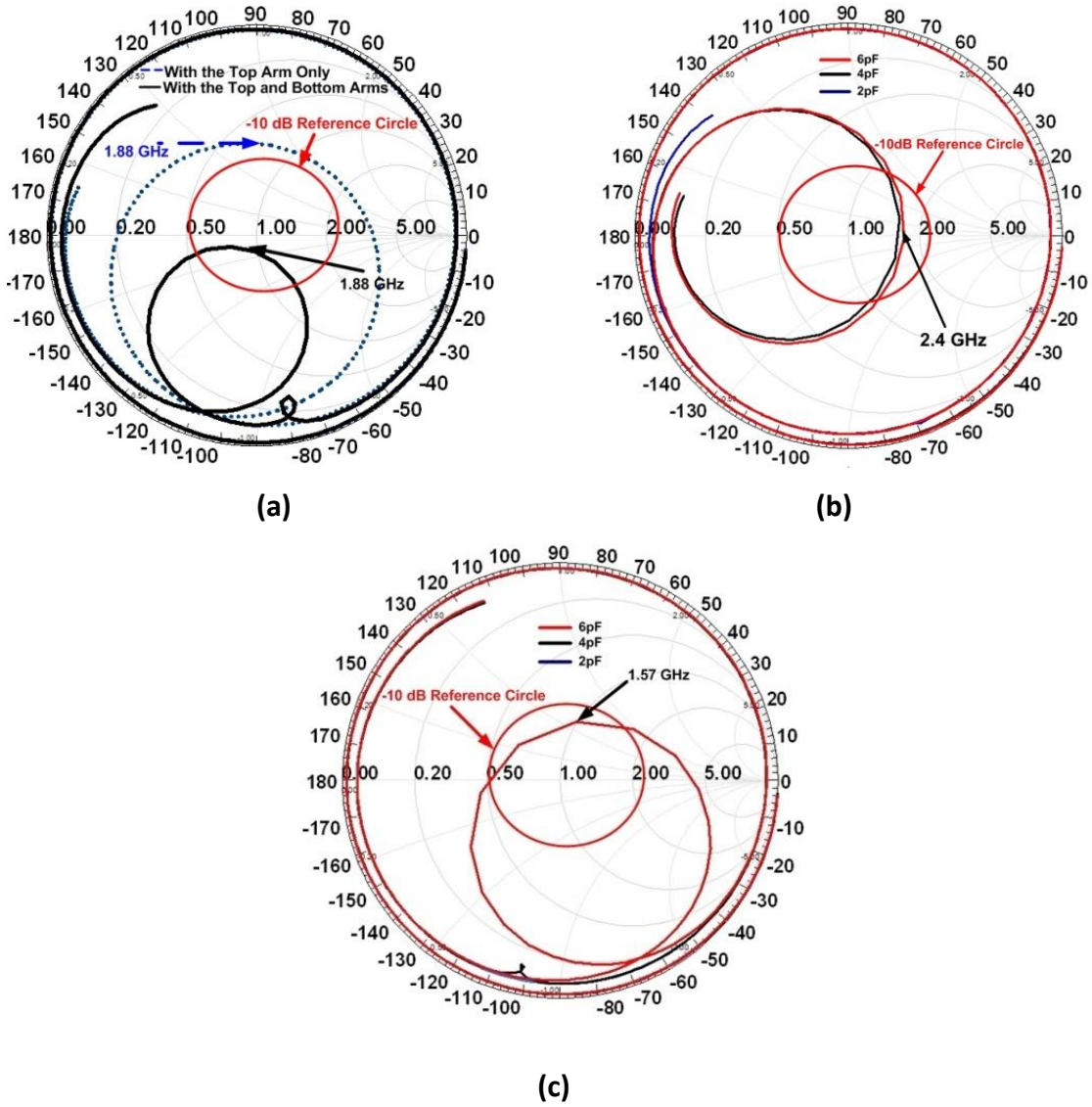

Figure 4-20: Simulated smith chart with (a) top arm only and tow arms with c=2pF, (b) LHS arms and c- 2, 4 and 6 pF and (c) RHS arms with C = 2, 4 and 6 pF.

4.4 Summary

This chapter has tackled the narrow band problem in patch antenna using switchable dual-patch elements allowing a wideband and multi-narrow bands characteristics to be obtained which can be used for cognitive radio applications. Moreover, this chapter has introduced a novel selectable method to select single, dual and tri bands. This method over comes the need to increase the surface area or add additional radiated elements to obtain multiple band operations.

Therefore, in section 4.2, a reconfigurable multiband and wideband patch antenna, employing dual-patch elements and C-Slots with a compact volume of 50 x 50 x 1.57 mm^3, has been presented and studied using simulation and measurement. Two PIN diode switches are used to switch ON and OFF two patch elements to operate the antenna in two different dual-band modes or a wideband mode (with a bandwidth of 33.52%). The frequencies in the dual-band modes can be independently control using the C-Slots without affecting the wideband performance. Simulation and calculation results have shown that the wideband performance is achieved by the coupling effects between the patch elements. The measured and simulated results have shown that radiation patterns across 5-7 GHz are stable in different modes. The main advantages of the proposed antenna include low profile, lightweight and easy to fabricate simple structure targeting future smaller wireless communication devices.

In section 4.3, a reconfigurable H-shaped antenna have been presented using a varactor to control three different operation modes, namely, a single-band mode to cover the GSM1900 system, a dual-band mode at 1.88 and 2.4 GHz to cover the GSM1900 and Bluetooth or WLAN systems, respectively, and a tri-band mode at 1.57, 1.88 and 2.4 GHz to cover the GSM1900, WLAN and GPS system, respectively. Simulation studies and measurements on the reflection coefficient, current density, antenna pattern and gain have been carried out to study the antenna behaviour. Results have shown that, by using the DC bias voltage across the varactor diode, which in turn controls the diode capacitance, the frequency bands in different operation modes can be turned for other applications. The proposed antenna is small and light weight, and so suitable for small wireless devices.

4.5 References

[1] P. Gardner, M. R. Hamid, P. S. Hall, J. Kelly, F. Ghanem, and E. Ebrahimi, “Reconfigurable antennas for cognitive radio: Requirements and potential design approaches,” in Proc. IET Seminar Wideband, Multiband Antennas Arrays Defense Civil Applications, pp. 89–94, Mar. 2008.

[2] H. Wang, X. B. Huang and D. G. Fang, "A Single Layer Wideband U-Slot Microstrip Patch Antenna Array", IEEE Antennas and Wireless Propagation Letters, vol. 7, pp. 9-12, 2008.

[3] C. L. Mak, R. Chair, K. F. Lee, K. M. Luk and A. A. Kishk, "Half U-slot patch antenna with shorting wall", Electronics Letters, vol. 39, pp. 1779-1780, 2003.

[4] Y. Li, R. Chair, K. M. Luk and K. F. Lee, "Broadband triangular patch antenna with a folded shorting wall," IEEE Antennas and Wireless Propagation Letters, vol.3, pp.189-192, 2004.

[5] S. Qu and Q. Xue, "A Y-Shaped Stub Proximity Coupled V-Slot Microstrip Patch Antenna", IEEE Antennas and Wireless Propagation Letters, vol. 6, pp. 40-42, 2007.

[6] Y. Lee and J. Sun, "A New Printed Antenna for Multiband Wireless Applications", Antennas and Wireless Propagation Letters, IEEE, vol. 8, pp. 402-405, 2009.

[7] J. Anguera, C. Puente, C. Borja and J. Soler, "Dual-Frequency Broadband-Stacked Microstrip Antenna Using a Reactive Loading and a Fractal-Shaped Radiating Edge", IEEE Antennas and Wireless Propagation Letters, vol. 6, pp. 309-312, 2007.

[8] K. Wong and W. Hsu, “A Broad-Band Rectangular Patch Antenna with a Pair of Wide Slits,” IEEE Transaction Antennas Propagation, vol.49, no.9, pp.1345-1347, Sep. 2001.

[9] F. Yang, X. Zhang, X. Ye, and Y. Rahmat-Samii,“ Wide-Band E-Shaped Patch Antennas for Wireless Communications,” IEEE Transaction Antennas Propagation, vol. 49, no. 7, pp. 1094-1100, July. 2001.

[10] R, Bhalla, L. Shafai, "Broadband patch antenna with a circular arc shaped slot," IEEE Antennas and Propagation Society International Symposium, 2002. vol.1, no., pp. 394-397 vol.1, 2002.

[11] E. Ebrahimi and P. S. Hall, "A dual port wide-narrowband antenna for cognitive radio", 3rd European Conference on Antennas and Propagation, pp. 809-812, 2009.

[12] F. Ghanem, P. S. Hall and J. R. Kelly, "Two port frequency reconfigurable antenna for cognitive radios", Electronics Letters, vol. 45, pp. 534-536, 2009.

[13] R. Kelly, P. S. Hall and P. Gardner, "Integrated wide-narrow band antenna for switched operation", 3rd European Conference on Antennas and Propagation, EuCAP 2009, pp. 3757-3760, 2009.

[14] D. Singh, C. Kalialakis, P. Gardner, and P. S. Hall, “Small H-shaped antennas for MMIC applications,” IEEE Transactions on Antennas and Propagation., vol. 48, pp. 1134–1141, July 2000.

[15] A.F. Sheta, “A novel H-shaped patch antenna”, Microwave Optical Technology Letter P.62–65, 2001.

[16] S.C. Gao, L.W. Li, M.S. Leong and T.S. Yeo, "Wide-band microstrip antenna with an H-shaped coupling aperture", IEEE Transactions on Vehicular Technology, vol. 51, pp. 17-27, 2002.

[17] T.Y. Yum, "A novel H-shaped active integrated antenna," Antennas and Propagation Society International Symposium, 2003. IEEE, vol. 2, pp. 708-711 vol.2, 2003.

[18] R. B. Hwang, "A broadband CPW-fed T-shaped antenna for wireless communications," Microwaves, Antennas and Propagation, IET Proceedings -, vol. 151, pp. 537-543, 2004.

[19] S.B. Chen, Y.C. Jiao, W.W. and F.S. Zhang, "Modified T-shaped planar monopole antennas for multiband operation," IEEE Transactions on Microwave Theory and Techniques, vol. 54, pp. 3267-3270, 2006.

[20] Y.L. Kuo and K.L. Wong, "Printed double-T monopole antenna for 2.4/5.2 GHz dual-band WLAN operations," IEEE Transactions on Antennas and Propagation, vol. 51, pp. 2187-2192, 2003.

[21] M. Sanad, “Double C-Patch Antennas Having Different Aperture Shapes,” IEEE Proceedings on Antennas and Propagation, pp.2116-2119, June 1995

[22] S. Yang, C. Zhang, H. Pan, A. Fathy and V. Nair, "Frequency-reconfigurable antennas for multiradio wireless platforms," IEEE Microwave Magazine, vol. 10, pp. 66-83, 2009.

[23] D. Kim, J. Lee, C. Sik Cho and T. K. Lee, "Design of a Compact Tri-Band PIFA Based on Independent Control of the Resonant Frequencies," IEEE Transactions on Antennas and Propagation, vol. 56, pp. 1428-1436, 2008.

[24] Lim, J.-H. Back, G.-T. Ko, Y.-I. Song, C.-W.; Yun, T.-Y.; , "A Reconfigurable PIFA Using a Switchable PIN-Diode and a Fine-Tuning Varactor for USPCS/WCDMA/m WiMAX / WLAN," IEEE Transactions on Antennas and Propagation, no.99, pp.1-1, 2010.

[25] Han, T.-Y. Huang, C.-T., "Reconfigurable monopolar patch antenna," Electronics Letters, vol.46, no.3, pp.199-200, Feb. 4 2010.

[26] Yong Cai, Y. Guo, A. Weily, "A Frequency-Reconfigurable Quasi-Yagi Dipole Antenna," IEEE Antennas and Wireless Propagation Letters, vol.9, pp.883-886, 2010.

[27] K. Boyle, P. Steeneken, "A Five-Band Reconfigurable PIFA for Mobile Phones," IEEE Transactions on Antennas and Propagation, vol.55, no.11, pp.3300-3309, Nov. 2007.

[28] A. Sheta, S. Mahmoud, "A Widely Tunable Compact Patch Antenna," IEEE Antennas and Wireless Propagation Letters, vol.7, pp.40-42, 2008.

[29] L. Yue, Z. Zhijun, C. Wenhua, F. Zhenghe, M. Iskander, "A Quadband Antenna With Reconfigurable Feedings," IEEE Antennas and Wireless Propagation Letters, vol.8, pp.1069-1071, 2009.

[30] B. Cetiner, G. Crusats, L. Jofre, N. Biyikli, "RF MEMS Integrated Frequency Reconfigurable Annular Slot Antenna," IEEE Transactions on Antennas and Propagation, vol.58, no.3, pp.626-632,March 2010.

[31] C. Zhang, S. Yang, El-Ghazaly, S. Fathy, A.E.; Nair, V.K., "A Low-Profile Branched Monopole Laptop Reconfigurable Multiband Antenna for Wireless Applications," IEEE Antennas and Wireless Propagation Letters, vol.8, pp.216-219, 2009.

[32] C. Jung, M. Lee, F. De Flaviis, "Reconfigurable dual-band antenna with high frequency ratio (1.6:1) using MEMS switches," Electronics Letters, vol.44, no.2, pp.76-77, January 2008.

[33] S. Haykin, 'Cognitive radio: brain-empowered wireless communications' IEEE Journal on Selected Areas in Communications, Vol. 23, No. 2. pp. 201-220. 2005.

[34] M. Dillinger, N. Alonistioti, and K. Madani, Software Defined Radio: Architectures, Systems and Functions, Wiley, 2003.

[35] C.A. Balanis, Antenna Theory, 2nd ed. New York: John Wiley & Sons, Inc., 1997.

[36] J. Volakis, "Antenna Engineering Handbook," McGraw Hill, 2007. Ch. 16.

[37] D. M. Pozar, Microwave Engineering, 2nd Ed., Toronto: John Wiley & Sons, 1998.

[38] A. A. Serra, P. Nepa, G. Manara, R. Massini, "A Low-Profile Linearly Polarized 3D PIFA for Handheld GPS Terminals," IEEE Transactions on Antennas and Propagation, vol.58, no.4, pp.1060-1066, 2010.

Chapter 5

Tunable Multiband Antennas

5.1 Introduction

Although fixed multiband antennas can widely be used in many different systems or devices, they lack the flexibility to accommodate new services compared with reconfigurable antennas as discussed earlier. This chapter presents tunable reconfigurable antennas, which is another type of frequency reconfigurable antennas.

Different reconfigurable (tunable) antennas have been proposed in [1] – [18]. Some of these techniques have the problems of 1) requiring high voltages to perform tuning, 2) being high profiles, 3) being large sizes or 4) having small tuning ranges and 5) services at lower frequencies such as DVB-H and GSM900 could not be covered as in [16]-[18].

Independent tuning on reconfigurable antennas has received much attention recently. A number of techniques have been proposed to achieve independent control for one or more bands over a wide range. For example in [19], a reconfigurable dual-band antenna has been reported with a wide tuning range (2020 MHz). However, a high voltage is required (30V) to achieve the independent tuning and the size of the antenna is large at 150 x 110 mm^2. In [20] a square-ring dual-band microstrip antenna was reported where the upper resonance frequency was fixed around 1.93 GHz and only the lower resonance frequency was tuned from 1.37 to 1.7 GHz using voltage from 0 to 30 V. Most of the reported techniques to independently tune and control each band are either using high voltage to perform the tuning or using high profile and large size antenna.

Although there is an extensive literature on frequency reconfigurable antennas [1] – [20], the following important issues needed to be addressed:

- The overall size and thickness of the antenna should be small and thin.
- The simplicity of the structure to reduce the cost of the fabrication.
- The number of reconfigurable elements (varactors) should be less to avoid complex biasing circuits.
- The multiplicity of bands generated from one antenna so the antenna can serve more than one application.
- Electrically Independent control with wide control range to cover more applications.
- The use of high voltages to perform reconfiguration.
- The effect of user's hand and housing of mobile phone when using reconfigurable antenna in mobile phone.

This chapter addressed all the above issues using the same antennas that were presented in chapter 3.

5.2 Tunable Multiband Antenna with Wide and Independent Tuning

5.2.1 Introduction

The results obtained in section 3.4 are used here to design a frequency reconfigurable antenna. By putting a varactor (diode) at each of the inputs to the sub-patches, four of the frequency bands can be controlled independently over wide ranges and the antenna becomes a reconfigurable design. The achievable tunability ranges for the four bands of 0.92, 1.73, 1.98 and 2.9 GHz are 23.5%, 10.30%, 13.5% and 3%, respectively.

The design presented in this section has tackled the large size and the limited number of bands. Moreover, the antenna presented in this section has the freedom to control one of the five-bands and tune it for other applications without affecting the other four bands.

5.2.2 Antenna structure and Design Procedure

The dimensions used to the proposed frequency reconfigurable antenna, as shown in Figure 5-1, are same as those of the fixed design, i.e .shown in Figure 3-24 and listed in Table 1. Four varactors, varactors #1, #2, #3 and #4, are placed at the inputs of the sub-patches. The positions of the varactors and the capacitor on the antenna are carefully selected and optimized so that the maximum tunable ranges with independent control can be accomplished.

A surface-mount-ceramic-chip capacitance is used for blocking the DC signal from the biased circuits for the varactors, preventing the DC signal from flowing to the antenna while allowing RF signal to go through. The inductors L_1, L_2, L_3, L_4 and L_5 are used as radio-frequency (RF) chokes, providing low impedance for the DC signal and high impedance for the RF signal. The resistors R_1, R_2, R_3, R_4 and R_5 are used to give extra protection to the varactors from being damaged. Detailed structure of the bias network is also shown in Figure 5-1(a)-(b). The EM simulation tool, HFSS, is used for study the antenna performance. Just to proof the design concept, practical varactors, BB184 from Philips, have been used. It is difficult to model the packaging of the capacitor in a full-wave solver, so the varactors are modelled using the Resistance, Inductance and Capacitance (RLC) boundary sheet which gives 0.6nH and 0.65ohm for the inductance and resistance, respectively.

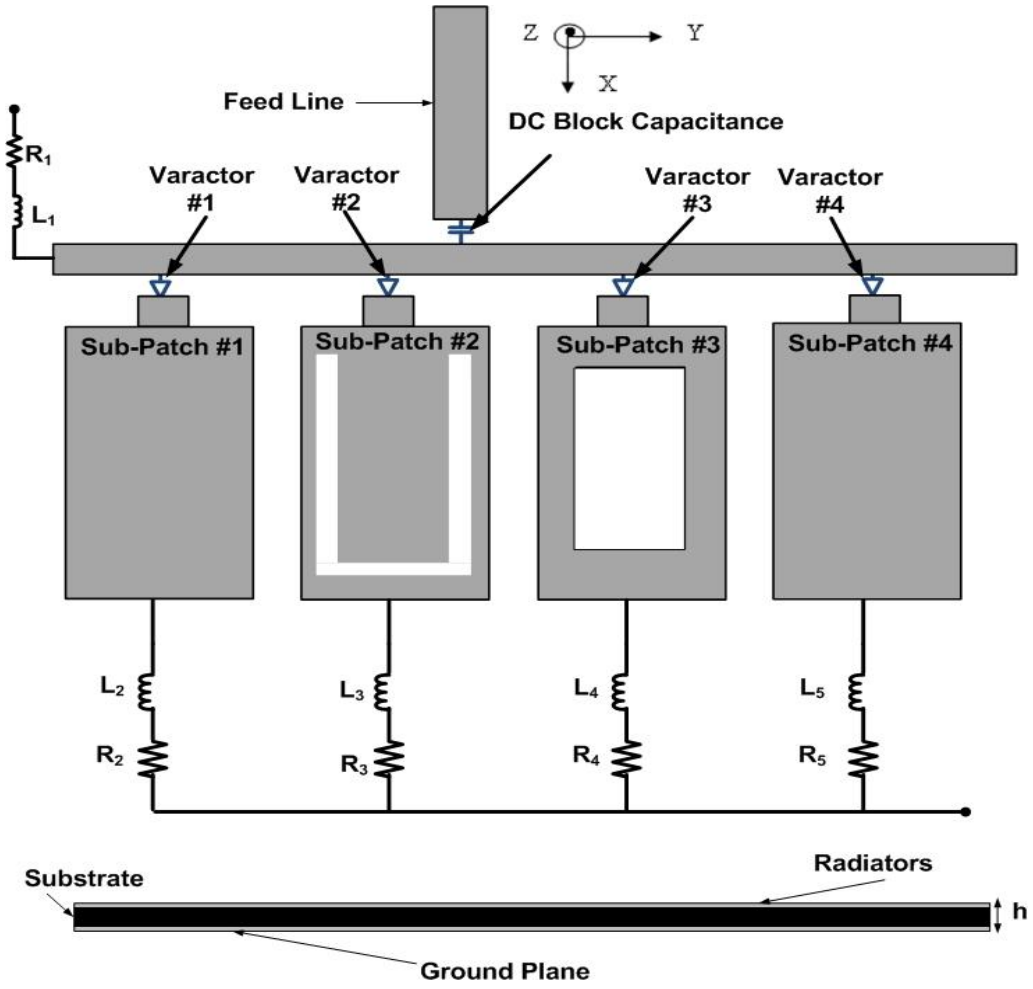

(a)

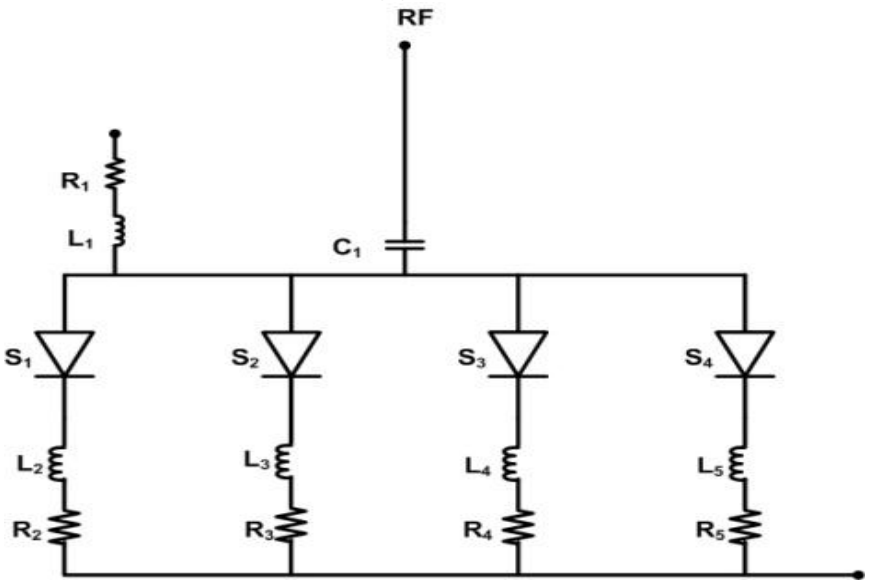

(b)

Figure 5-1: (a) Structure of proposed reconfigurable design and (b) biasing network

5.2.3 Independent Tuning and Control Range

A DC biased voltage of 1V is applied to all varactors, leading to a capacitance of 14 pF, simulation results have shown that all the resonant frequencies remain the same as those in the fixed antenna design, i.e., the varacitors under such biased condition have no effect on the resonant frequencies. However, if the biased voltage of all varactors is increased to about 1.5 V simultaneously, all resonant bands slightly shift up. Here, a study of the tuning range for each band using the corresponding varactor is conducted while at the same time keeping all other bands fixed. To study the tuning range of band #1 at 0.92 GHz, the biased voltage for varactor #1 was varied, while keeping the biased voltages for other varactors at 0.5 V. Figure 5-2(a) shows the effect of varying the capacitance of varactor #1 on the resonant frequency 0.92 GHz band. It can be seen the 0.92 GHz band can be independently tuned between 0.92 to 1.16 GHz without disturbing much the other four bands. For the tuning range of band #3 at 1.98 GHz, the biased voltage for varactor #4 is varied. Here to illustrate the flexibility of the design, the biased voltage was fixed at a higher value of 1.5 V to other varactors, which slightly shifts all five bands, bands #1, #2, #3, #4 and #5 to 1.08, 1.75, 1.99, 2.48 and 2.98 GHz, respectively. The simulation results are shown in Figure 5-2(b). It can be seen that band #3 at 1.99 GHz band can be tuned independently without affecting much the other four bands. Note that band #4 is determined by the main patch and so cannot be tuned in the reconfigurable design. For the tuning range of band #5 at 2.9 GHz, the biased voltage for varactor #3 is varied. Results have shown that, for the capacitance varied from 3–12 pF, the 2.9 GHz band is only moved by about 3% which is quite small. This might be due to the location of the slot which did not allow the current on this sub-patch to be changed. For the tuning range of band #2, varactor #2 is used. However, the simulated result in Figure 5-2(c) shows that the undesirable frequency band at 1 GHz is emphasised and moved, instead of band #2 at 1.73 GHz. The reason is that the varactor capacitance improves the matching at this frequency. To solve this problem, we re-design U-slot in sub-patch #2 and move the varactor to the slot gap as shown in Figure 5-2(d). The effect of varying the capacitance of varactor #2 on the resonant frequency 1.73 GHz band is shown in Figure 5-2(d). It can be seen that now, the 1.73 GHz band can be tuned independently from 1.73–1.56 GHz, while the other four bands remain unchanged. Table 5-1 summarise these results.

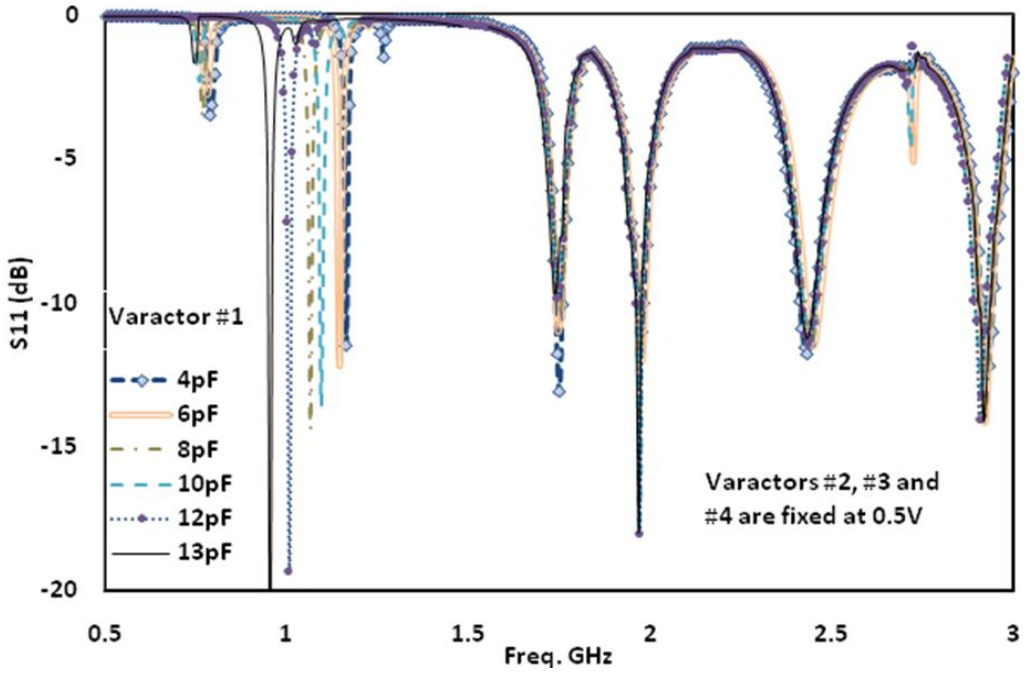
0
-5
-10
-15
-20
S11 (dB)
Varactor #1
4pF
6pF
8pF
10pF
12pF
13pF
Varactors #2, #3 and
#4 are fixed at 0.5V
0.5
1
1.5
2
2.5
3
Freq. GHz

(a)

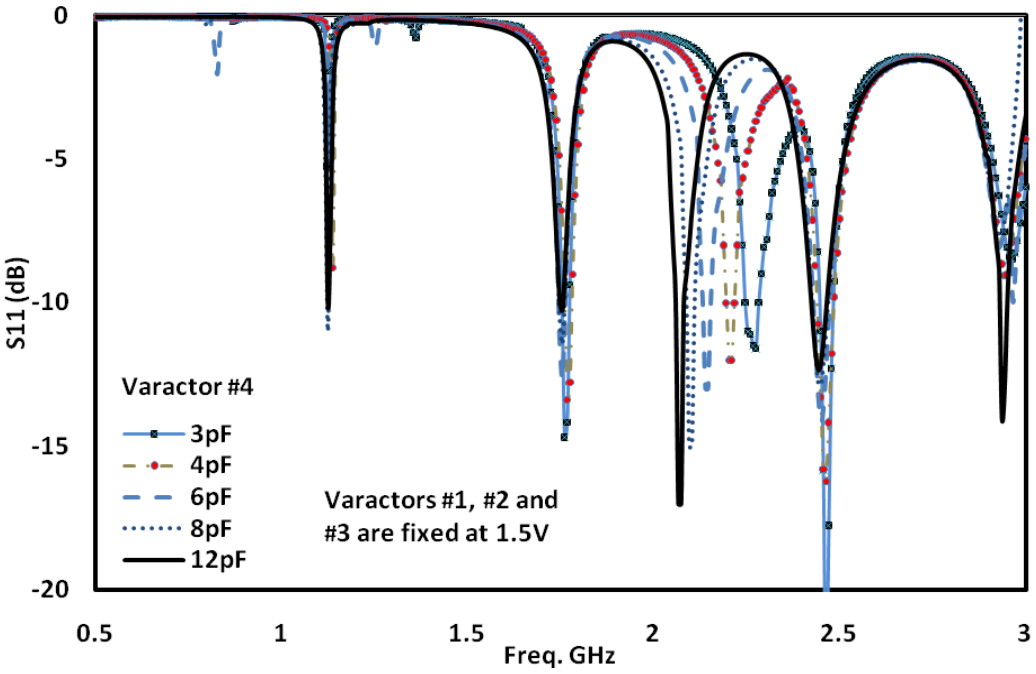
0
-5
-10
-15
-20
S11 (dB)
Varactor #4
3pF
4pF
6pF
8pF
12pF
Varactors #1, #2 and
#3 are fixed at 1.5V
0.5
1
1.5
2
2.5
3
Freq. GHz

(b)

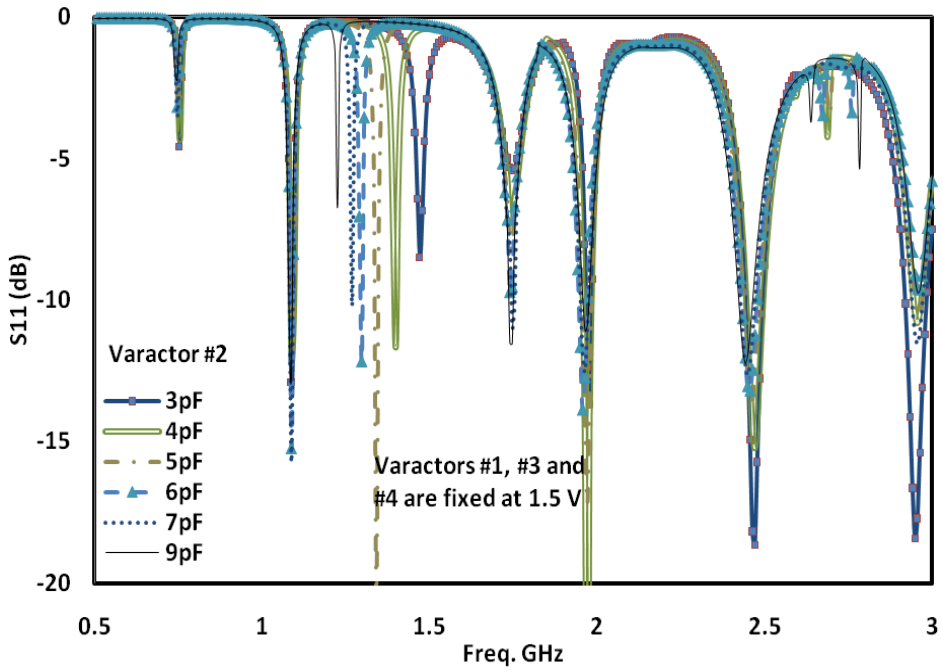

(c)

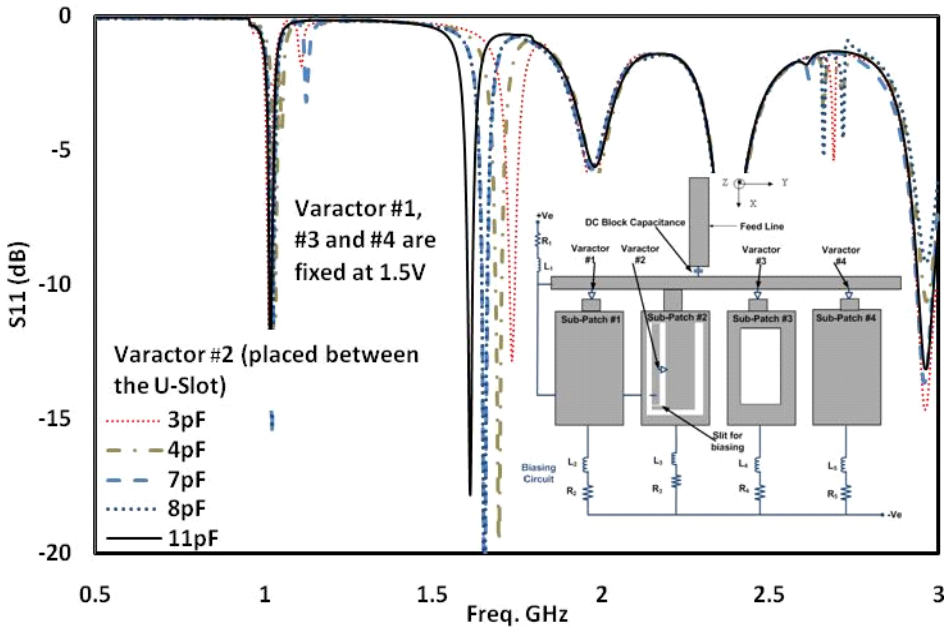

(d)

Figure 5-2: Measured S_{11} for reconfigurable design with independent control using (a) Varactor #1, (b) Varactor #4, (c) Varactor #2 (at the input of sub-patch #2), and (d) Varactor #2 (re-located on the U-Slot).

Table 5-1: Effect of varying capacitances of varactors independently and/or simultaneously

	Band #1	Band #2	Band #3	Band #4	Band #5
Varactor #1	920 – 1165 MHz	Fixed	Fixed	Fixed	Fixed
Varactor #2	Fixed	1560-1730 MHz	Fixed	Fixed	Fixed
Varactor #3	Fixed	Fixed	Fixed	Fixed	2900 - 2990MHz
Varactor #4	Fixed	Fixed	1980 – 2267MHz	Fixed	Fixed
Bandwidth covered	23.5%	10.3%	13.5%	--	3%

For the reconfigurable design, the effects of the varactor capacitance on the radiation patterns in three bands i.e., bands #1, #2 and #3 were studied. The measured results are shown in Figure 5-3 (a) - (c), indicating that the effects are insignificant. The study was not done for band #4 (which is not tunable) or band #5 (which has a very small tunable range of only 3%).

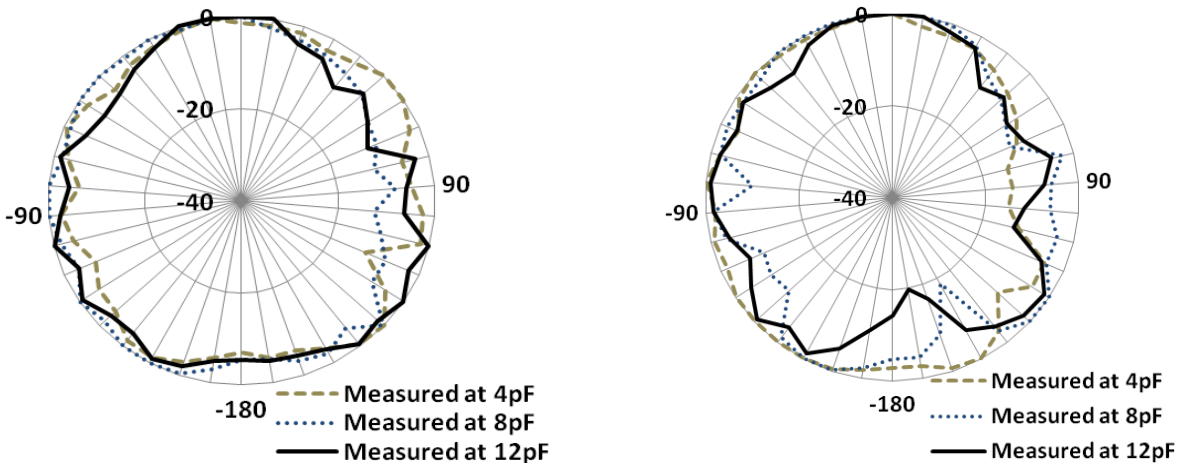

(a)

X-Z **Y-Z**

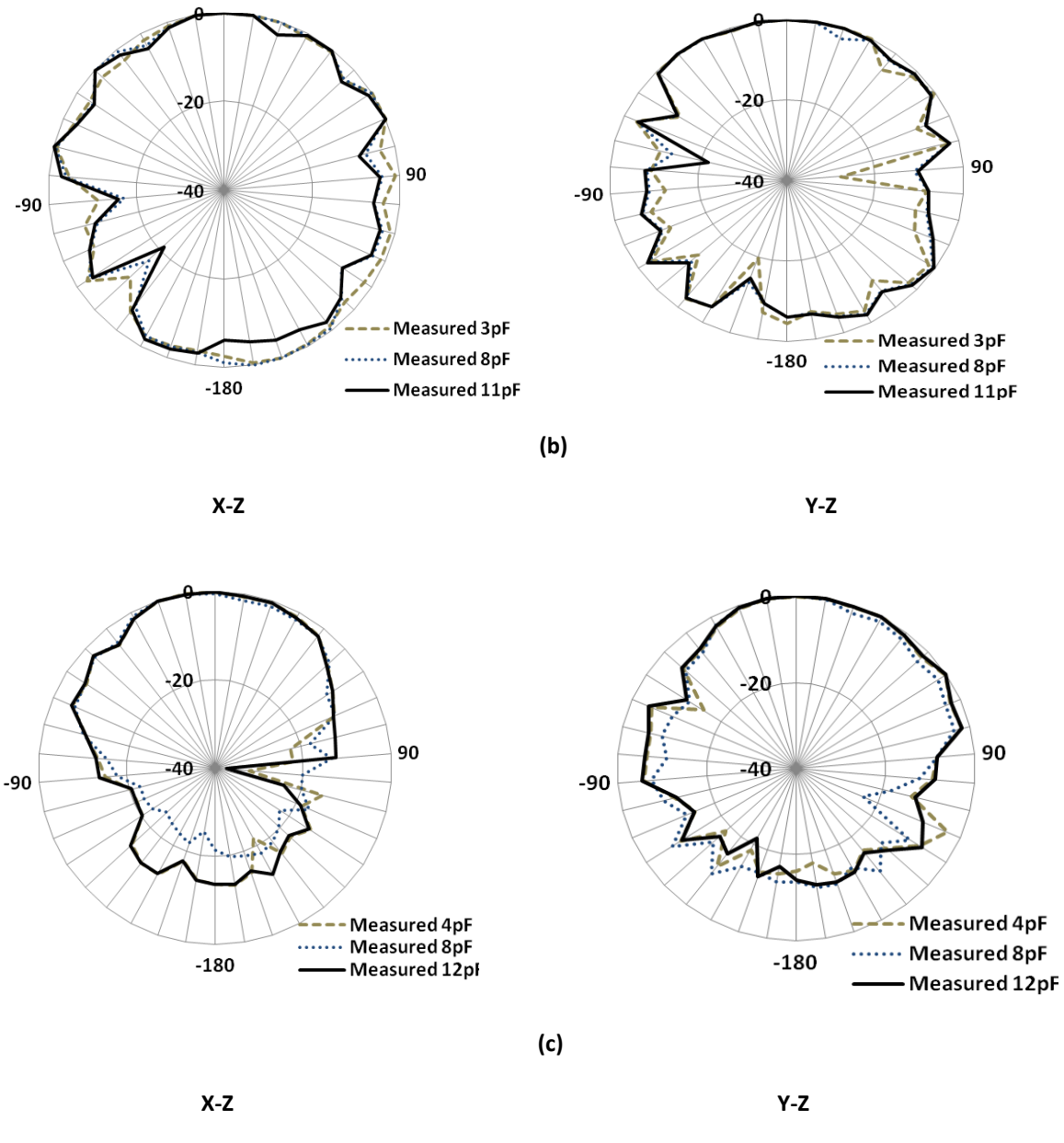

Figure 5-3: Measured Co-Pol radiation patterns for the reconfigurable design for X-Z and Y-Z planes at (a) first band (b) Second band and (c) third band

5.3 Reconfigurable Penta-Band PIFA for Small and Slim Mobile Handsets

5.3.1 Introduction

In this section, as part of the comprehensive study on the fixed PIFA antenna presented in section 3.3, investigation is carried out to analyse the possibilities of making the PIFA tunable or switchable so other applications in the lower frequencies such as GSM, GPS, DVB-H and other bands can be achieved without changing the shape of the antenna. It is found that, when using varactor or PIN diodes, the antenna can serve more standards and applications than the fixed PIFA that was previously discussed in section 3.3. Yet, the size of the ground plane is small and slim which can be fitted in small and slim modern mobile phones. The proposed reconfigurable PIFA is simple and practically implementable.

Therefore, the antenna consists of two radiators and connected together using two PIN or varactors diodes. Frequency reconfigurability is obtained by i) tuning using varactor diodes or ii) switching using PIN diodes. In the study, when varactors are used, the PIFA is optimized to operate in five frequency bands centered at 0.72, 1.35, 1.98, 3.6 and 5 GHz. Varying the voltages across the varactors can tune these five bands over the range of 45.33% (5.8-9.2 GHz), 17.77% (1.23-1.47 GHz), 26% (1.57-2.04 GHz), 6.66% (3.48-3.72 GHz) and 0.97% (4.99-5.04MHz), covering the DVB-H, GSM 800/900, GPS, PCS, DCS, UMTS, Wibro phase III, WiMAX and WLAN systems etc. If PIN diode switches are used instead, the frequency bands can be switched among different standards, including the DVB-H, GSM, UMTS, DCS, GPS, WiMAX and WLAN systems, depending on the switching states. The two radiators are supported using a shorting wall and a shorting pin connected to a small ground plane.

5.3.2 Design Structure

The structure and dimensions of the proposed reconfigurable PIFA are shown in Figure 5-4 (a), where two radiators, radiators #1 and #2, are optimized to excite multiple resonances in the antenna as described in section 3.3 and in [21]. These two radiators are separated by a slot, but connected together by a pair of varactor or PIN diodes. The varactors and PIN diodes operate like variable capacitors and switches, respectively. The

positions of the varactor or the PIN diodes on the structure are optimized using the HFSS simulator software to achieve the widest tunable range. The antenna was fabricated using an FR-4 substrate with thickness of 1.57 mm and a relative permittivity of 4.4, as shown in Figure 5-4(b). To prove the design concept, a practical PIN diode, SMP1320-079 from Skyworks Solutions Inc was employed with size of 1.5 x 0.7 mm^2, for the switching function in the prototype. For the tuning , a practical varactor diode, BB184 from NXP with a capacitance value ranging from 2 pF to 14 pF controlled by a DC bias voltage varying from 1 V to 14 V was employed. The dimension of the varactor diode is approximately 1 x 1 mm^2. In the simulations, the PIN diodes were modelled using Resistance, Inductance and Capacitance (RLC) boundary sheet with 0.9 Ω as the impedance value of the PIN diode in the ON state and 0.3 pF as the capacitance value in the OFF state. These PIN diodes were turned "ON" and "OFF" using a DC biased signal. Similarly, the RLC boundary sheet was used to simulate the antenna performance when the capacitance of the varactor diodes varied from 2 pF to 14 pF. Figure 5-4(a) also shows the DC bias setup using a Bias-Tee for the PIN or varactor diodes for the antenna. The RF signal from a VNA is fed to the Bias-Tee, combined with the DC biased voltage and then fed to feed line of the antenna. In order to maintain a DC potential difference between the two radiators for biasing the PIN or varactor diodes, the shorting wall is cut open and connected together using a 10 pF capacitance, as shown in Figure 5-4 (a). Studies have shown that the position of this capacitor on the shorting wall is not sensitive to impedance matching of the antenna.

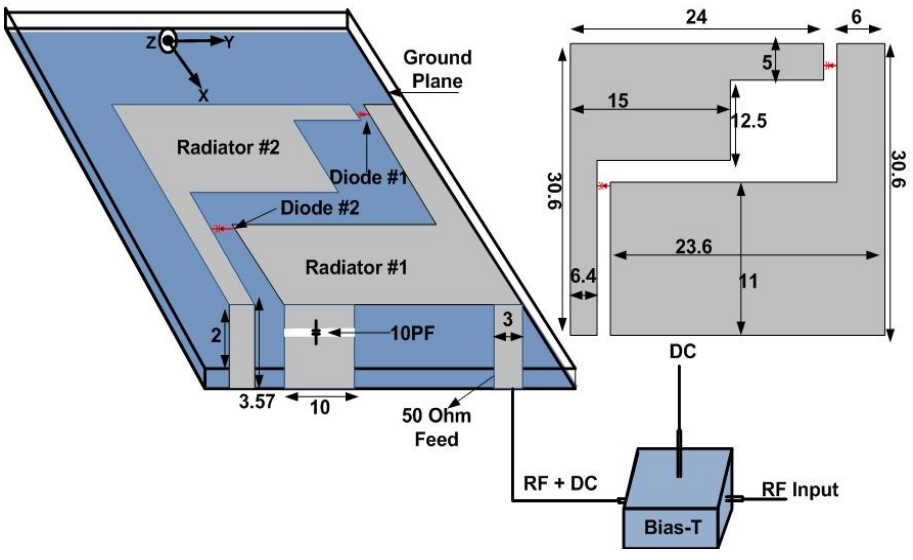

(a)

(b)

Figure 5-4: Layout of proposed antenna (a) 3D View and detailed dimensions and (b) prototype antenna

5.3.3 Simulated and Measured Results

5.3.3.1 Using Varactor Diode

The reflection coefficients (S_{11} in dB) of the proposed antenna for different bias voltages across the varactors are shown in Figure 5-5. It can be seen that, with the capacitance varied from 2 to 6 pF, the operating frequency bands of the antenna can be tuned over the range of 45.33% (0.580-0.920 GHz), 17.77% (1.230-1.470 GHz) and 26% (1.570-2.040 GHz). Thus the antenna can be used to serve many wireless and mobile applications, including the DVB-H, GSM800/900/1800/1900, GPS, PCS, DCS, UMTS, WLAN, HaiperLAN/2 and the middle and higher bands of the WiMAX applications, as listed in Table 5-2. Further results of simulations have reviewed that varying the capacitance values of the varactor diodes alters the surface current distributions of the antenna, hence changing the operating frequencies of these bands. If the capacitance is further increased to more than 6pF by reducing the biased voltage, the impedance of the first and second bands are affected and no longer matched, i.e., S_{11}>-6 dB.

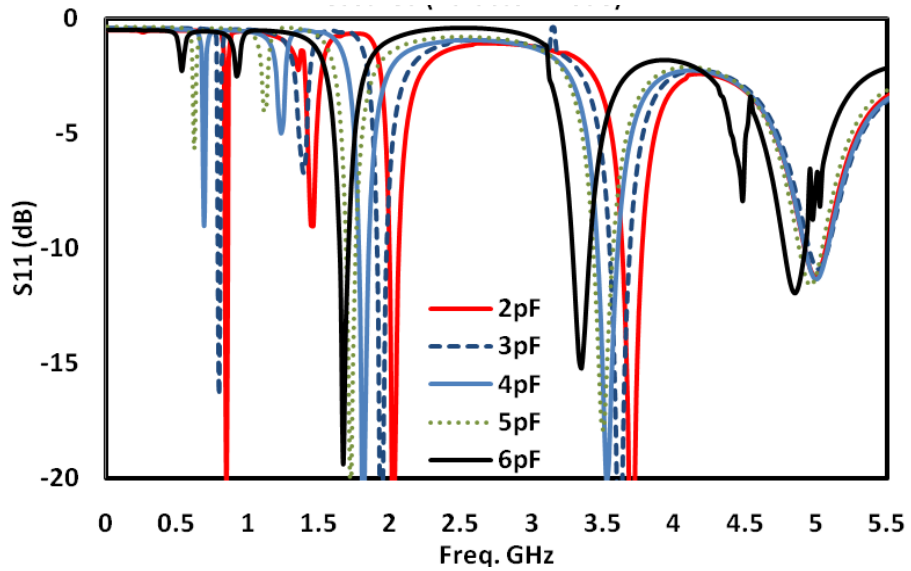

Figure 5-5: Measured S_{11} when using varactor diode

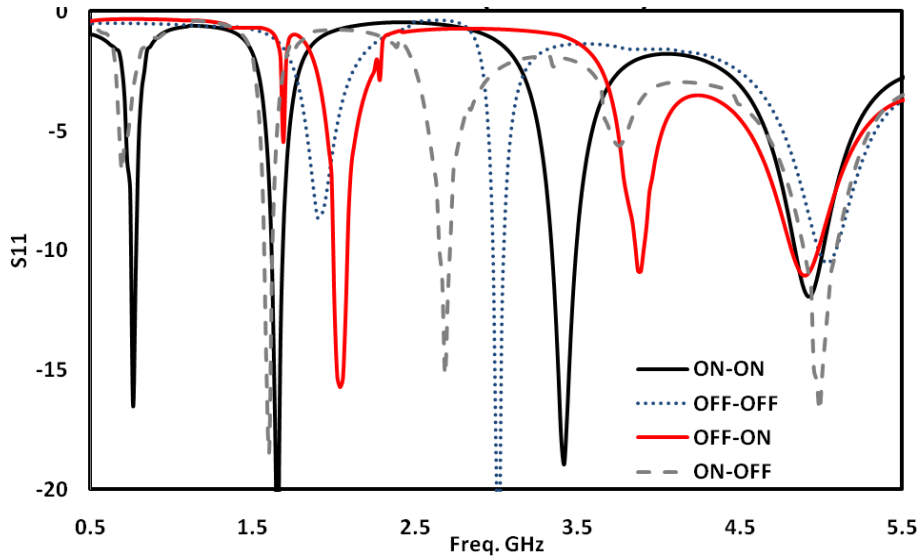

Figure 5-6: Measure S_{11} when using PIN diode

5.3.3.2 Using PIN Diodes

The two diodes, diodes #1 and #2, connecting the two radiators can have four possible switching states, i.e., ON-OFF, OFF-ON, ON-ON and OFF-OFF states, which affect the current distributions on the radiators and hence the operating frequencies of the antenna. The measured S_{11} in these four possible states are shown in Figure 5-6. It can be seen that,

when both diodes are in the ON state, the antenna can cover the DVB-H, DCS, m-WiMAX and WLAN system. When diode #1 is OFF and diode #2 is ON i.e. in the OFF-ON state, the antenna can cover the UMTS, m-WiMAX and WLAN systems. In the ON-OFF state, the antenna covers the DVB-H, GPS, m-WiMAX and WLAN systems. Finally, when both diodes are in the OFF state, the antenna operates in three frequency bands, covering the GSM1900 and WLAN as listed in Table 5-2.

The dimensions of the PIFA are obtained by modifying the fixed PIFA antenna discussed in section 3.3. Results have shown that the radiation patterns of this reconfigurable antenna are similar to those of the antenna reported in section 3.3 [22]. The simulated efficiency when using the PIN or varactor diodes ranges between 78%-95%. The measured efficiency will be less than that as the losses of the parasitic elements will have some effects.

Table 5-2: Band generated when using PIN or varactor diodes

Switch	Remarks	F_1	F_2	F_3	F_4	F_5
Varactor	Tuning range (MHz)	580 – 920 45.33%	1230 – 1470 17.77%	1570 – 2040 26%	3480 – 3720 6.66%	4990 – 5040 0.97 %
Varactor	Services	DVB-H & GSM800/900	--	DCS, PCS, GSM1800 / 1900 & UMTS	m-WiMAX & WiBro phase III	WLAN / h-WiMAX / HaiperLAN/2
PIN	ON-ON	0.72 / DVB-H	--	1.75 / DCS	3.63/m-WiMAX	5.00 / WLAN
PIN	OFF-ON	--	--	2.05 / UMTS	3.89/m-WiMAX	5.10 / WLAN
PIN	ON-OFF	0.72 / DVB-H	--	1.58 / GPS	2.82/m-WiMAX	5.19 / WLAN
PIN	OFF-OFF	--	--	1.93 / GSM1900	3.03	5.35 / WLAN

5.3.4 Human Interaction and Ground Plane Size

5.3.4.1 Effect of Ground Plane Size

In some PIFA designs, the ground plane can have a direct impact on the antenna performance as discussed in the earlier work in section 3.3. However, changing the size of the ground plane in the proposed reconfigurable antenna when using PIN diode in the ON-ON state did not affect its S_{11} response as shown in Figure 5-7. Similarly when using varactor diodes, the S_{11} did not change when the size of the ground plane was changed.

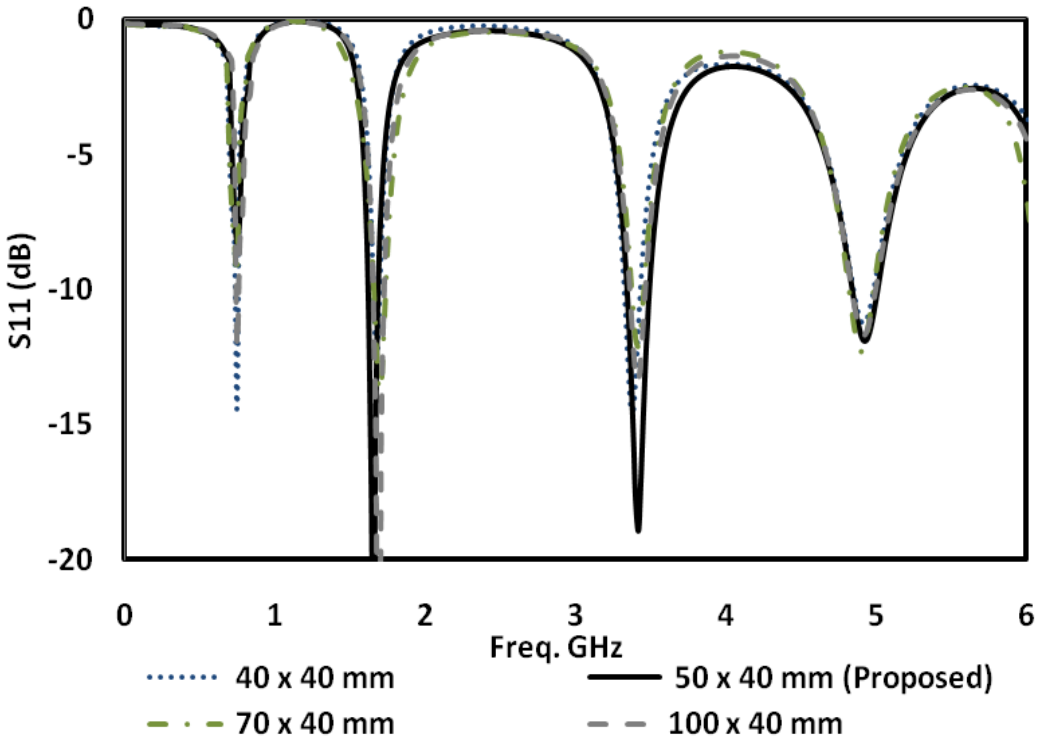

Figure 5-7: Effects of ground plane size when using PIN diode (ON-ON)

5.3.4.2 Effect of User's Hand

When designing antennas for mobile phones, the effect of user's hand on the performance needs to be studied in order to avoid too much human interactions with the antennas [22].

Figure 5-8 (a)-(c) shows the simulation model of the PIFA antenna with the human-hand model in three different positions. The fingers and the palm are attached directly to the ground plane and the main substrate, respectively. The relative permittivity and conductivity of 54 and 1.45 S/m, respectively, for human hand model [23] have been used for simulations.

In position #1, the upper part of the antenna is covered by the hand model. In position #2, the middle part of the antenna is covered. While in position #3, the antenna is not covered by the hand model. Two scenarios have been investigated. The first scenario is when the fingers are placed 1 mm above the radiators and the hand (palm) is touching the ground plane directly on the other side. The results in Figure 5-9(a) show that the human hand only slightly affects the third and fourth bands but very little in the first and the second bands. In a real situation, there will be a gap of at least 2 mm between the antenna (radiators) and the mobile phone housing. If the gap between the antenna and the housing is 2 mm and the housing thickness is 2 mm, it will make a total distance of 4 mm between the antenna and the hand. This is the second scenario studied, i.e. when the fingers are placed 4 mm above the top of the radiators and the hand (palm) is touching the ground plane directly on the other side. The results for the second scenario are shown in Figure 5-9(b). It can be seen that the human hand increases the return losses in the two lower frequency bands and slightly increases it in the higher frequency bands. Thus, the results in Figure 5-11 indicate that, in these three positions studied, the performance of the antenna is not sensitive to the user's hand. Results have shown that the best position, in terms of maximum efficiency and gain, is when the user is holding the mobile phone at the bottom of the antenna, i.e., position #3. If the user's hand gets closer to the radiator, the gain and the radiation efficiency drop slightly compared with the case when the antenna is in free space. However, even in the worse scenarios where the user's hand is covering the radiators with 1 mm and 4 mm gap between them, as in positions #1 and #2, simulation results have showed that the antenna still can attain an efficiency of above 50% which is considered quite acceptable for mobile phone applications.

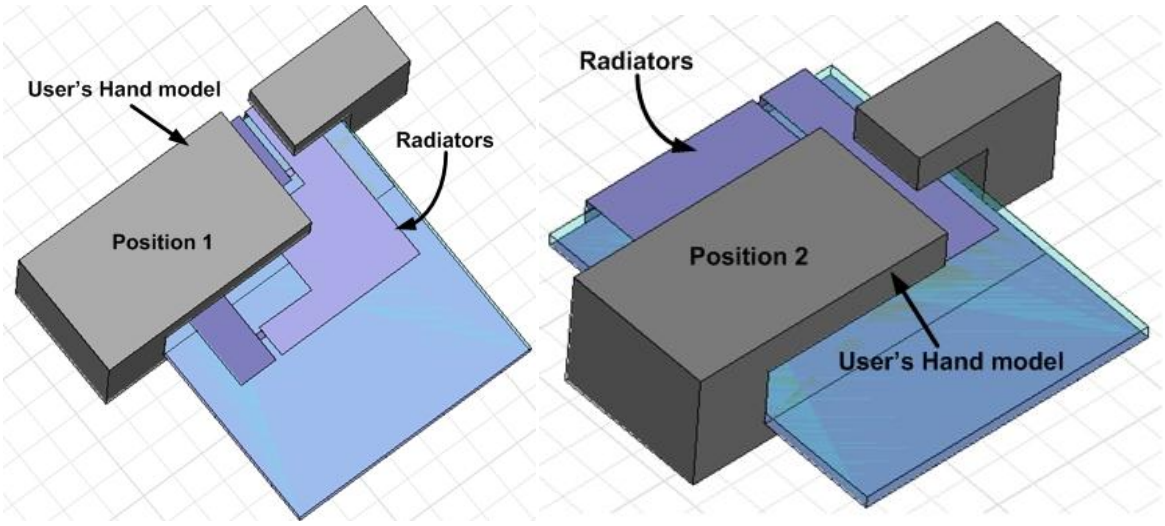

(a) **(b)**

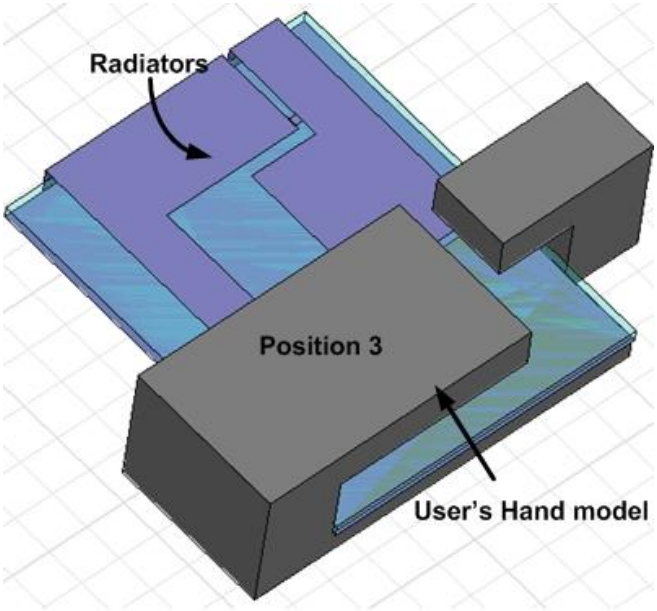

(c)

Figure 5-8: Simulation model for different positions of user's hand (a) User's hand covering radiators, (b) User's hand partly covering radiators and (c) User's hand not covering radiators of antenna.

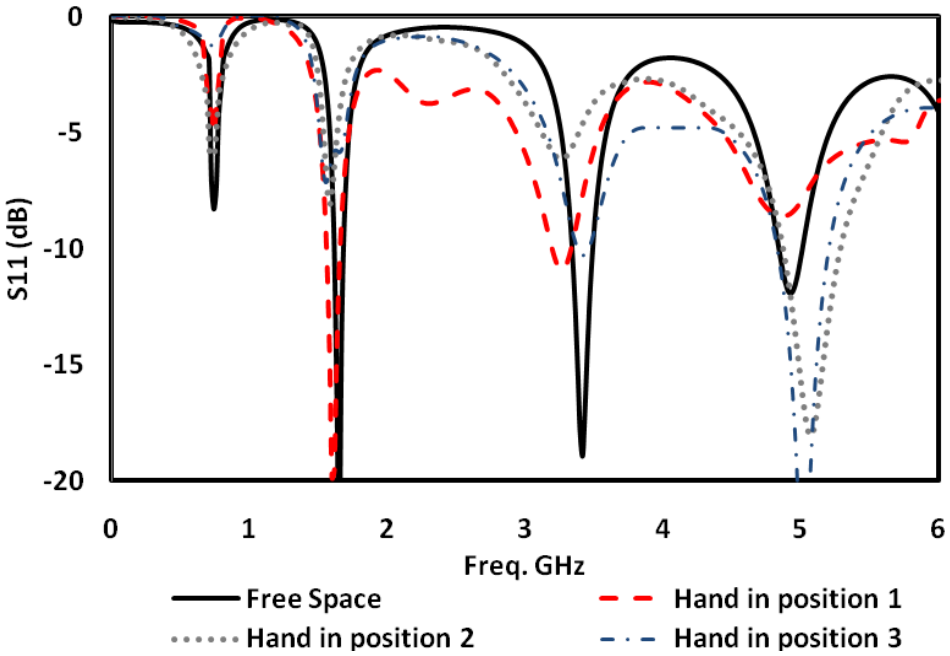

(a)

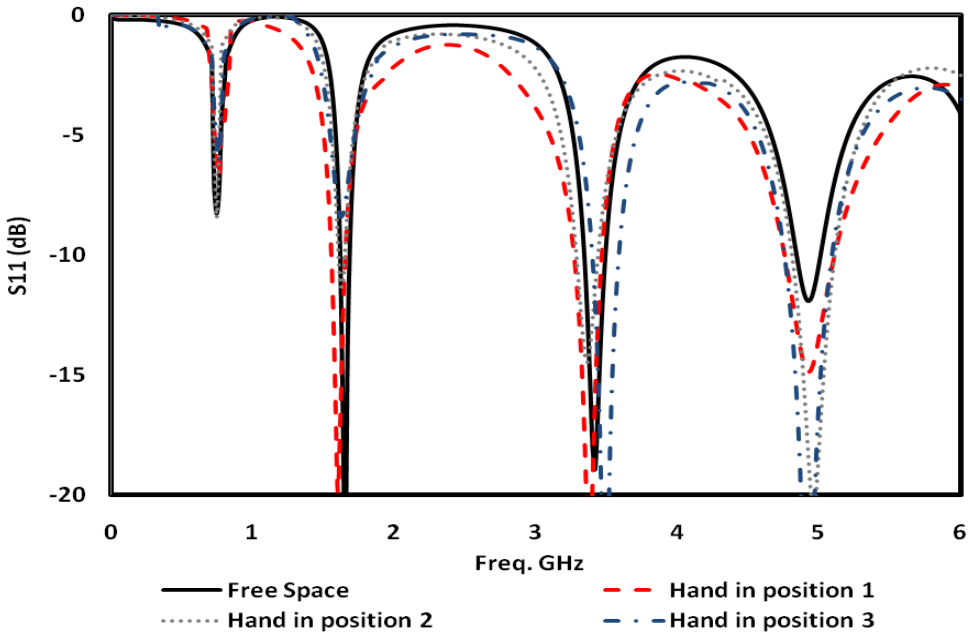

(b)

Figure 5-9: Effect of user's hand in different position when the PIN diode is in the ON ON state (a) fingers are 1mm away 1mm from radiators (b) fingers are 3mm away from radiators.

5.4 Summary

In this chapter, tunable antennas have been proposed with wide tunability range.

Many designs presented in the literature have reported excellent designs with tunable frequency bands. Some of these antennas suffer from large size, high profile, limited number of band, complicated structure that can affect the fabrication cost and most important the freedom of tuning each band independently without affecting the other bands. All of the above issues have been tackled in this chapter. All the antennas presented in this chapter are small and thin that makes them become attractive for compact and slim handsets or wireless device.

In section 5.2, printed antenna has been designed to operate in five-band. These five-band can be tunable over a wide range from 0.9 to 3 GHz. This will eliminate the need to increase the service area or dimensions that needed to design multiple bands antenna. In addition, many different wireless and mobile standard can be access from a single antenna. Indepednate tuning of each band has been performed.

In section 5.3, a small and slim tunable PIFA for modern mobile phone handsets has been presented. The operating frequencies of the proposed antenna can be switchable or tunable over a wide range. The antenna can be used to serve most of the mobile and wireless applications including: DVB-H (470 MHz - 702 MHz), GSM, GPS, DCS (1710 1880 MHz), PCS (1750 1870 MHz, 1850 1990 MHz), UMTS (1920 2170 MHz), Wibro (2.3-2.4GHz), WLAN, WiMax and WiBro phase III (3.1- 4.5 GHz) and many more. The size of the ground plane is insignificant to the antenna performance. The effect of user's hand on the antenna performances has been investigated at different position and at different locations on the antenna which thought to be insensitive.

5.5 References

[1] S. Yang, C. Zhang, H. Pan, A. Fathy and V. Nair, "Frequency-reconfigurable antennas for multiradio wireless platforms," IEEE Microwave Magazine, vol. 10, pp. 66-83, 2009.

[2] Y. Guo, A. R Weily, "A Frequency-Reconfigurable Quasi-Yagi Dipole Antenna," IEEE Antennas and Wireless Propagation Letters, vol.9,pp.883-886, 2010.

[3] H. F AbuTarboush, R. Nilavalan, K. Nasr, H. Al-Raweshidy, D. Budimir, "A reconfigurable H-shape antenna for wireless applications," Proceedings of the Fourth European Conference on Antennas and Propagation (EuCAP), pp.1-4, 12-16 April 2010.

[4] L. M. Feldner, C. T. Rodenbeck, C. G. Christodoulou, and N. Kinzie, "Electrically small frequency-agile PIFA-as-a-package for protable wireless devices," IEEE Transaction on Antennas Propagation, vol. 55, no. 11, pp. 3310–3319, Nov. 2007.

[5] Pei-Yuan Qin, A.R Weily, Y. J. Guo, T. S. Bird, Chang-Hong Liang, "Frequency Reconfigurable Quasi-Yagi Folded Dipole Antenna," IEEE Transactions on Antennas and Propagation, ,vol.58,no.8, pp.2742-2747, Aug. 2010.

[6] S. Yang, A. Kishk, K. Lee, "Frequency Reconfigurable U-Slot Microstrip Patch Antenna," IEEE Antennas and Wireless Propagation Letters, vol.7, pp.127-129, 2008

[7] C. White, G. Rebeiz, "A Shallow Varactor-Tuned Cavity-Backed Slot Antenna With a 1.9:1 Tuning Range," *IEEE Transactions on Antennas and Propagation,* vol.58, no.3, pp.633-639, March 2010.

[8] S. Shynu, G. Augustin, C. Aanandan, P. Mohanan, K. Vasudevan, "C-shaped slot loaded reconfigurable microstrip antenna," Electronics Letters , vol.42, no.6, pp. 316- 318, March 2006.

[9] B.R. Holland, R. Ramadoss, S. Pandey and P. Agrawal, " Tunable coplanar patch antenna using varactor," Electronics Letters, vol.42, no.6, 2005.

[10] C. Song, Z. Hu, J. Kelly, P. Hall, P. Gardner, "Wide tunable dual-band reconfigurable antenna for future wireless devices," *Loughborough Antennas & Propagation Conference, LAPC 2009*, pp.601-604, 16-17 Nov. 2009.

[11] V. Nguyen, R. Bhatti, S. Park, "A Simple PIFA-Based Tunable Internal Antenna for Personal Communication Handsets," IEEE Antennas and Wireless Propagation Letters, vol.7, pp.130-133, 2008.

[12] S. V. Shynu, G. Augustin, C. Aanandan, P. Mohanan, K. Vasudevan, "Development of a varactor-controlled dual-frequenciy reconfigurable microstrip antenna," Microwave Optical Technology Letter V. 46, no. 4, P.375–377, 2005.

[13] D. Anagnostou, A. Gheethan, "A Coplanar Reconfigurable Folded Slot Antenna Without Bias Network for WLAN Applications," IEEE Antennas and Wireless Propagation Letters, vol.8, pp.1057-1060, 2009.

[14] S. Shynu, G. Augustin, C. Aanandan, P. Mohanan, K. Vasudevan, "C-shaped slot loaded reconfigurable microstrip antenna," *Electronics Letters* , vol.42, no.6, pp. 316- 318, 16 March 2006.

[15] S. Xiao, B. Z.Wang, and X. S.Yang, "A novel frequency reconfigurable patch antenna," Microwave Optical Technology Letter, vol. 36, pp. 295–297, 2003.

[16] V. Nguyen, M-T Dao, Y.T. Lim and S-O Park, "A Compact Tunable Internal Antenna for Personal Communication Handsets," IEEE Antennas and Wireless Propagation Letters, vol. 7, pp. 569 - 572, 2008.

[17] J-H Lim, G-T Back, Y-I Ko, C-W Song and T-Y Yun, "A Reconfigurable PIFA Using a Switchable PIN-Diode and a Fine-Tuning Varactor for USPCS/WCDMA/m-WiMAX/WLAN," IEEE Transactions on Antennas and Propagation, vol.58, no.7, pp.2404-2411, July 2010.

[18] S - K Oh, H - S Yoon and S - O Park, "A PIFA - Type Varactor-Tunable Slim Antenna With a PIL Patch Feed for Multiband Applications," IEEE Antennas and Wireless Propagation Letters, vol. 6, pp. 103 - 105, 2007.

[19] N.Behdad, K.Sarabandi, "Dual-band reconfigurable antenna with a very wide tunability range," IEEE Transactions on Antennas and Propagation, vol.54, no.2, pp.409-416, 2006.

[20] k M. Alkanhal and A. F. Sheta, "A Novel Dual-Band Reconfigurable Square-Ring Microstrip Antenna," Progress In Electromagnetics Research, PIER 70, 337-349, 2007.

[21] Hattan F. AbuTarboush, R. Nilavalan, T. Peter and S. Cheung, "Multiband Inverted-F Antenna with Independent Bands for Small and Slim Cellular Mobile Handsets," IEEE Transaction on Antennas and Propagation, Vol. 59, No. 7, 2011.

[22] Y-W Chi and K-L Wong, "Internal Compact Dual-Band Printed Loop Antenna for Mobile Phone Application", IEEE Transactions on Antennas and Propagation, vol. 55, No. 5, pp. 1457 - 1462, 2007.

[23] D. Zhou, R. Abd-Alhameed, C. See, A. Alhaddad and P. Excell, "Compact Wideband Balanced Antenna for Mobile Handsets", IET Microwave Antennas and Propagation Journal, vol. 4, pp. 600 - 608, 2010.

Chapter 6

Conclusion and Future Work

6.1 Conclusion

Planar antennas are extensively used in various wireless and mobile applications. The continuous growth and commercial interest in wireless communications, especially in personal and mobile communication systems significantly increases the demand for low cost, compact size, multiple bands and high performance antennas, which are the key components used in any communication systems. The reduction of the antenna's size, the multiplicity of bands, the ease of designing the antenna (simple structure) and the need for flexible specifications such as independent control, is very important in the design of new antennas.

Reconfigurable antennas have more advantages in terms of increasing the antenna capabilities by tuning or switching its performances. Therefore, the needs to design compact size, simple structure, low profile, multiple bands antennas are required.

The object of the thesis was to develop fixed and reconfigurable compact antennas with high performance, which are easy to design and cheap to manufacture. Other aims were also to investigate the independent control feature on the operating frequencies and to develop simple design guidelines.

The proposed antennas in this these are all small and slim which make it easy to integrate any of them into small mobile handsets or wireless devices.

Different antennas were developed in this thesis mainly for three categories:

- Fixed terminal (non-reconfigurable)
- Switchable terminals

- Tunable terminals

In the fixed designs, the proposed multiple-band antennas have been designed to serve the wireless standards such as WiMAX, WLAN and many others applications. The antennas reported in the fixed designs have been designed in a way that they can be optimized to other operating frequencies easily. Not only that but also they have the options of optimizing each band independently without affecting the performance of the other operating frequencies.

In the fixed designs, the following have been achieved: i) Employed U-slots to minimise the size of the antenna. ii) Enhanced the performance of PIFA by adding additional features such as independent control over a wide range. iii) Reduced the effect of the ground plane which intern reduces the effect of user's hand and mobile phone housing. Finally, proposed a new printed antenna capable of operating in five-band with small and slim structure and with cost effective. This antenna has the flexibility to control the five-band independently adding additional feature to design the five-band to any application of interest with respect to the maximum variation range.

In the switchable designs, the proposed antennas also have small and slim size. The application considered for the switchable antennas are cognitive radio and wireless applications. The antenna proposed for cognitive radio can operates in wide-band mode or in multiple-narrow bands mode (four bands in total). This antenna is suitable for cognitive radio applications where cognitive radio system needs reconfigurable antenna (switchable) that can operate in two different modes (wideband and narrow bands) where the wideband mode can search for free slots in the spectrum before the antenna changes to the narrow bands for transmitting. The proposed switchable technique allowed to overcome the need to increase the surface area of the antenna to obtain wideband operations.

Another design has been introduced with a novel method to select the number of operating frequencies with some tuning capabilities. The antenna has a simple shape based on H-shape. In this design, the antenna is capable of switching amongst three bands and it is capable of operating in a single, dual or/and three bands mode. In addition to this, the three bands can be further tuned to lower frequencies without the need to change the size of the shape of the antenna. All these features have been performed using a single varactor

diode which reduced the complexity of using many switches to achieve these results and eliminate the need for complicated filters that usually attached with the fixed multiple bands antennas to reject the unwanted bands.

In the switchable designs, the following have been achieved: i) overcome the narrow band problem in patch antenna by using switchable technique that allowed the antenna to operate in different mode (wide and narrow). ii) Novel method to select the number of bands was achieved to eliminate the need for filter which can reduce the overall size of the wireless system. Only one varactor diode was used which also reduces the complexity of the biasing.

In the tunable designs, the proposed antennas in the fixed design have been made reconfigurable in order to serve more applications when needed without changing the antenna or change the size. The tunable five-band antenna for wireless applications was able to be tunable over a wide band and can tune each band independently without affecting the performances of the other bands. For mobile phone application, the fixed PIFA design is also made reconfigurable (switchable or tunable) by using PIN or varactor diodes. Different applications can be covered when using PIN or varactor diodes such as DVB-H, GSM, UMTS, DCS, GPS, WiMAX and WLAN.

All the designs reported in this thesis have been fabricated and measured where the measured results were compared with the simulated results. The simulated and measured results agreed well in most results.

6.2 Future research

Many issues still have not been solved and can be the basis for future investigations. These are summarised in the following points:

- The material used in the antennas presented in this thesis is FR-4, which is considered as a lossy material. Therefore, the efficiency of the antennas can be further enhanced by using expensive lossless materials.
- PIN diode and varactor diodes might have some impact on the gain and efficiency of the antennas. The use of MEMS switches is recommended which has less losses than PIN and varactor diodes.

- Cognitive radio might needs antennas to operate at the very low frequency bands. Therefore, designing an antenna with wideband and narrow bands feature for the low frequencies is a great challenge.
- In some designs, the bandwidth of the operating frequencies is narrow. Therefore, some techniques can be used to enhance the bandwidth to few more percentages.
- In the H-Shape antenna, the selectivity of the bands can be further enhanced to be more flexible and to have more choice by adding additional H-shape radiators within the same substrate. This will increase the number of bands as well making the method more flexible.
    - Some of the reconfigurable antennas proposed in this thesis operate in GPS bands. The GPS applications may need antennas that operate with circular polarization. Therefore, frequency and polarization reconfigurablility can be achieved from the same antenna to be used in the GPS band and other bands.
    - The studies of the effect of user's hand on the reconfigurable PIFA can be confirmed by measurements. Phantom of human head and hand is essential to complete this study.
    - All the switchable/tunable antennas presented in this thesis have used practical switches just to prove the concept of the designs. Better switches with the same values can be found which might be more expensive.